Comparison of differentiation protocols of SH-SY5Y cells for use as an *in vitro* model of Alzheimer's disease

by

Nooreen Mullah

A dissertation submitted in fulfilment of the requirements for the degree

Magister Scientiae

in

Pharmacology

in the

Faculty of Health Sciences

at the

University of Pretoria

Supervisor: Prof V Steenkamp
Co-supervisor: Prof W Cordier

September 2021

Declaration of originality

I,	Nooreen Mullah
Student Number	10258486
Subject of work	Dissertation
Title	"Comparison of differentiation protocols of SH-SY5Y cells for use as an *in vitro* model of Alzheimer's disease"

Declaration

1. *I understand what plagiarism is and am aware of the University's policy in this regard*
2. *I declare that this dissertation is my own original work. Where other people's work has been used, this has been properly acknowledged and referenced in accordance with applicable requirements*
3. *I did not make use of work previously presented by another student and submitted it as my own*
4. *I have not allowed, and will not allow, anyone to copy my work with the intention of passing it off as his or her own work*

Signature

.....

Date

19 September 2021

Acknowledgements

To my supervisors, Prof Vanessa Steenkamp and Prof Werner Cordier:

Thank you for being supportive and helping me through this journey. I am grateful for the knowledge you both have imparted on me.

To Prof Duncan Cromarty:

Thank you for seeing my potential, I am truly grateful for the opportunity that you have given to me.

To Mrs Margo Nell:

Thanks for being my mentor, assisting me when help was required and for your continuous support and motivation. Thank you for your friendship and guidance throughout my research.

To Dr Chrisna Durandt:

Your assistance and time spent assisting me with flow cytometry is greatly appreciated. I have learnt much from you.

To my parents and siblings:

Thank you for your prayers and unwavering belief in me. I am grateful to have such a strong support system.

To my husband:

Thank you for choosing to accompany me on my weekend trips to the laboratory and for your endless encouragement. I appreciate you and all that you do for me.

Abstract

Alzheimer's disease (AD) is caused by decreased levels of acetylcholine (ACh) and accounts for 60-80% of dementia cases worldwide. Current AD treatment modalities (i.e. cholinesterase inhibitors and N-methyl-D-aspartic acid receptors antagonists) only offer symptomatic relief as there is currently no cure. *In vitro* studies are more economical as they are capable of large-scale production of cell cultures, and are less labour intensive. In an attempt to make neurotoxicity models more representative, neuronal cell lines (such as SH-SY5Y neuroblastoma cells) are differentiated to a more mature phenotype. However, literature describes several different differentiation procedures, and thus it becomes necessary to assess their applicability in determining specific neurotoxicity parameters. The aim of the study was to compare two differentiation protocols of SH-SY5Y neuroblastoma cells for the purpose of developing an *in vitro* AD drug development platform.

Two published methods were compared for their ability to yield differentiated cells: a six-day and an eighteen-day differentiation procedure. The most representative differentiation model was determined by assessing various endpoints relating to maturity of both differentiation models in comparison to undifferentiated cells: morphological and viability changes of the cells were monitored via light microscopy, sulforhodamine B staining, protein content determination, and live-dead staining. The ACh/acetylcholinesterase (AChE) levels were measured by the Amplex Red assay; and protein expression relating to mature (amyloid precursor protein [APP] and β-secretase APP-cleaving enzyme-1 [BACE-1]) and immature (proliferating cell nuclear antigen [PCNA]) phenotypes by flow cytometry.

Live-dead staining confirmed that cells remained viable after treating with the differentiation cocktails. The cellular density of differentiated cells of both differentiation methods by Shipley *et al*. and Forster *et al*. significantly ($p \leq 0.001$) increased, thus confirming that there are more cells at the end of the differentiation processes which also correlates to the increased protein content of cultures. The six-day differentiation method had a significantly ($p \leq 0.01$) higher cellular density of differentiated cells (2.3-fold) than the eighteen-day differentiation method. Despite the difference in cellular densities between the two methods, there were sufficient cells at the end of the differentiation methods to continue with further testing. The protein content of differentiated cells of both differentiation methods significantly (six-day: $p \leq 0.001$; eighteen-day: $p \leq 0.01$) increased compared to the undifferentiated cells (six-day: 2.1-fold; eighteen-day: 1.3-fold). There was a significant ($p \leq 0.001$) decrease in protein content in the

supernatant of both differentiation methods (six-day: 1.2-fold; eighteen-day: 1.4-fold). There was a significant ($p \leq 0.001$) decrease in ACh levels in the cell lysates (six-day: 0.57-fold; eighteen-day: 0.64-fold) and supernatants (six-day: 0.60-fold; eighteen-day: 0.65-fold) of both differentiation methods. Similar to ACh levels, a significant ($p \leq 0.001$) decrease in the AChE level was observed between respective undifferentiated and differentiated cell lysates (six-day: 0.58-fold; eighteen-day: 0.51-fold) and supernatants (six-day: 0.48-fold; eighteen-day: 0.50-fold). The differentiation methods did not produce the expected increase in ACh and AChE levels after cellular differentiation. All three biomarkers (PCNA, APP, BACE-1) were expressed in undifferentiated, six-day differentiation method and the eighteen-day differentiation method. The undifferentiated cells and the cells differentiatited via the six-day differentiation method expressed higher levels of PCNA and APP than BACE-1. However, lower levels of PCNA expression were exhibited after cellular differentiation, with the eighteen-day differentiation method expressing the lowest PCNA levels. The undifferentiated cells expressed higher BACE-1 levels than the differentiated cells. The differentiation methods did not produce the expected increase in mature biomarkers after cellular differentiation. However, morphologically both differentiation methods produced a high number of long neuritic projections that connected to other cells which were evenly distributed, exhibiting a pyramidal shaped cell body, although a reduction in cellular proliferation was observed.

The results support morphological differentiation, but it is not recommended to use these preparations to investigate the mature cholinergic system. Further method development will be needed to ascertain the correct cocktail of differentiation factors to yield a mature phenotype expressing markers relevant to AD, including APP and BACE-1, and functional neurotransmitter systems, such as ACh and AChE.

List of abbreviations

Aβ	β-amyloid
ACh	Acetylcholine
AChE	Acetylcholinesterase
AD	Alzheimer's disease
Akt	Protein kinase B
Apo-E	Apolipoprotein E
APP	Amyloid precursor protein
BACE-1	β-secretase APP-cleaving enzyme-1
BBB	Blood-brain barrier
BCA	Bicinchoninic acid
BDNF	Brain-derived neurotrophic factor
BSA	Bovine serum albumin
Ca^{2+}	Calcium
CD40	Cluster of differentiation 40 protein
ChAT	Choline acetyltransferase
CNS	Central nervous system
CoA	Coenzyme A
CO_2	Carbon dioxide
CREB	Cyclic adenosine monophosphate response element binding protein
CRP	C-reactive protein
CSF	Cerebrospinal fluid
CT	Computed tomography
db-cAMP	Dibutyryl cyclic adenosine monophosphate
DMEM	Dulbecco's Modified Eagle's Medium
DMTs	Disease-modifying therapies
DNA	Deoxyribonucleic acid
ECM	Extracellular matrix
EDTA	Edetic acid

ERK	Extracellular signal–regulated kinases
EOAD	Early-onset Alzheimer's disease
FAD	Familial Alzheimer's disease
FBS	Foetal bovine serum
FDA/PI	Fluorescein diacetate/ propidium iodide
FDG	Fluorodeoxyglucose
G0	Gap 0
G1	Gap 1
GluN2B	Glutamate ionotropic receptor NMDA type subunit 2B
HRP	Horseradish peroxidase
H_2O_2	Hydrogen peroxide
ID-1	Differentiation inhibiting basic helix-loop-helix transcription factor-1
ID-2	Differentiation inhibiting basic helix-loop-helix transcription factor-2
ID-3	Differentiation inhibiting basic helix-loop-helix transcription factor-3
IgG	Immunoglobulin G
IL-1β	Interleukin-1 beta
IL-6	Interleukin-6
IMR	Immunomagnetic reduction
iPSCs	Induced pluripotent stem cells
KCl	Potassium chloride
LDL	Low-density lipoproteins
LOAD	Late-onset Alzheimer's disease
mAbs	Monoclonal antibodies
MAP2	Microtubule-associated protein 2
MAPK	Mitogen-activated protein kinase
MCI	Mild cognitive impairment
MCP-1	Monocyte chemoattractant protein-1
MKK6	MAPK kinase 6
mTOR	Mammalian target of rapamycin

Na^+	Sodium
Ng	Neurogranin
NFL	Neurofilament light chain
NFTs	Neurofibrillary tangles
NF-κB	Nuclear factor-kappa B
NMDA	N-methyl-D-aspartic acid
NMDAR	N-methyl-D-aspartic acid receptors
NO	Nitric oxide
Nrf2	Nuclear factor E2-related factor 2
PBS	Phosphate-buffered saline
PCNA	Proliferating cell nuclear antigen
PET	Positron emission tomography
Pen2	Presenilin enhancer 2
PI3K	Phosphatidylinositol 3-kinase
PS1	Presenilin 1
PS2	Presenilin 2
RA	Retinoic acid
RAGE	Receptor for advanced glycation end-products
RIPA	Radio-immunoprecipitation assay
ROS	Reactive oxygen species
sAPPα	Soluble APP-α
$sAPP_\beta$	Soluble APP-β
Simoa	Single-molecule array technology
SPs	Senile plaques
SQUID	Superconducting quantum interference device
SRB	Sulforhodamine B
STNFR-1	Soluble tumour necrosis factor receptor-1
STNFR-2	Soluble tumour necrosis factor receptor-2
TCA	Trichloroacetic acid

TGF-β1	Transforming growth factor beta 1
TNF-α	Tumour necrosis factor-α
TREM2	Triggering receptor expressed on myeloid cells 2
TrkB	Tropomyosin kinase B
tRNA	Transfer ribonucleic acid
US FDA	United States Food and Drug Administration
YKL-40	Chitinase-3-like protein 1

List of Figures

List of Tables

Table of Contents

Chapter 1 Literature review

1.1. Introduction

Neurodegeneration is a detrimental series of events that decreases neuronal functioning, due to progressive loss of neuronal tissue.[1] Neurodegeneration is most frequent in people over the age of 65 years.[2] It is a multifactorial process with various aetiologies, such as imbalanced antioxidant defence mechanisms leading to oxidative stress,[1] environmental toxicants (i.e. pesticides, mercury, aluminium), and genetic predisposition.[3,4,5] Neurodegeneration is a complex process and can occur as a result of neuronal loss and consequently reduced associated enzymatic functions responsible for the synthesis and degradation of neurotransmitters.[6] The abnormal polymerisation of proteins and possible mutations in genes also contributes to neurodegeneration which leads to dementia.[7] Dementia is the umbrella term used for diseases that affect the brain.[7]

Worldwide, there are currently 50 million people living with dementia, and it is estimated to increase to 152 million cases by 2050.[8] There were 4 million dementia cases reported in Africa in 2015, of which an estimated 186,000 people were diagnosed in South Africa. It is expected that this will increase to 275,000 cases by 2030 (Figure 1) due to the constant increase in untreated neurodegenerative disorders such as human immunodeficiency virus and alcohol dependence.[9] The most common form of dementia is Alzheimer's disease (AD), which ultimately impacts cognitive function[7] and memory loss.[10]

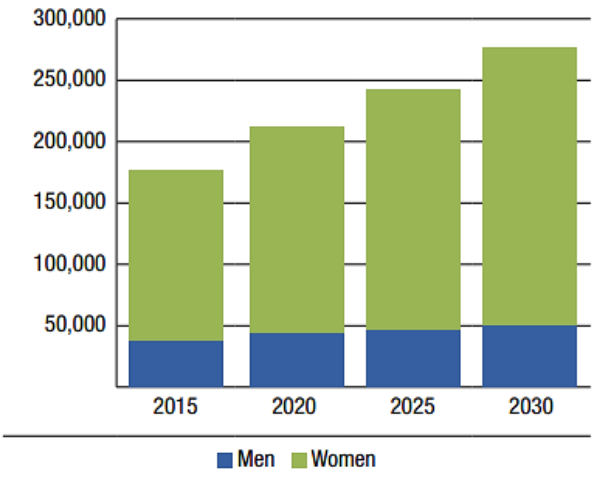

Figure 1: The estimated number of people with dementia in South Africa between the years 2015 and 2030.[9] (Reproduced with permission from the Alzheimer's Disease International)

1.2. Alzheimer's disease

Alzheimer's disease accounts for 60-70% of dementia cases worldwide.[8] Progressive loss of memory, reasoning and orientation are characteristics of AD, which are correlated to the stages of progression.[8,11] However, a pre-clinical AD stage before mild cognitive impairment (MCI) exists in which slight cognitive changes, such as reduced attention, is noticed.[12,13] The pre-clinical stage refers to patients who do not exhibit symptoms as yet but do exhibit slight cognitive decline.[12] Dr Barry Reisberg of the New York University's Aging and Dementia Research Center developed the Global Deterioration Scale to clinically measure the progression of AD (Table 1).[11] The classification of the stages of AD assist in prognostic determinants, treatment selection and psychosocial advisement,[14] and can also aid in designing clinical trials.[15]

Table 1: Global Deterioration Scale in Alzheimer's disease.[11]

Stage	**Symptoms**
1. No impairment	• There are no visible symptoms
2. Very mild cognitive decline	• Forget names and location of objects, and trouble finding words • Memory generally becomes slightly weaker as people get older
3. Mild cognitive decline	• Difficulty travelling to new location, handling work-related problems, planning and organizing events • Family may become aware of certain symptoms
4. Moderate cognitive decline	Duration of 2 years • Difficulty in complete daily tasks (i.e. manage finances, preparing meals, shopping) • Patients may suffer with short-term memory loss
5. Moderately severe cognitive decline	Duration of 1.5 years • Need supervision and assistance with daily tasks • Are unable to recall personal history
6. Severe cognitive decline	Duration of 2.5 years • Tend to wander • Wear their daytime clothing over their night time clothes • Personality and behavioural problems become worse • Patients can only remember people closest to them • Are unable to recall personal history
7. Very severe cognitive decline	• Decline in speech • Inability to eat or swallow • Loses the ability to walk • Involuntary movement

Alzheimer's disease is categorised as two forms: early-onset AD (EOAD) and late-onset AD (LOAD).[16] The neurological hallmarks of both forms of AD are identical, however, their clinical profiles differ.[17] Early-onset AD, also called familial AD (FAD), usually occurs between the ages 30 and 50 years, and accounts for less than 0.5% of AD cases.[16] Early-onset AD can occur spontaneously or by an inherited mutation in one of three genes: *amyloid precursor protein* (*APP*), *presenilin 1* (*PSEN1*), and *presenilin 2* (*PSEN2*)[18] on chromosomes 1, 14 and 21, respectively.[17] Early-onset AD is characterised by the inability to learn new information, easily forgetting names and short-term memory loss.[17]

Late-onset AD occurs in people over the age of 65, and is the most prevalent form.[17] Genetic risk factors, age, vascular disease, diet and metal exposure contributes to late-onset AD.[19] Polymorphisms in the apolipoprotein E (*Apo-E*) gene (*Apo-E4*) on chromosome 19 are the predominant risk factor for sporadic AD.[17,20] Genes encoding for Apo-E neuronal receptors, such as sortilin related receptor 1, may also be involved.[17] Decreased Aβ clearance and increased aggregation, decreased cholesterol transport, increased neurotoxicity, neuroinflammation and brain atrophy contribute to LOAD through *Apo-E4* dysfunction.[18] Specialised pro-resolving mediators reduce inflammatory molecules (i.e. cytokines) thus, equalising the inflammatory response (discussed in Section 1.3.1.1) which may give rise to LOAD.[21] Symptoms of late-onset AD include loss of cognitive function, loss of memory, disorientation, as well as behavioural and personality changes.[17] The Genome-Wide Association Study (GWAS) has identified ten genomic loci (*Apo-E* gene, *clusterin*, *phosphatidylinositol-binding clathrin assembly protein*, *complement receptor type 1*, *bridging integrator-1*, *ephrin type-A receptor 1*, *membrane-spanning 4A* gene, *ATP-binding cassette sub-family A member 7*, *CD33*, and *CD2 associated protein*) that are linked to AD risk and are coupled with various biological processes (i.e. Aβ metabolism, endocytosis, immune system and lipid homeostasis).[18] This provides a new direction for drug treatments of AD by elucidating physiological mechanisms whose disruption may predispose individuals to neurodegenerative changes.[18]

1.2.1. Hallmarks of Alzheimer's disease

The progression of AD is accompanied by neuronal loss,[22] with brain atrophy as repercussion (Figure 2).[23] Atrophy of the brain occurs first in the medial temporal lobe.[24] Initially, the

entorhinal cortex,[25] which is responsible for memory, thinking and planning, shrivels up.[24] Thereafter, atrophy progresses to the hippocampal areas (responsible for forming new memories) and the amygdala.[24] There is an approximate 20-30% and 15-25% reduction in the entorhinal cortex and hippocampal volume, respectively, in patients with MCI.[26] The shrinkage of the hippocampus is followed by the degeneration of the neocortical regions. Thereafter, the ventricles become enlarged.[27]

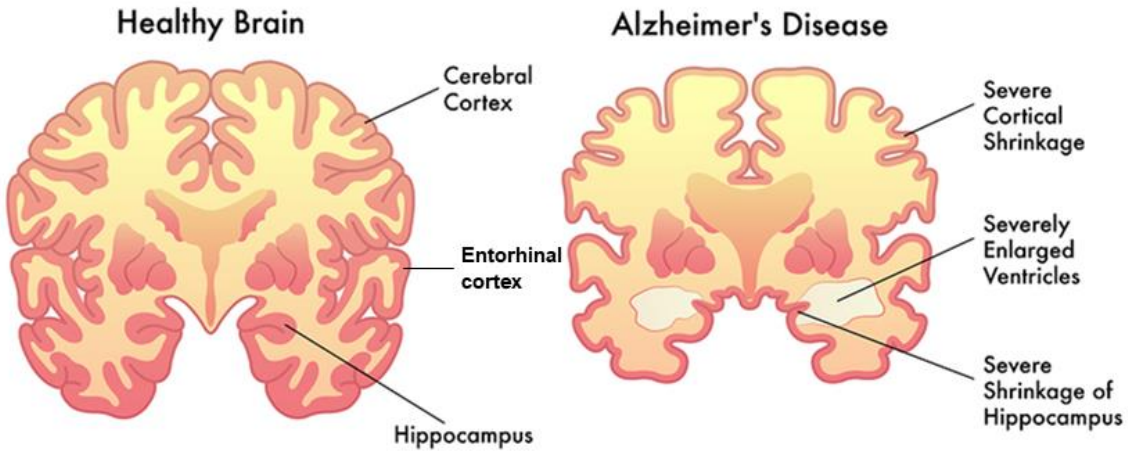

Figure 2: A coronal view of a schematic diagram comparing a healthy brain to a brain affected by AD. (Reproduced with permission from the Creative Commons Attribution License (CC BY)).

Protein expression changes are noted in a number of regions in the brain.[28] The hippocampus, entorhinal cortex and the cingulate gyrus exhibits approximately 30% change in protein expression, whereas the cerebellum shows approximately 20% change.[28] Neuronal development, survival and regeneration occur via pathways in the cerebellum.[28] In relation to other regions of the brain, the changes in protein that occur in the cerebellum are unique; it is suspected that the cerebellum is relatively unaffected by early AD.[28] However, it has been observed that in later stages of AD, the cerebellum undergoes atrophy and changes in glucose metabolism.[28] Changes to other regions, such as the hippocampus, entorhinal cortex and the cingulate gyrus, correspond to the severity of the disease, resulting in cellular death.[28] Thus, a temporospatial element of AD exists as pathology of different regions of the brain do not occur simultaneously (i.e. earlier or later stages of AD).[28] The highest number of biological pathways that are disrupted by AD are observed in the hippocampus, entorhinal cortex and the cingulate gyrus.[28] It is suspected that the cellular response to AD is different in the cerebellum as it acts as a defence mechanism.[28] By increasing oxidative defence proteins and decreasing electron transport chain (ETC) complex 1 proteins, less reactive oxygen species (ROS) are produced by

the ETC.[28] Alzheimer's disease triggers an innate immune response that is present through the brain (global activation), and it is associated with neuroinflammation.[28] Complement family proteins may be possible AD biomarkers as global activation of the immune response is suggested to occur at an earlier stage in the disease process, prior to atrophy.[28]

Altered glucose use in the brain is another characteristic associated with AD,[28] and can be visualised using positron emission tomography (PET) scans.[2] High glucose use is an indication of healthy brain activity, while use thereof decreases with AD progression as brain function is perturbed.[2] Free glucose levels are increased in the hippocampus, entorhinal cortex, cingulate gyrus and the cerebellum, as the pathways that metabolise monosaccharides (such as glucose) are hindered.[28] It has been reported that the ketogenic/fatty acid β-oxidation pathway was used as an alternative to aerobic glycolysis in severely affected regions of the brain in AD patients.[28]

Brain morphology may be altered by inflammation, which in turn affects cognitive execution.[21] Patients aged 60 and older express decreased hippocampal volume and increased levels of interleukin-6 (IL-6), C-reactive protein (CRP), soluble tumour necrosis factor receptor-1 (STNFR-1) and STNFR-2.[21] Furthermore, increased IL-6 levels are observed in parallel to a reduced total brain volume and decreased cortical thickness of the inferior occipital and temporal gyri.[21]

Two fundamental hallmarks of AD include extracellular amyloid-β (Aβ) plaques and intracellular neurofibrillary tangles (NFTs).[16,22] Other lesions or characteristics include granulovacoular degeneration[29] and Hirano bodies (a.k.a. eosinophilic rod-like bodies).[30] The intensity and size of the Aβ plaques does not increase as AD progresses, however, the number and distribution thereof does.[31] Amyloid-β plaques are found in the isocortical region (stage 1), allocortical or limbic regions (stage 2) and finally the subcortical region (stage 3).[31] Unlike Aβ, NFTs intensity and distribution increases with the progression of AD, and is categorised by six stages.[31] Abnormal tau-protein or NFTs occur in stages: (1) stage 1 and 2, transentorhinal and entorhinal regions; (2) stage 3, limbic allocortex regions; (3) stage 4, adjoining neocortex; and (4) stage 5 and 6, neocortex.[32,33]

The cholinergic pathway consists of cholinergic neurons which are present in most regions of the brain.[34] Due to its extensive distribution, various physiological processes are mediated by the cholinergic pathway including learning, memory, sensory information and other neural functions.[34] The presence of Aβ and NFTs adversely affects neuronal cells, thus injuring the cholinergic pathway.[35] Amyloid-β accumulation blocks the transmission of ACh in the synaptic

cleft, which results in low levels of synaptic ACh.[35] As will be discussed in Section 2.1, ACh is formed by ChAT from choline and acetyl coenzyme A (CoA). Acetylcholine in turn, is broken down by AChE to form choline and acetate.[36] The cholinergic hypothesis suggests that the decline in cognitive function is age-related whereby a reduction in ChAT is mainly observed in the hippocampus, amygdala and the cortex, resulting in ACh deficiency.[16] The reduction of ACh levels and consequently the loss of associated enzymatic functions responsible for the synthesis and degradation of ACh can occur as a result of the destruction of cholinergic systems.[35] This depletion leads to deficits in overall cognition and neuroprotection.[34]

1.2.1.1. Amyloid-β plaques

In a healthy brain, Aβ have a modulatory role on memory and transmission in the hippocampal regions when present at low concentrations.[6] Equilibrium is maintained between the production and clearance of Aβ.[16] Amyloid-β aggregates form and accumulate when the equilibrium is disturbed by metabolic disorders and excitotoxicity.[16] Synaptic activity is also hindered by aggregated Aβ thus provoking neurodegeneration.[22] Extracellular Aβ aggregation and accumulation forms fibrillary Aβ and Aβ-oligomers,[17] as well as activates tau-kinase.[6] The fibrillary Aβ causes inflammation, oxidative stress,[16] mitochondrial dysfunction,[30] and leads to the formation of Aβ plaques.[1,17] The accumulation of Aβ plaques and the hyperphosphorylation of tau proteins disrupt nerve cells and transmission of signals, thus inducing neuronal loss, synaptic and axonal dysfunction which causes dementia.[16,17] This process is known as the amyloid cascade hypothesis (Figure 3).[16]

Amyloid precursor protein (APP) is a transmembrane protein which is processed by two pathways that are mutually exclusive: non-amyloidogenic and amyloidogenic.[17] The non-amyloidogenic pathway (Figure 4) cleaves APP at the +83 site[6] with α-secretase[17] to produce soluble APP-α fragments ($sAPP_{\alpha}$).[6] The $sAPP_{\alpha}$ fragments are important for early CNS development, control of neural stem cell proliferation, allow neuronal survival, and are neuroprotective against excitotoxicity.[6] The $sAPP_{\alpha}$ fragments are further cleaved by γ-secretase which produces a p3 fragment.[6] There is no plaque formation when APP is cleaved via the α- and γ-secretase pathway (Figure 4).[17] γ-Secretase is a multi-protein complex which comprises

four proteins: presenilin (PS) 1 or 2, nicastrin, presenilin enhancer 2 (Pen2) and anterior pharynx defective 1.[37,38]

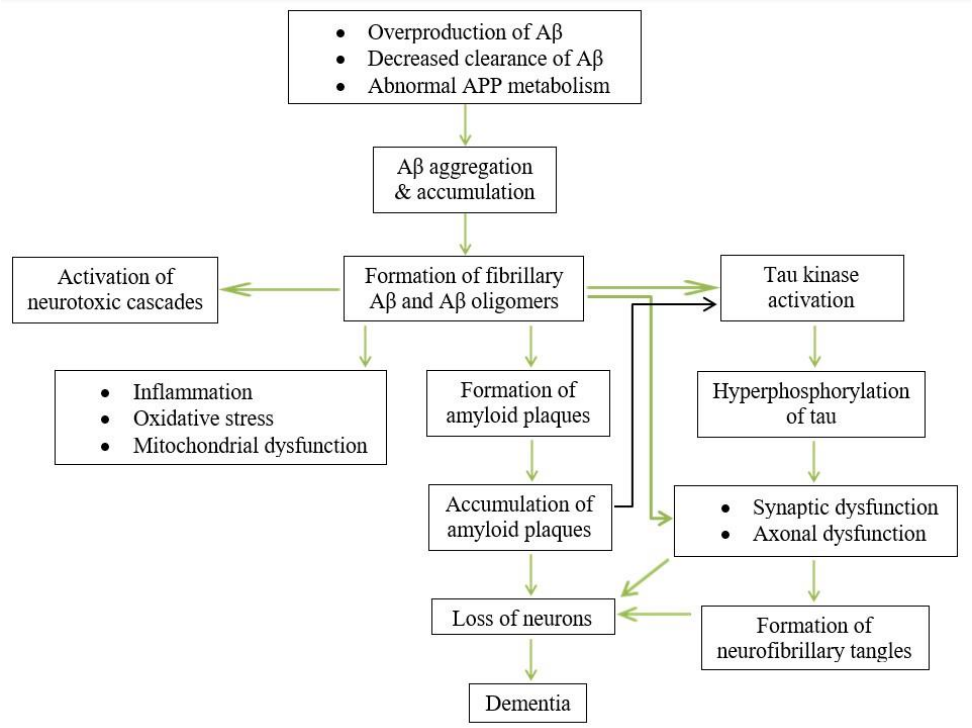

Figure 3: Amyloid cascade hypothesis. β-amyloid (Aβ); Amyloid Precursor Protein (APP).

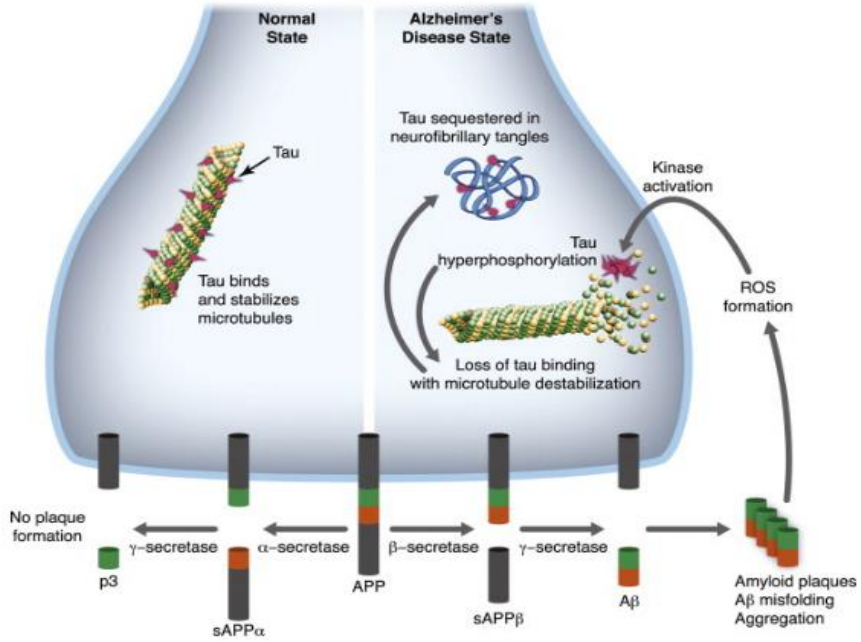

Figure 4: Amyloid plaque formation and tau hyperphosphorylation via cleavage by amyloid precursor protein.[39] (Reproduced with permission from Elsevier). β-amyloid (Aβ); Amyloid Precursor Protein (APP); Reactive Oxygen Species (ROS); soluble APP-α fragments (sAPPα); soluble APP-β fragments (sAPPβ).

The amyloidogenic pathway (Figure 4) cleaves APP at a site which is located at 99 amino acids away from the C-terminus with the main β-secretase enzyme, β-secretase APP-cleaving enzyme-1 (BACE-1), to produce soluble APP-β fragments ($sAPP_{\beta}$).[6] The $sAPP_{\beta}$ fragments mediate axonal pruning and neuronal cell death.[40] The $sAPP_{\beta}$ fragments are further cleaved by γ-secretase which produces extracellular Aβ ($A\beta_{42}$ and $A\beta_{40}$) peptides and APP-intracellular domain.[6] Paired helical filaments, dense and membranous bodies, and microglial cells are present in SPs.[6] Amyloid-β aggregate and accumulate forming Aβ plaques between neurons (Figure 5).[17,35] The Aβ accumulation prevents transmission of chemical signals (ACh) from presynaptic to postsynaptic neurons.[17,35]

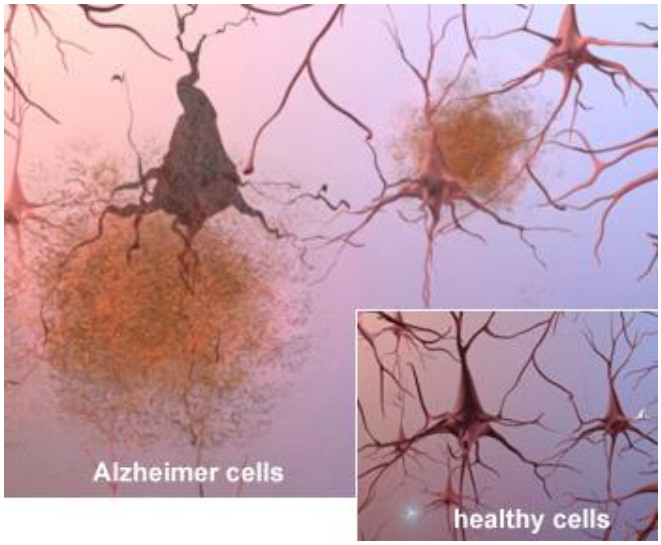

Figure 5: The comparison between healthy neuronal cells and cells with Aβ accumulation between the neurons, such as seen in Alzheimer patients.[41] (Reproduced with permission from ©2021 Alzheimer's Association. www.alz.org. All rights reserved. Illustrations by Stacy Jannis).

A misfolded protein is a functionally inactive protein with exposed hydrophobic regions which can interact with hydrophobic regions on other misfolded proteins.[42] This interaction tends to produce cellular aggregates (such as Aβ) which accumulate in brain tissue.[30] Misfolded proteins can occur due to factors that may act independently such as mistakes in trafficking, environmental changes such as temperature and pH, and posttranslational modification.[1] One of the factors that cause the accumulation of misfolded proteins is the expenditure of aminoacyl transfer ribonucleic acid (tRNA) synthetase (nuclear and mitochondrial) in the cerebellum.[28] *In vitro* formation of Aβ40 and Aβ42 are characterised by simple strand-bend-strand conformations.[43] However, $A\beta_{40}$ from a patient showed a kink in residues 19-23 which allowed side chains to be buried in the structure.[43] Interaction with other $A\beta_{40}$ molecules occurs when the side chains point in opposite directions due a twist at G33.[43] Amyloid-β in its constitutional

form is an unfolded protein.[6] The constitutional form folds from random-coil-rich state to α-helical-rich intermediate, which then forms amyloid fibrils (β-sheet-rich amyloid monomer).[6]

An accumulation of Aβ in the brain is an abnormal occurrence which triggers a stress response.[44] Stress stimulates the innate immune response of microglial cells and astrocytes which results in neuroinflammation and subsequently, neuronal death (Figure 6).[44,45] The immune cells (microglial cells) bundle up at Aβ deposition sites and contribute to the loss of dendritic spines.[21,45] The production and release of pro-inflammatory cytokines are activated: interferon gamma, interleukin-1 beta (IL-1β) and tumour necrosis factor-α (TNF-α).[45] The cytokines activate a secondary response by triggering an astrocyte.[45] An increase in production of Aβ42 is initiated by the astrocyte.[45] The binding of CD40 ligand (astrocytic signalling molecule) to its cognate receptor triggers a pro-inflammatory effector molecule (TNF-α) which causes tissue destruction.[44] It is thus likely that neuroinflammation may be conducive to AD progression.[44] It is suggested that the elevated levels of cytokines have a direct impact on cognitive decline as lengthy cytokine exposure can be damaging to astrocytes.[45]

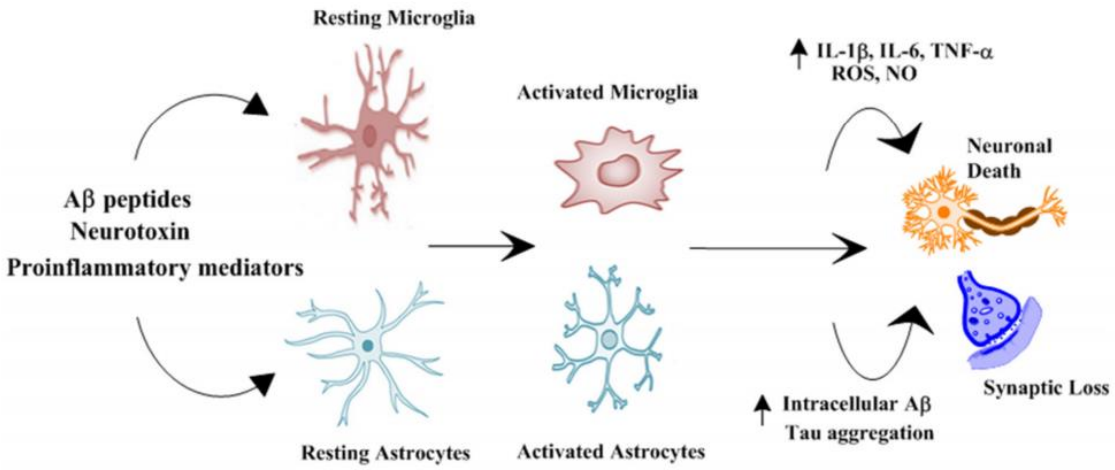

Figure 6: Schematic representation of the role of glial cells in the pathophysiology of Alzheimer's disease.[45] (Reproduced with permission under Frontiers in Pharmacology's open-access copyright law). Interleukin-1 beta (IL-1β); Interleukin-6 (IL-6); Tumour necrosis factor-α (TNF-α); Reactive Oxygen Species (ROS); Nitric Oxide (NO).

Various neuroinflammatory pathways and signalling cascades occur in AD. These include: nuclear factor-kappa B (NF-κB), protein kinase B-phosphoinositide-3-kinase (Akt/PI3K), mitogen-activated protein kinase (MAPK), nuclear factor E2-related factor 2 (Nrf2) and cyclic-AMP response element binding protein (CREB) pathways.[45] Nuclear factor-kappa B transcribes genes which are involved in inflammation and immunity.[45] Neurotoxicity, caused

by the production of Aβ, activates signalling of NF-κB in neural and microglial cells.[45] Cellular proliferation, migration growth and survival are managed by the Akt/PI3K pathway.[45] Substrates that are involved in cellular signalling, such as glycogen synthase kinase-3-beta is pertinent and mammalian target of rapamycin (mTOR) are activated by protein kinase B.[45] Toxicity caused by Aβ induction results in hyperactivity of mTOR.[45] Mitogen-activated protein kinase signals oxidative stress and cell cycle control thus, contributing to the control of neuronal survival or death.[45] Impaired hippocampal function and memory occurs due to increased levels of activated extracellular signal regulated kinases (ERK), which is a MAPK.[45] An immediate upstream activator of the p38 pathway is MAPK kinase 6 (MKK6).[45] Alzheimer's disease increases MKK6 which activates the p38 pathway.[45] Activated MKK6-p38 is suspected to be directly conducive to neuronal degeneration as it is more eminent in neurons than astrocytes.[45] The transcription factor, Nrf2, shifts from the cytoplasm of cells into the nucleus in response to oxidative stress.[45] The expression of genes encoding antioxidant activity is activated by Nrf2.[45] In AD, Nrf2 is upregulated as a response to excessive oxidation, with subsequent antioxidant response element modulation to reduce oxidative damage.[45] However, disruption of the pathway is evident as there is a decrease in ARE-containing gene products.[45] Thus, a decline in antioxidant activity and an increase in inflammation and oxidative stress occurs.[45] In AD, CREB levels in the prefrontal cortex have decreased.[45] Cyclic-AMP response element binding protein is imperative in memory development.[45] It is speculated that neuroinflammation may activate and boost Aβ formation and tau-associated events (as is discussed in Section 1.6.1).[21]

1.2.1.2. Neurofibrillary tangles

Tau is a microtubule-associated neuronal protein (MAP2) which is localised in the cell body of neuronal axons.[6,46] It is a multi-protein complex which comprises four regions: a proline-rich domain, a microtubule-binding domain, an N- and a C-terminal region.[47] Tau can undergo several post-translational modifications, including phosphorylation, aggregation and oxidation.[47] In a healthy brain, normal functioning of the tau protein enables the mediation of signal transduction,[17] axonal transport regulation[47] and allows for the construction of tubulin into the microtubules which provides stability in the cell (Figures 4 and 7).[6] The aggregation and accumulation of Aβ activates ROS, which in turn activates tau-kinase (GSK-3β); this

process initiates tau-hyperphosphorylation (Figure 4).[6] Activated Akt inhibits GSK-3β by phosphorylation.[45] However, in AD, GSK-3β causes the separation of tau proteins from the microtubules due to phosphorylation of tau.[45] During this process, tau repositions itself in the somatodendritic compartments of neurons.[46,47] Once in the somatodendritic compartments, tau binds to a tyrosine-kinase, thus the excitatory N-methyl-D-aspartate receptor (NMDAR), glutamate ionotropic receptor NMDA (N-methyl-D-aspartate) type subunit 2B (GluN2B) is subjected to phosphorylation and is stabilised.[47] This intensifies Aβ toxicity by causing an influx of intracellular Ca^{2+} (as discussed in Section 1.3) as a result of an increase in glutamate signalling.[47]

Hyperphosphorylated-tau protein results in the loss of tau binding with microtubules, thus destabilising microtubules (Figures 4 and 7).[1] Hyperphosphorylated and aggregated tau are the major components in the paired helical filaments, NFTs.[17] The accumulation of NFTs causes cognitive impairment and dementia as signal transduction and cellular stability is lost due to tau-hyperphosphorylation.[6,17]

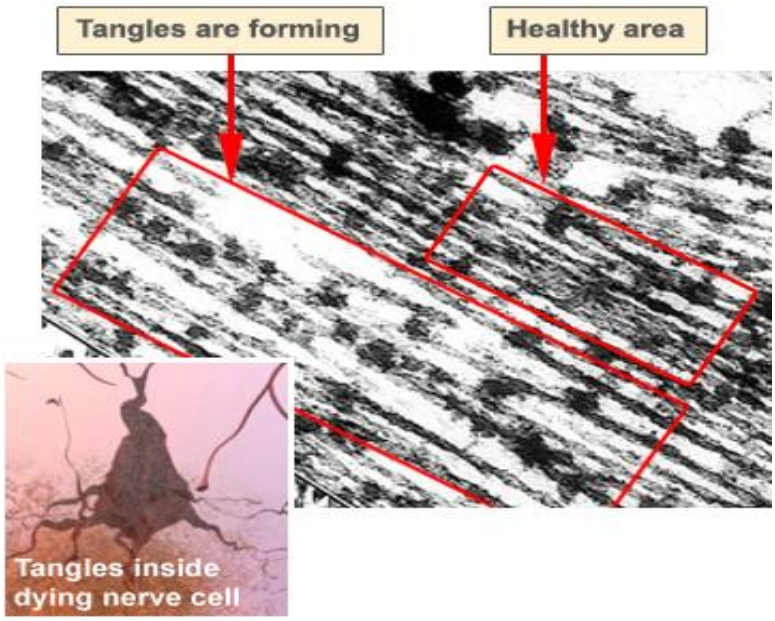

Figure 7: The comparison between healthy tau binding and cells with the formation of tangles within the cell body of neurons.[41] (Reproduced with permission from ©2021 Alzheimer's Association. www.alz.org. All rights reserved. Illustrations by Stacy Jannis).

1.3. Acetylcholine

Acetylcholine (ACh) is the most important neurotransmitter[48] found in the cholinergic nerve system.[49] Acetylcholine is present in all pre-ganglionic sympathetic and all pre- and post-ganglionic parasympathetic neurons.[34] In the peripheral nervous system, ACh activates the cardiac and skeletal muscle functions, as well as enables the contraction of smooth muscles.[50] Additionally ACh is associated with memory, learning, and is responsible for excitatory actions (i.e. arousal, reward and excitability) in the CNS.[51] Acetylcholine is formed by choline acetyltransferase (ChAT) from choline and acetyl.[36] Acetylcholine in turn, is broken down by acetylcholinesterase (AChE) to form choline and acetate which undergoes recycling processes.[36]

Cholinergic receptors consist of two receptor families: nicotinic and muscarinic.[52] The receptors serve different functions based on their location.[52] Muscarinic receptors are described as G-coupled protein receptors that are associated with the parasympathetic nervous system which controls parasympathetic reactions such as peristalsis, lacrimation and bronchoconstriction.[53] The modulation of ion channels and intracellular processes are controlled by the G-coupled protein receptors which also has the potential of altering genetic activity and protein expression.[52] The release of neurotransmitters can be suppressed by the reduction in cAMP signalling which is regulated by the presynaptic muscarinic acetylcholine receptors that are known to have inhibitory effects on the calcium (Ca^{2+}) channels.[52] The activation of postsynaptic muscarinic acetylcholine receptors leads to depolarization of the membrane and enhancements in NMDA currents and phospholipase C signalling.[52] Nicotinic receptors are ionotropic receptors that are involved in the CNS.[54] Nicotinic ACh receptors are expressed pre- and post-synaptically.[55] The influx of Ca^{2+} or terminal depolarization regulates the release of the neurotransmitter.[52] The nicotinic ACh receptors depolarise the serotonergic (5HT6) receptors by ACh[52] and are present on GABAergic interneurons, cellular activity is regulated by the latter.[55] Learning, memory and the regulation of synaptic plasticity and transmission are controlled by nicotinic ACh receptors.[55] However, both nicotinic and muscarinic receptors are both activated by ACh.[34,52] The thalamus, hippocampus and the cerebral cortex are associated with cognitive function and express nicotinic receptors in the CNS.[54] The release of neurotransmitters (such as ACh and glutamate) and synaptic function is regulated by nicotinic receptors.[54] Nicotinic receptor agonists display neuroprotective activity, supporting the necessity of healthy, active cholinergic systems for neuroprotection.[34,56]

Synaptic transmission allows for the development of neural signals, required for functioning of the brain (Figure 8).[52,57] The presynaptic axon receives an action potential which opens sodium (Na^+) and Ca^{2+} channels, causing an influx of Na^+ and Ca^{2+}, respectively, into the cell.[58,59] Increased concentrations of Ca^{2+} in the cell results in a signalling cascade.[23] Synaptic vesicles containing ACh travel to the presynaptic membrane, thus, releasing ACh into the synaptic cleft via exocytosis.[52] Upon release, ACh binds to both nicotinic and muscarinic receptors[34,52] on the postsynaptic neuron membrane.[51] After activation of receptors, ACh is degraded by AChE in the synaptic cleft, and choline is taken back into the neuron for ACh synthesis in the synaptic knob.[52] A block in synaptic transmission would result in noticeably reduced levels of ACh in the synaptic cleft, thus having a negative impact on neuronal cells.[52] In turn, this will lead to reduced skeletal functions and a decline in cognitive abilities, including perception, memory and learning.[50] Some mechanisms which may incur neurotoxicity include Ca^{2+}-induced excitotoxicity, leading to membrane depolarisation, surplus of mitochondrial Ca^{2+}, oxidative stress, post-synaptic damage and apoptotic cellular death.[47]

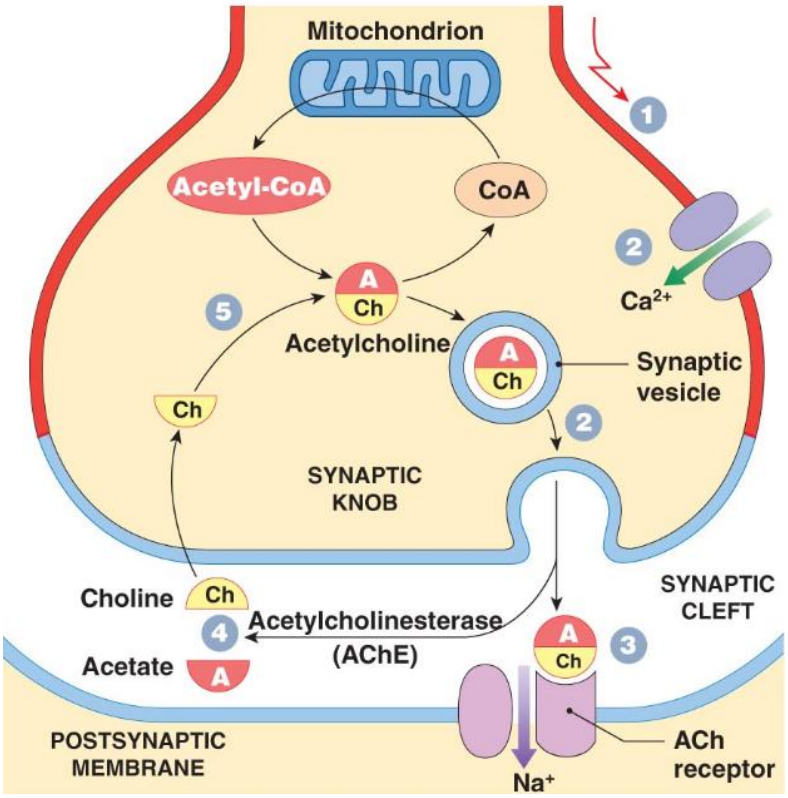

Figure 8: Schematic representation of synaptic transmission across neurons.[60] (Reproduced with permission).[60] Acetylcholine (ACh); Acetylcholinesterase (AChE); Calcium (Ca^{2+}); Coenzyme A (CoA); Sodium (Na^+).

1.4. Diagnosis and biomarkers of Alzheimer's disease

As not many effective treatments have been discovered for AD, focus is now being shifted to the early stages of the disease process.[21] It is believed that treating AD in its pre-clinical phase would most likely change its course.[12] For this, early-stage biomarkers need to be identified (i.e. neurological and pre-clinical markers).[21] The biomarkers being researched are associated with Aβ and tau pathology, axonal and synaptic degeneration, glial activation (neuroinflammation) and TAR DNA-binding protein-43 pathology.[61]

Neuroimaging biomarkers are mostly used for research; however, clinical diagnosis is possible.[18] Positron emission tomography imaging is used as a biomarker for NFTs as increased levels of cortical tau protein can be detected using PET imaging (Figure 9).[18] Structural MRI is used as a biomarker for neurodegeneration/neuronal injury to detect brain atrophy.[18] Fluorodeoxyglucose (FDG)-PET imaging detects a decline in glucose metabolism.[18] Amyloid-specific imaging agents for PET-computed tomography (CT) can be used to identify Aβ deposition 15 years prior to AD symptoms.[18] Cerebral hypometabolism (FDG-PET/CT) is observed 10 years prior to the onset of AD symptoms.[18] Positron emission tomography requires a radioactive probe to be injected into the blood which will cross the BBB and remain in the system for some time.[61] This is a more invasive and expensive procedure.[61]

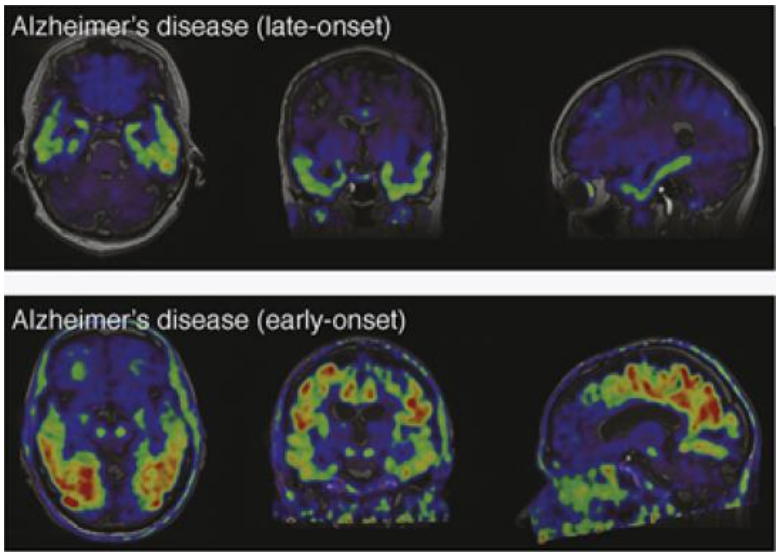

Figure 9: Positron emission tomography images of late-onset and early-onset Alzheimer's disease exhibiting tau deposition.[61] The binding of AV1451 to tau produces the red colour.[61] (Reproduced with permission from Prof. Michael Scholl).

Total tau, hyperphosphorylated-tau and $A\beta_{42}$ are known as the core biomarkers and are the most appropriate cerebrospinal fluid (CSF) biomarkers as they are present in early prodromal AD and exhibit a steady change in later stages.[18] The diagnostic AD criteria have incorporated these CSF biomarkers due to their high diagnostic performance.[18] Non-demented patients exhibit reduced $A\beta_{42}$ levels[61] which corresponds with brain atrophy, thus suggesting a preclinical stage.[18] However, brain atrophy corresponds with the elevated levels of tau and hyperphosphorylated-tau concentrations in CSF.[18] Therefore, the development of cognitive decline symptoms is more effectively predicted via tau and hyperphosphorylated-tau than Aβ.[18] The reduction in $A\beta_{42}$ in CSF can also be detected in patients with MCI.[61]

Cerebrospinal fluid neurofilament light chain (NFL), neurogranin (Ng), and chitinase-3-like protein 1 (YKL-40) proteins are new biomarkers that are at an advanced clinical validation stage.[18] Neurofilament light chain can be used as a marker to measure total tau levels for axonal degeneration – the higher the total tau levels, the more axonal neurodegeneration.[61] The core CSF biomarkers and CSF NFL were suggested by meta-analysis to be strongly connected to AD.[18] Several markers of glial activation in AD are increased, including YKL-40, triggering receptor expressed on myeloid cells 2 (TREM2), C-C chemokine ligand 2.[18,61] Neurogranin is a protein which participates in synaptic dysfunction and degeneration and it is somewhat specific to AD as the levels do not change in any other neurodegenerative diseases.[18,61] Higher CSF levels of Ng are observed in AD patients.[18,61] The decrease in glucose metabolism, the severity of cognitive decline and brain atrophy in early stages of AD correspond with Ng.[61] The drawback of CSF analysis is that a lumbar puncture is necessary as the CSF is less accessible.[61]

The disease processes can be monitored with blood-based biomarkers which can also be used for primary care screening.[18] This method is inexpensive and suitable for multiple measures. Plasma biomarkers for AD include total tau and Aβ.[18] Plasma total tau is suspected to have a strong connection to AD.[18] It is suspected that 30-50% of Aβ originates from the CNS and has the ability to cross the BBB.[18] Lower levels of plasma $A\beta_{42}$ and $A\beta_{40}$ are observed in AD – the $A\beta_{42}$ corresponds with Apo-E4 allele and age.[18] The major drawback in developing blood biomarkers is the low concentration of CNS-specific proteins in the blood which makes it tricky to quantify and may lead to inconsistent results using standard immunochemical technology.[18] However, the levels of plasma total tau and plasma hyperphosphorylated-tau as well as total tau and hyperphosphorylated-tau have been found to be higher in AD dementia when compared to the cognitively unimpaired patients when using improved technology, namely single-

molecule array (simoa) technology.[18] It has also been noted that plasma hyperphosphorylated-tau has a connection with Aβ and tau PET.[18] The concentration of plasma NFL corresponds with those found in CSF and YKL-40 levels are increased in plasma levels.[61] Sensitive technology such as superconducting quantum interference device (SQUID) immunomagnetic reduction (IMR) assay allows the clinical diagnosis of AD by detecting plasma $A\beta_{42}$ and tau. Furthermore, the cognitive decline in early AD patients can be detected using the concentrations of plasma hyperphosphorylated-tau by measuring low-level proteins in blood, which makes SQUID IMR suitable for AD diagnosis.[18] Markers of mitochondrial dysfunction, oxidative stress, inflammation and neuronal injury are also detected via blood-based biomarkers.[18]

Neuroinflammation is a prospective pre-clinical marker as it is suggested that neuroinflammation may occur before Aβ and tau formation.[21] The pre-clinical markers that are used are IL-1β, IL-6, TNF-α and CRP.[21] However, in pre-clinical studies, the variability of cognitive ability is evident as inflammation is not always exhibited.[21] The inflammatory biomarkers provide a more accurate classification/diagnosis by indicating pre-clinical AD in healthy adults.[21]

1.5. Treatment of Alzheimer's disease

The two major drug groups that have been approved by the United States Food and Drug Administration (US FDA) to treat AD are cholinesterase inhibitors (donepezil, rivastigmine and galantamine) and non-competitive NMDAR antagonists (memantine).[17] Cholinesterase inhibitors[62] and NMDARs aim to restore cognitive function in AD patients.[63]

Donepezil (Aricept), rivastigmine (Exelon) and galantamine (Reminyl)[62] are three cholinesterase inhibitors used as first-line treatment of mild-to-moderate AD (earlier stages: 1-4).[64] Acetylcholinesterase inhibitors inhibit the enzyme AChE thus preventing the rapid reduction in acetylcholine levels in the synaptic cleft thereby enhancing cholinergic neurotransmission.[35] Cholinesterase inhibitors have been shown to delay cognitive function decline and result in improved memory, thinking, language and a longer attention span.[17]

β-amyloids and tau-phosphorylation induces glutamate excitotoxicity and leads to synaptic dysfunction.[63,65] N-methyl-D-aspartate receptor mediates synaptic transmission and is

associated with cognitive functions such as learning and memory.[63] It is reported that in AD, abnormal NMDAR activity causes synaptic dysfunction.[63] Memantine (Namenda) is a non-competitive NMDAR antagonist that is used to treat moderate-to-severe AD (later stages: 5-7)[17,63] by preventing DNA fragmentation, neurite retraction, neuronal necrosis and the disruption of axonal transport trafficking.[65] Memantine, used in low doses, blocks chronic extra-synaptic NMDARs without impeding on synaptic NMDAR activity.[2] The non-competitive antagonist is reported to protect neurons from excitotoxicity,[66] and improves cognitive functions and behaviour of continuous usage.[67] The adverse effects of memantine are dizziness, headaches, confusion and agitation.[17] Memantine has no effect on β-amyloids; however, it reduces tau-phosphorylation and excitation.[65] A combination treatment of memantine and donepezil, Namzaric, is used to treat moderate-to-severe AD.[64]

Aducanumab is Aβ monoclonal antibodies (mAbs) which induce the clearance of Aβ, resulting in a reduction in amyloid plaques and hyperphosphorylated-tau.[68] The US FDA accelerated the approval of aducanumab due the trial's clinical benefit.[69] However, a post-approval trial is still required.[69]

Current AD treatment modalities only offer symptomatic relief as there is currently no cure. The drugs are accompanied by adverse effects such as abdominal cramps, nausea and vomiting, syncope and bradycardia rates, dizziness, headaches, confusion and agitation.[17] Current research studies are searching for new targets for AD drug therapy.

1.5.1. Combination therapies undergoing clinical trials

Combination therapy consists of combination and add-on trials.[70] With add-on trials, patients who are currently on standard-care are tested by comparing a new drug to a placebo.[70] With combination trials, the drugs of interest are tested individually, in combination with each other and with a placebo.[70] This is advantageous as these methods provide an indication of both individual and synergistic effects of the drugs.[70]

1.5.1.1. Add-on therapy

Studies are being conducted on drugs as 'add-on' to standard-care therapy.[70] These drugs are disease-modifying therapies (DMTs) which target Aβ, BACE-1, mAbs, tau protein, inflammation or other disease processes.[70]

Posiphen is drug currently being investigated to delay the onset or the progression of AD by blocking the production of APP in order to target Aβ.[71] Posiphen, which passes through the BBB, reduces Aβ, tau and inflammatory indicators in CSF tests.[71] Posiphen is still in phase 2 clinical trials.[72] A selective monoamine oxidase (MAO) inhibitor, rasagiline is currently in phase 2 trials. [73] Patients with mild-to-moderate AD are selected and this can be prescribed as an add-on to standard-care therapy of AChE or memantine.[70] Cleavage of APP is moderated by rasagiline by stimulating the non-amyloidogenic pathway thus, reducing the production of Aβ.[70] Rasagiline is also reported to have neuroprotective, anti-apoptotic effects, as well as mitochondrial protection.[70]

Beta-secretase APP-cleaving enzyme-1 cleaves APP which allows Aβ to form and accumulate.[74] Verubecestat (MK-8931) and atabecestat (JNJ-54861911) are drugs that inhibit BACE-1[70] and are administered orally in the form of a pill.[74] In phase 1 of the study, treatment with verubecestat decreased levels of Aβ.[15] However, verubecestat was discontinued as there was a poor positive risk-benefit ratio in patients with mild-to-moderate AD.[15,70] This suggests that patients that already have severe Aβ accumulation would be unlikely candidates for BACE-1 inhibition.[70] Thus, BACE-1 inhibition may work prior to Aβ accumulation with monotherapy in primary or early secondary prevention.[70] Atabecestat was undergoing phase 3 studies[71] trials were aborted the study due to an increase in liver enzymes, suggesting hepatotoxicity.[15,70] Elenbecestat (E2609) and umibecestat (CNP520) and are in phase 2 and 3 trials, respectively.[15] Individuals that are asymptomatic with increased levels of Aβ are tested using umibecestat (CNP520)[15] which is administered orally.[75]

Gantenerumab, and crenezumab are Aβ mAbs that are in the placebo-controlled phase 3 trials.[70] These drugs are tested on patients with early or mild AD.[70] Monoclonal antibodies induce the clearance of Aβ by binding to an immunological response towards AD.[70] Gantenerumab is currently in phase 3 trials[76] and is administered via subcutaneous injections.[77] Solanezumab and bapineuzumab in passive mAB immunisation studies exhibited positive results in earlier studies; however, bapineuzumab has been discontinued due to the lack of clinical benefits in

phase 3 trials.[70,75] However, solanezumab is currently in phase 3 trials.[75] The combination of solanezumab and gantenerumab is also in phase 3 trials.[70,75]

One of the drugs currently being researched is AADvac1 which targets abnormal tau protein. The clinical trials of the AADvac1 vaccine have been completed and the vaccine has been deemed safe in patients with mild AD, however, more in depth trials are being considered.[78] AADvac1 can be used as an add-on to an AChE inhibitor or memantine.[70] A reduction in tau levels was observed, however, there was no change in cognitive function,[78] it is therefore suggested that AADvac1 could halt the advancement of AD.[71]. The reversal or prevention of tau aggregation can be achieved via tau-aggregation inhibitors.[70] Methylene blue (TRx0237), a second generation tau-aggregation inhibitor is currently in phase 3 trials.[70,79] TRx0237 which is aimed at treating patients with mild-to-moderate AD, failed to produce clinical benefits.[70] However, it is speculated that patients who are not receiving standard-care therapy would benefit.[70] Thus, due to the post-hoc analyses, TRx0237 is favoured as a monotherapy treatment; however, further studies are required.[70]

Sargramostim is a drug developed to target inflammation.[71] The accumulation of Aβ in the brain triggers microglial cells which overstimulate inflammatory responses, thus, causing inflammation.[71] Patients with mild-to-moderate AD[70] are being recruited for trials with this drug. Sargramostim[80] is currently in phase 2 clinical trials,[80] and it has been found to stimulate the innate immune system.[71] Sargramostim can be used as an add-on drug to AChE inhibitors or memantine.[70] Neuroinflammatory pathways are targeted by masitinib (selective tyrosine-kinase inhibitor) which is a drug that incidentally controls pro-inflammatory mediators.[70] In a phase 2 trial, notable improvements in the cognitive scale and a mini-mental examination were observed when patients with mild-to-moderate AD were treated with either memantine or cholinesterase inhibitors in conjunction with masitinib as an add-on.[70] Although a placebo-controlled phase 3 trial has been completed,[70] the drug is still currently in phase 3 clinical trials.[80]

The 5HT6 receptor regulates the releases of neurotransmitters (such as ACh), The accumulation of Aβ and hyperphosphorylated-tau decreases serotonergic neurons,[81] thus reducing their availability.[71] Decline in these neurotransmitters may result in neuropsychiatric symptoms such as depression, agitation, aggression and anxiety.[70] By activating the 5HT6 receptor, the expected release of the neurotransmitters can restore normal functioning and communication between the neurons[71] to achieve as symptomatic therapy.[70] Pimavanserin is

an antagonist which binds to the 5-HT2A receptor which increases communication between neurons.[71] Dementia-related psychosis may be reduced.[71] Pimavanserin is in phase 3 of clinical trials.[82] Idalopirdine and intepirdine, selective 5HT6 antagonists, were tested in placebo-controlled phase 2 trials as an add-on drug to donepezil.[70] The combinations were found to improve cognition in AD patients, however, failed phase 3 trials in patients with mild-to-moderate AD.[70] Brexpiprazole is a second generation drug that is approved as an add-on treatment for depressive disorders.[70] Patients with mild-to-severe AD were selected for phase 3 trials targeting agitation.[70] The endpoints of the studies were not met; however, further studies are in the pipeline.[70]

1.5.1.2. Combination therapy

ALZT-OPT1 and Gamunex are DMTs that are currently undergoing phase 3 trials.[70] Patients with early AD are being selected for the ALZT-OPT1 trial.[70] ALZT-OPT is a combination of two agents; an anti-amyloid agent (cromolyn) and an anti-inflammatory agent (ibuprofen), which combats several pathological pathways.[70] There is structural similarity between cromolyn and other anti-amyloid agents, and the former has the ability to cross the BBB.[70] Cromolyn is administered nasally whereas ibuprofen is administered orally in the form of a pill.[70] Patients that are on standard-care treatment (AChE or memantine) can continue with their treatment as well as ALZT-OPT1, thus making ALZT-OPT1 an add-on option.[70] *In vitro* studies of cromolyn exhibited reduced Aβ, Aβ fibrilisation and oligomerisation,[70] and increased Aβ phagocytosis *in vivo*.[83]

The transport of Aβ from the blood to the brain is made possible by the receptor for advanced glycation end-products (RAGE); this receptor has become a possible drug target for the treatment of AD.[70] The inhibition of RAGE combats multiple pathways affecting AD such as neuroinflammation and the levels of Aβ.[70] Azeliragon, a RAGE inhibitor, failed phase 3 trials and was discontinued as treatment did not exhibit cognitive or functional improvement in patients.[70]

1.5.2. Herbal remedies

Treatments that are currently available only serves as palliative care by managing the symptoms of AD which causes limitations to treating the disease itself.[45] Due to these limitations and adverse effects, studies on alternative treatments are being executed.[45] Herbal remedies, such as those that are antioxidant and flavonoid rich, are being studied through *in vivo* and *in vitro* models.[45] There are various classes of phytochemicals that have neuroprotective effects in AD, which include; steroidal, alkaloidal, terpenoidal, and phenolic phytochemicals.[45] *Dioscorea nipponica* (steroidal sapogenin; diosgenin), *Coptis chinensis* (alkaloid; berberine), *Panax ginseng* (terpenoid; ginsenoside Rg3) and *Camellia sinensis* (phenol; epigallocatechin-3-galate) are a few examples of the various plants and their respective phytochemicals.[45] These plants have been reported to prevent the formation of inflammatory factors (i.e., MCP-1, TNF-α and NO and inhibits the MAPK/ NF-κB and p38 pathway) by way of its anti-neuroinflammatory and neuroprotective properties.[45]

Centella asiatica (Gotu Kola), is traditionally used in Chinese and Ayurvedic medicine to enhance cognitive function.[84] *B*oth *in vivo* and *in vitro* studies have indicated neuroprotective and cognitive enhancing effects of the plants.[84] In 5xFAD mice, improved cognitive performance, induced expressions of both antioxidant and mitochondrial response genes and improved hippocampal mitochondrial function were observed due to reduced levels of Aβ in the hippocampus induced by the plant extract.[84]

The mushroom, *Hericium erinaceus*, is reported to have anticarcinogenic, antibiotic, antidiabetic, antifatigue as well as neuroprotective properties.[85] *Hericium erinaceus* is also reported to alleviate anxiety and depression, and assist with cognitive function.[85] An *in vivo* rat model indicated antioxidant activity through the inhibition of ROS production.[85] Furthermore, the nerve growth factor in *in vitro* astrocytes was found to be stimulated by *H. erinaceus*.[85]

1.6. Models used to investigate Alzheimer's disease pathogenesis and pathology

1.6.1. *In vivo* models for Alzheimer's disease

Alzheimer's disease is a progressive disorder which occurs over many years,[11] and the majority of the AD cases are caused by sporadic AD or LOAD.[86,87] Rodents are used in *in vivo* models for AD studies,[87,88] however, these models are based on FAD instead of LOAD.[21,88] The disadvantage arises when treatments are successful in mouse models affected by FAD, but are unsuccessful when tested in patients with LOAD.[87,88] There are ethical constraints when conducting tests using humans and/or human samples, thus the use of *in vivo* models allows for the analysis of certain aspects of AD not otherwise possible.[21,88] Unfortunately, animal models are limited to one or two aspects to be studied at a time.[87,88] During the AD timeline in a human brain, neuronal loss occurs which leads to an increase in brain atrophy.[88] Unfortunately, rodents have a short lifespan and as such extensive neuronal loss does not occur.[87] Neuronal loss can be induced into a transgenic mouse model by eliminating doxycycline from the test animals' diet,[88] as doxycycline has been reported to decrease neuroinflammation and increase BDNF in the neurons.[89]

Cognitive decline in humans occurs due the accumulation of Aβ plaques, tau-hyperphosphorylation and neuronal loss.[88] However, cognitive decline in rodent models is observed before the presence of Aβ plaques.[88] Transgenic mice with mutant APP produce Aβ.[87,88] The Aβ plaques formed by both humans and rodents are morphologically comparable; however, the biochemical composition of Aβ differs.[21] The formation of NFTs occurs in humans with AD, but not in rodent models; reasons for this may be due to tau being structurally different in rodents and/or not having adequate time for NFTs to form due to the short life span of rodents.[88] Mutated APP, tau and PS1 have been developed into the 3xTg-AD mouse model.[88] The strains of rodents used for *in vivo* studies show different characteristics for example, C57/Bl6 shows resistance to excitotoxicity.[88]

Neuroinflammation may occur prior to Aβ formation and/or accumulation.[90] It is reported that, IL-1β and IL-6 were detected in transgenic mice after microglial stimulation.[91] The mice were three months old at the time of IL-1β and IL-6 detection and had not yet produced Aβ.[91] Expressions of monocyte chemoattractant protein-1 (MCP-1) and TNF-α in the entorhinal cortex, has been detected in three-month old 3xTg mice.[92] The authors found that the formation and the ultimate accumulation of intracellular Aβ correlated with the increased expressions of

the cytokines and chemokines, although, extracellular Aβ formation only occurred at twelve-months of age.[92]

In vivo studies are more expensive[93] and time-consuming than *in vitro* studies.[94] Furthermore, *in vivo* testing is laborious and variability from animal-to-animal exists which leads to difficulties in reproducing results.[95]

1.6.2. *In vitro* models for Alzheimer's disease

In vitro studies are more cost effective and less labour intensive than *in vivo* studies, and allows for large-scale production of cell cultures to facilitate analysis.[96] Neuronal cell lines, such as the rat PC12 and B35 cells, mouse Neuro-2A cells, induced-pluripotent stem cells (iPSCs)[97] and SH-SY5Y human neuroblastoma cells are available for *in vitro* AD.[98]

These rodent cell lines have the ability to proliferate and differentiate on their own accord to mature neurons, which express markers such as neurofilament protein and glial fibrillary acid protein.[99] The disadvantages of using cell lines derived from rodents is that the Aβ formed by the cells do not form fibrils as in the adult human brain,[99] and the results obtained from these cells may not necessarily have a similar outcome to that found in a human-derived cell line, as the differences in gene expression across species are vast.[100] As mentioned earlier, spatial elements of AD exists as pathology of different regions of the brain occur temporally.[28] This aspect of AD is not expressed in *in vitro* studies.[28]

IPSCs are derived from primary human fibroblasts specific to FAD.[99] However, as stated above, this is a disadvantage as the majority of the AD cases are caused by sporadic AD or LOAD.[86] Induced-pluripotent stem cells are able to differentiate into many cell types, neurons being one of them.[93,101] The neurons that are derived from these stem cells are electrically active[101] and form a synaptic network thus recapulating neurons in the human brain.[93,102] Another disadvantage of iPSCs is the inability to mimic the biological aging *in vitro* as AD is a progressive disorder that occurs over many years.[101] Induced-pluripotent stem cells have a large likelihood of mutating.[97]

The SH-SY5Y cell line which originated from a human neuroblastoma patient,[103] can be differentiated into mature neurons which are capable of expressing human-specific

proteins.[98,104] The SH-SY5Y cells are also able of producing phenotypically homogenous cells with a uniform genetic background. The SH-SY5Y cells are chromosomally stable cells.[98] Primary SH-SY5Y cells are immature and possess an epithelial-like phenotype,[103] which lacks important neuronal markers that would be representative of an accurate model (Table 2).[97,98] Differentiation mediates the transition from a primary SH-SY5Y state of cells to a neuronal phenotype which possesses branched neuritic processes that connect to other cells, and possess neuronal markers that are present in mature cells (Table 2).[97,98]

Retinoic acid (RA), dibutyryl cyclic AMP (db-cAMP)[98] and BDNF are used to differentiate SH-SY5Y cells.[97,98,105] Retinoic acid is a powerful differentiation factor,[106] which differentiates cells by seizing the cell cycle at Gap 0/Gap 1 (G0/G1), stimulating phosphatidylinositol 3-kinase/protein kinase B (PI3K/Akt) activity,[97] or by intensifying cyclin-dependent kinase inhibitors and apoptotic proteins.[98] Treatment with RA reduces cellular proliferation, thus lowering the population growth and allowing for even distribution.[106] The SH-SY5Y cells present longer, thicker neurites, and exhibit a more neuronal phenotype when treated with a combination of RA and BDNF.[97,106] Brain-derived neurotrophic factor is a neurotrophin which further enhances neuronal differentiation.[97,98] Absence of BDNF induces cellular apoptosis, thus BDNF allows longer cell survival and withdrawal from the cellular cycle.[98] Dibutyryl cyclic adenosine monophosphate enhances neurite extension.[98]

Table 2: Characteristics of undifferentiated versus differentiated SH-SY5Y cells.[97,98,105]

	Undifferentiated Cells	**Differentiated Cells**
Proliferation	Rapid	Decreased proliferation
Phenotype	• Large, flat epithelial-like • Few, short processes • Grow in clumps	• Reduced cell clumping • Long, branched processes • Connecting neuritic processes
Markers	Express immature neuronal markers • Proliferating cell nuclear antigen (PCNA) • Nestin • Differentiation inhibiting basic helix-loop-helix transcription factors (ID-1, ID-2, ID-3)	Express mature neuronal markers • Growth-associated protein • Neuronal nuclei • Synaptophysin • Synaptic vesicle protein II • Neuron specific enolase (NSE) • Microtubule-associated protein (MAP2) • βIII-tubulin • β-site amyloid precursor protein-cleaving enzyme 1 (BACE-1) • Amyloid precursor protein (APP)

The addition of neurotoxins in *in vitro* assays allows the pathological hallmarks of AD to be studied.[107] Metals such as zinc, iron and aluminium are known to promote Aβ aggregation, result in toxicity and lead to neuronal cell death.[107] Mercury[108] and cadmium exposure have also been found to increase the levels of Aβ.[107] Furthermore, iron, cadmium and aluminium also stimulate GSK-3β kinase which results in tau-hyperphosphorylation *in vitro*.[107]

Higher cholesterol levels are associated with the increased risk of dementia in older adults[109] by binding to the C99 terminus of APP which promotes Aβ formation.[110] *In vitro* studies have shown that SH-SY5Y cells exposed to low-density lipoproteins (LDL) decrease cell viability,[111] increase the activity of APP and BACE-1, and induce Aβ formation.[112]

1.7. Project overview

A cure for AD is yet to be discovered as the current AD treatments available only serve as palliative care by managing the symptoms and are associated with uncomfortable adverse effects.[17] Alternative therapies are being investigated as possible effective treatments.[45] However, this requires potential drug leads to be tested on a viable in-house *in vitro* model of AD. Thus, in an attempt to make a more mature phenotypic representation of SH-SY5Y cells, differentiation processes need to be assessed,[98] as well as *in vitro* neurotoxicity parameters. The differentiation process is expected to produce viable, homogenous, differentiated mature neuronal cultures. Evaluating different differentiation protocols is required in order to select which one provides the best *in vivo* representative model.

1.8. Study aim and objectives

The aim of the study was to compare two differentiation protocols of SH-SY5Y neuroblastoma cells for the purpose of developing an *in vitro* AD drug platform.

The objectives of the study were to compare a six- and eighteen- day SH-SY5Y differentiation protocol to select the most representative model with relevance to a mature neuronal phenotype, as defined by:

- Morphological changes by light microscopy;

- ACh and AChE levels by fluorescence assay kits;
- Cellular density by sulforhodamine B (SRB) colourimetric assay;
- Protein content by bicinchoninic acid (BCA) assay;
- Cellular viability by fluorescein diacetate/ propidium iodide (FDA/PI) staining; and
- Mature (APP and BACE-1) and immature (PCNA) neuronal biomarkers by flow cytometry.

Chapter 2 Materials and methods

Ethical approval (212/2018) for the project was obtained from the Research Ethics Committee of the Faculty of Health Sciences, University of Pretoria (Appendix I). All reagents used, including their preparation, are listed in Appendix II.

2.1. Cell culture and maintenance

SH-SY5Y neuroblastoma cells (ATCC® CRL-2266™) were gifted from the North-West University. Cells were cultured in 75 cm^2 flasks with Dulbecco's Modified Eagle's Medium (DMEM)/Ham's F12 (1:1) medium (Sigma-Aldrich, USA), supplemented with 10% heat-inactivated foetal bovine serum (FBS; Thermo Fisher, Massachusetts, USA) and 1% penicillin/streptomycin (Sigma-Aldrich, USA) at 37°C in a humidified atmosphere of 5% carbon dioxide (CO_2). Cells were washed as needed with phosphate-buffered saline (PBS; Sigma-Aldrich, USA) to remove any debris, and medium was exchanged.

Once confluent (between 80 and 90%), medium was discarded, and cells washed with PBS. Cells were enzymatically detached using TrypLE express solution (Thermo Fisher, USA), and collected using centrifugation at 200 *g* for 5 min. Pelleted cells were resuspended in 1 mL DMEM/Ham's F12 medium and were counted using the trypan blue (0.1% w/v in PBS) exclusion assay. Cells were diluted to 1×10^5 cells/mL in 10% FBS-supplemented medium.

2.2. Cellular differentiation

Cells were differentiated to establish a more mature neuronal phenotype. Various models of differentiation are available, though downstream implications relevant to in-house needs are not ascertained. Given the purpose of the cellular model, it is imperative to assess which would be most representative. Two methods were compared for their ability to yield differentiated cells: a six-day and an eighteen-day differentiation procedures by Forster *et al.*[105] and Shipley *et al.*,[98] respectively.

2.2.1. Cellular density optimisation

For the six-day differentiation method, cells were seeded at 85 × 10^3 cells/well according to the methods of Forster *et al.*,[105] however, this resulted in cellular clumping in this study which is discussed in Section 3.1. A pilot study for the six-day differentiation method (Section 2.2.2) was carried out to determine the seeding density of cells/well. Cells were cultured as stated in Section 2.1 and were seeded at 75 × 10^3 cells/well, 80 × 10^3 cells/well and 85 × 10^3 cells/well. Wells seeded with 85 × 10^3 cells/well and 80 × 10^3 cells/well exhibited 90% confluence in the wells which resulted in cells forming clusters, whereas wells seeded with 75 × 10^3 cells/well exhibited 80% confluence, thus allowing the cells to transform into a colony of connecting neurons (Section 3.1). A seeding density of 75 × 10^3 cells/well was selected for the six-day differentiation process.

According to the methods of Shipley *et al.*,[98] cells were seeded at 1 × 10^5 cells/well and included two passaging steps that occurred on Days 7 and 10 of the eighteen-day cycle. This resulted in a lower cellular density with single neurons present instead of the expected colonies of neurons (Section 3.1). A pilot study for the eighteen-day differentiation method (Section 2.2.3) was carried out to determine the seeding density of cells/well. Cells were cultured as stated in section 2.1 and were seeded at 7 × 10^4 cells/well and 85 × 10^3 cells/well. In addition, the passaging step on Day 7 was eliminated, leaving one passaging step (Day 10). Colonies of connecting cells were produced by eliminating one passaging step and by seeding the cells at 85 × 10^3 cells/well (Section 3.1). The latter was selected for the eighteen-day differentiation process.

2.2.2. Six-day differentiation

The six-day differentiation method of Forster *et al.*[105] was followed with modification to the volumes and seeding density used. Two phases of differentiation took place using phase I and II medium. Phase I medium consisted of DMEM/Ham's F12 (1:1 v/v), 1% penicillin/streptomycin, 5% FBS and RA (10 µM; added immediately before use; Sigma-Aldrich, USA). Phase II medium consisted of neurobasal medium (Thermo Fisher, USA) supplemented with penicillin/streptomycin (1%), GlutaMAX (2 mM; Thermo Fisher, USA),

N-2 supplement 100x (1%; added immediately before use; Thermo Fisher, USA) and BDNF (50 ng/mL; added immediately before use; Sigma-Aldrich, USA). The SH-SY5Y cells (75 × 10^3 cells/well) were cultured in 6-well plates (Sigma-Aldrich, USA) for three days in phase I medium, after which medium was replaced with phase II medium for three days (Figure 10). A total volume of 3 mL of the respective medium was added per well.

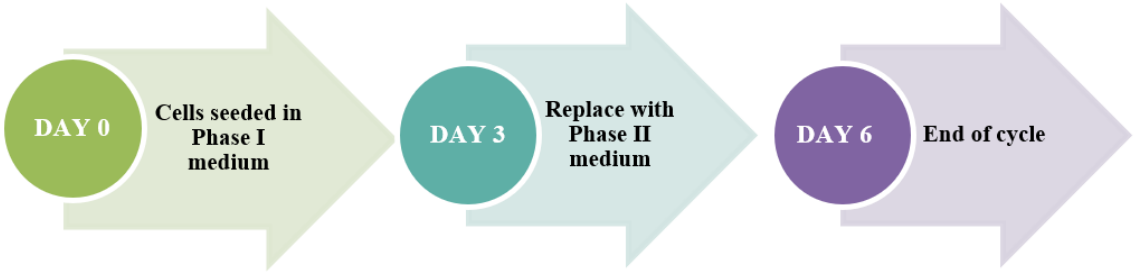

Figure 10: The six-day differentiation cycle was used to differentiate SH-SY5Y cells from an immature phenotype to a mature phenotype.

2.2.3. Eighteen-day differentiation

The eighteen-day differentiation method of Shipley *et al.*[98] was followed with modification to the volumes used. The SH-SY5Y cells (85 × 10^3 cells/well) were cultured in 6-well plates.

Various cell culture mediums were used to ensure differentiation of the cells; standard medium, differentiation medium I, differentiation medium II and differentiation medium III. Standard medium consisted of DMEM/Ham's F12 (1:1 v/v), 1% penicillin/streptomycin and 10% FBS. Differentiation medium I consisted of DMEM/Ham's F12 (1:1 v/v) medium supplemented with 2.5% FBS, 1% penicillin/streptomycin and 10 µM RA (added immediately before use). Differentiation medium II consisted of DMEM/Ham's F12 (1:1 v/v) medium supplemented with 1% FBS, 1% penicillin/streptomycin and 10 µM RA (added immediately before use). Differentiation medium III consisted of neurobasal medium supplemented with B27 supplement (1:50 v/v; Thermo Fisher, USA), potassium chloride (20 mM; Sigma-Aldrich, USA), GlutaMAX (2 mM; Thermo Fisher, USA), penicillin/streptomycin (1%), db-cAMP (2 mM; Sigma-Aldrich, USA), BDNF (50 ng/mL; added immediately before use; Sigma-Aldrich, USA), RA (10 µM; added immediately before use). Cells (85 × 10^3 cells/well) were seeded

(Day 0) in 6-well plates in standard culture medium (total volume of 3 mL per well). Standard medium was replaced with differentiation medium I on Days 1, 3, 5 and 7.

On Day 8, differentiation medium I was replaced with differentiation medium II. On Day 9, an extracellular matrix (ECM; Sigma-Aldrich, USA) mixture (2 mL) was added to a new 6-well plate as a coating, and incubated at 37°C under 5% CO_2 for 1 h. The ECM mixture was aspirated, and the cells were split at a 1:1 ratio onto ECM-coated plates (Day 10) in differentiation medium II. On Days 11, 14 and 17, medium was replaced with differentiation medium III. Day 18 was taken as the end of differentiation (Figure 11).

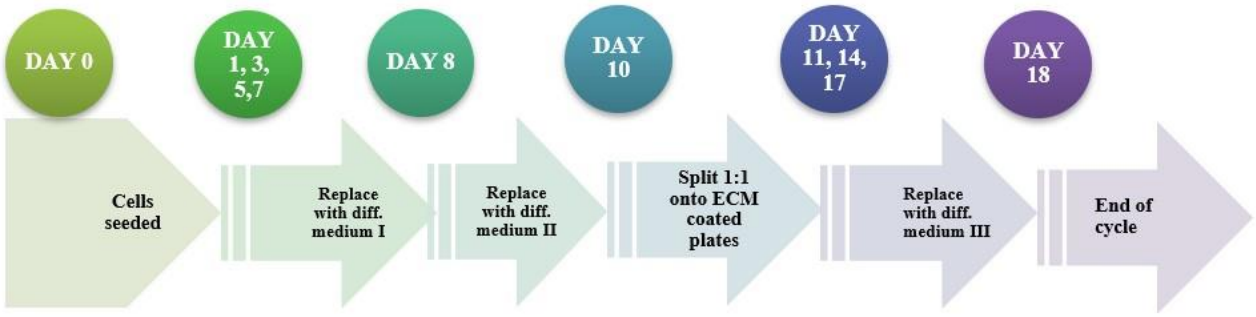

Figure 11: The eighteen-day differentiation cycle was used to differentiate SH-SY5Y cells from an immature phenotype to a mature phenotype. Differentiation (Diff); Extracellular matrix (ECM).

The most representative differentiation model as surrogate for a mature phenotype was determined by assessing various endpoints.

2.3. Differentiation endpoint assessment methods

2.3.1. Light microscopy

Light microscopy (Zeiss Axiovert CFL40 microscope, Zeiss Axiovert MRm monochrome camera, Axiovert 40 CFL microscope; Zeiss, Oberkochen, Germany) images of the cells were taken during the differentiation process at 20X magnification. Images were taken on Days 1, 3 and 6 (six-day differentiation), and Days 1, 8, 10, 11 and 18 (eighteen-day differentiation). Axiovision software was used to analyse the micrographs of the cells. Morphological signs of differentiation in SH-SY5Y cells such as a reduction in cell clumping and long, branched neuritic processes which connect to surrounding cells, were monitored.

2.3.2. Acetylcholine assay

A fluorescence assay was used to assess the levels of ACh and AChE activity. Acetylcholine is converted to choline by AChE.[113] Hydrogen peroxidase is then produced by the oxidation of choline which produces resorufin.[113] Resorufin is a fluorescent product used in both ACh and AChE assay kits (Thermo Fisher, USA, A12217), which is formed as a result of an enzymatic reaction between the Amplex Red reagent and hydrogen peroxide (H_2O_2) in the presence of horseradish peroxide (HRP).[113] Acetylcholine levels were measured using the method provided by Molecular Probes Incorporated.[113]

The supernatant and cell lysates of undifferentiated and differentiated SH-SY5Y cells were used to quantify ACh levels. The supernatants and cell lysates of undifferentiated cells were taken on day 1 of both six- and eighteen-day differentiation processes and the supernatant and cell lysates of differentiated cells were taken at the end of both six- and eighteen-day, respectively of the differentiation cycles. The SH-SY5Y cells and the supernatant were separated through centrifugation (1,500 *g* for 5 min), collected and stored separately at -80°C until analysed. The samples were prepared by diluting 50 µL supernatant or 50 µL cell lysate with 50 µL 1X reaction buffer. The working solution contained 200 µL Amplex Red reagent (400 µM), 100 µL HRP (2 U/mL), 100 µL choline oxidase (0.2 U/mL), 100 µL AChE (1 U/mL) and 9.5 mL reaction buffer (1X). Hydrogen peroxide (10 µM) and ACh (50 µM) were used as positive controls, and reaction buffer (1X) was used as a negative control. The samples consisted of reaction buffer, the positive control, and the negative control, which were plated (100 µL) in triplicates into respective wells of a 96-well white microplate. The working solution (100 µL) was added to the wells to initiate the reaction. Plates were incubated for 30 min at room temperature in the dark. The fluorescence was measured using a fluorescence microplate (Synergy II, BioTek instruments Inc, Highland Park, USA) reader set at an excitation wavelength of 544 nm and emission wavelength of 590 nm.

The ACh fluorescence values were normalised relative to the average protein concentration of the samples (Section 2.3.6). The ACh levels were then calculated relative to the undifferentiated samples. The fold-change of ACh concentration was calculated based on the formula:

$$ACh\ (fold-change) = \frac{ACh\ of\ differentiated\ samples}{ACh\ of\ undifferentiated\ samples}$$

2.3.3. Acetylcholinesterase assay

Acetylcholinesterase levels were measured using the method provided by Molecular Probes Incorporated (A12217).[113] The supernatant and cell lysates of undifferentiated and differentiated SH-SY5Y cells were used to detect AChE levels. The samples were prepared as described in Section 2.3.2. The working solution contained 200 µL Amplex Red reagent (400 µM), 100 µL HRP (2 U/mL), 100 µL choline oxidase (0.2 U/mL), 10 µL ACh (1 U/mL) and 9.5 mL reaction buffer (1X). Hydrogen peroxide (10 µM) and AChE (0.2 U/mL) were used as positive controls and reaction buffer (1X) was used as the negative control. The diluted samples and controls were plated into 96-well plates as in Section 2.3.2. The working solution (100 µL) was added to the wells to start the reaction. Plates were incubated for 30 min at room temperature in the dark. The fluorescence was measured using a fluorescence microplate (Synergy II, BioTek instruments Inc, Highland Park, USA) reader set at an excitation wavelength of 544 nm and emission wavelength of 590 nm.

The AChE fluorescence values were normalised relative to the average of protein concentration of the samples (Section 2.3.6). The AChE levels were then calculated relative to the undifferentiated samples. The fold-change of AChE concentration was calculated based on the formula:

$$AChE\ (fold-change) = \frac{AChE\ differentiated\ samples}{AChE\ of\ undifferentiated\ samples}$$

2.3.4. Sulforhodamine B assay

Cellular density was determined using the SRB colourimetric assay.[114] The assay is performed on cells fixed with trichloroacetic acid (TCA).[114] Under mildly acidic conditions, SRB (bright-pink dye) binds to basic protein amino acid residues, and is released when alkalinised.[114] There is a direct relationship between the amount of dye that binds to the fixed proteins to the density of cells as SRB binds stoichiometrically.[114,115]

Differentiated and undifferentiated cells were subjected to the SRB assay. In order to fix the cells to the bottom of the plate, 1 mL TCA solution (50%; Sigma-Aldrich, US) was added to

each well and then incubated overnight at 4°C. Post incubation, the plate was washed thrice under running tap water and dried in the oven. Once dried, 1 mL SRB stain solution (0.057%; Sigma-Aldrich, USA) was added to each well. The plate was incubated for 30 min at room temperature, after which the wells were washed three times with 1 mL acetic acid solution (1%; Merck chemicals, South Africa) and dried in the oven. Once dried, 1 mL TRIS-buffer solution (10 mM; pH 10.5; Sigma-Aldrich, USA) was added to each well. The plate was placed on a shaker for 1 h. A spectrophotometer, ELX800UV microplate reader (BioTek instruments Inc, Highland Park, USA) was used to determine the absorbance of the plate, at a wavelength of 540 nm and a reference wavelength of 630 nm.

The fold-change of cellular density was calculated based on the formula:

$$Cellular\ density\ (fold-change = \frac{Absorbance\ of\ differentiated\ cells}{Average\ absorbance\ of\ undifferentiated\ cells}$$

2.3.5. Fluorescein diacetate/propidium iodide staining

Differentiated cells were subjected to the live-dead fluorescein diacetate/propidium iodide (FDA/PI) staining. Fluorescein diacetate is converted to fluorescein, a compound with green fluorescence in the cytoplasm by de-acetylating FDA using non-specific esterases.[116] Propidium iodide is impermeable to in-tact membranes.[117,118] Fluorescein diacetate stains viable cells green by converting FDA to fluorescein under blue light, and PI stains membrane-compromised/dead cells red.[119,120]

The differentiated and undifferentiated cells were rinsed with PBS and 1 mL FDA/PI staining solution. The stained cells were incubated at room temperature for 5 min in the dark. The cells were washed two to three times with PBS in order to remove the excess dye. The stained cells were analysed using a Zeiss Axiovert CFL40 microscope, Zeiss Axiovert MRm monochrome camera, Axiovert 40 CFL microscope (Zeiss, Oberkochen, Germany) set at an excitation wavelength of 488 nm and emission wavelength of 530 nm for FDA, and at an excitation wavelength of 540 nm and emission wavelength of 625 nm for PI. ImageJ was used to analyse and create composite micrographs of the cells.

2.3.6. Bicinchoninic acid protein assay

Protein content was assessed using a sensitive, colourimetric BCA protein assay.[121,122] During this process copper (II) ions are reduced to copper in an alkaline medium which forms a purple solution when it reacts with BCA.[121] Bicinchoninic acid protein assays is the most used method to determine the protein concentrations of an unknown sample.[122] The intensity of the colour (deep violet/purple being the most intense) that is produced depends on the amount of protein present in the sample.[123] The BCA assay was carried out in order to determine the change in protein concentration between undifferentiated and differentiated cells.

Differentiated and undifferentiated cells were collected through trypsinisation and washed with PBS and centrifuged (200 *g*, 5 min). The supernatant of the differentiated and undifferentiated cells was collected and centrifuged at 200 *g* for 5 min. Radio-immunoprecipitation assay (RIPA) buffer (150 µL) was used to lyse the cells on ice for 5 min, whereafter they were centrifuged at 16 000 *g* for 10 min. The supernatant was collected, and the samples were stored at -80°C till analysis.

Samples (5 µL) and BCA solution (100 µL) were added to a 96-well plate. The sample consisted of either RIPA buffer (blank), bovine serum albumin (BSA; dilutions of 2.5 mg/mL) standard, lysate or supernatant. Plates were shaken for 10 min at room temperature, then covered with foil and incubated at 37°C for 30 min. Plates were cooled to room temperature, and read spectrophotometrically using an ELX800UV microplate reader (BioTek instruments Inc, Highland Park, USA) at 562 nm.

The protein concentrations of the cells were interpolated using linear regression obtained from the BSA standard curve. The fold-change in protein content (protein content [mass] per sample) was calculated by dividing the protein concentration of differentiated cells by the protein concentration of undifferentiated cells. The fold-change of protein concentration was calculated based on the formula:

$$Protein\ content\ (fold-change) = \frac{Protein\ content\ of\ differentiated\ cells}{Protein\ content\ of\ undifferentiated\ cells}$$

2.3.7. Flow cytometry

The expression of cell surface and intracellular molecules can be analysed by flow cytometry.[124] Flow cytometry is most used to sort cells for further testing.[125] The proteins of interest are stained with a fluorophore and detected individually when the targeted proteins emit light after being excited by a laser.[124] Cell populations can be identified by their characteristics via fluorescent and scattered light signals (forward and side scatter).[125] The detection of mature neuronal biomarkers such as APP and BACE-1 is indicative that the cells have differentiated. The presence of the immature marker (PCNA) is indicative of undifferentiated cells. A series of fluorophore conjugated antibodies are described in Appendix II.

2.3.7.1. Positive control and method optimisation

The positive control for flow cytometry was established by following the four-day differentiation by treatment of RA on SHSY-5Y cells by Lv *et al.*[126] Cells were cultured as described in Section 2.1. Standard medium consisted of DMEM/Ham's F12 (1:1 v/v) medium which was supplemented with 1% penicillin/streptomycin and 10% FBS. Medium 1 consisted of DMEM/Ham's F12 (1:1 v/v) medium supplemented with 10% FBS, 1% penicillin/streptomycin and 10 µM RA (latter compound added immediately before use). The SH-SY5Y cells (80 x 10^3 cells/well) were seeded (day 0) in 6-well plates in standard medium, after which medium was replaced with medium 1 (day 1) for four days (Figure 12). A total volume of 3 mL of the respective medium was added per well. The cells were then analysed via flow cytometry using a CytoFLEX V5-B5-R3 Flow Cytometer (Beckman Coulter, Inc, Indianapolis, USA) on day 4.

Figure 12: The differentiation cycle for the positive control.

The cells from three wells of the same population were pooled, centrifuged at 200 *g* for 5 min and resuspended in 1 mL DMEM/ Ham's F12 (1:1) medium. Cell suspension (140 µL) was added to all flow tubes (i.e. cells-only, APP-only, BACE-1-only, PCNA-only and a combination tube). A combination tube contained all the antibodies (anti-APP, anti-BACE-1 [Sigma-Aldrich, USA] and anti-PCNA [Miltenyi Biotec, Germany]) that were tested. Anti-APP antibody (2 µL) was added to each APP-only and combination flow tubes. All flow tubes were incubated for 30 min, after which the cells were washed once with PBS (2 mL), centrifuged at 200 *g* for 5 min and aspirated. The cells in all flow tubes were resuspended with formaldehyde (100 µL) and incubated for 30 min. The cells were washed once with PBS (1 mL), centrifuged at 200 *g* for 5 min and aspirated. Permeabilization buffer (200 µL) was added to each flow tube except the tube containing APP-only. Anti-BACE-1 (1 µL) and anti-PCNA (2 µL) were added to their individual and combination flow tubes and incubated at room temperature for 30 min in the dark. The cells were washed once with PBS (1 mL), centrifuged at 200 *g* for 5 min and aspirated. The cells were resuspended in PBS (500 µL) and analysed via flow cytometry using a CytoFLEX V5-B5-R3 Flow Cytometer (Beckman Coulter, Inc, Indianapolis, USA).

2.3.7.2. Mature and immature protein detection

Once the positive control was established, flow cytometry was employed to assess protein content. The cells from three wells of the same population (i.e. undifferentiated, six- and eighteen-day differentiated cells) were pooled, centrifuged at 200 *g* for 5 min and resuspended in 1 mL DMEM/ Ham's F12 (1:1) medium. Cell suspension (140 µL) was added to 'cells only' which acted as the control, and 'Combination' flow tubes. Combination tubes contained all the antibodies (anti-APP, anti-BACE-1 and anti-PCNA) that were being tested. Anti-APP antibody (2 µL) was added to the combination flow tube. The 'cells only' and combination flow tubes were incubated for 30 min, after which the cells were washed once with PBS (2 mL), centrifuged at 200 *g* for 5 min and aspirated. The cells were resuspended with formaldehyde (100 µL) and incubated for 30 min. The cells were washed once with PBS (1 mL), centrifuged at 200 *g* for 5 min and aspirated. Permeabilization buffer (200 µL) was added to each flow tube. Anti-BACE-1 (1 µL) and anti-PCNA (2 µL) were added to the combination flow tube and incubated at room temperature for 30 min in the dark. The cells were washed once with

PBS (1 mL), centrifuged at 200 *g* for 5 min and aspirated. The cells were resuspended in PBS (500 µL) and analysed via flow cytometry using a CytoFLEX V5-B5-R3 Flow Cytometer (Beckman Coulter, Inc, Indianapolis, USA).

2.4. Statistics

All experiments were carried out in triplicate on at least three different occasions. Statistical changes were analysed using GraphPad Prism 5.0. The Student's t-test was employed for comparisons between the undifferentiated and differentiated samples. Data is expressed as the mean ± SEM. Significance was set at $p < 0.05$.

Chapter 3 Results and discussion

3.1. Method optimisation

3.1.1. Seeding density

Optimisation of seeding density was undertaken in order to ensure that cultures remained viable through the differentiation period up until the day of analysis. The pilot study for the six- and eighteen-day differentiation methods was performed using six-well plates.

3.1.1.1. Six-day differentiation

To implement the six-day differentiation protocol, the method by Forster *et al.*[105] was followed with modifications to the seeding density, where the cells were seeded in a six-well plate at a density of 30×10^4 cells/well. As this seeding density was too high, the cells had reached confluence to the point of being overgrown and thus detached (not shown).

For the six-day differentiation method, wells were seeded with 85×10^3 cells/well, 80×10^3 cells/well and 75×10^3 cells/well. Densely packed cells were noted in wells seeded with 85×10^3 cells/well (Figure 13A) and 80×10^3 cells/well (Figure 13B), whereas wells seeded with 75×10^3 cells/well (Figure 13C) indicated diffusely spread cells. No cell clumps were noted in the wells seeded with 75×10^3 cells/well, however, cell clumping was evident in wells seeded at the higher densities. Cellular debris was evident in the wells seeded with 85×10^3 cells/well (Figure 13A) which was ascribed to overgrowth in the wells. As the seeding density of 75×10^3 cells/well did not result in overgrowth or clumping of the cells in the wells, this seeding density was selected for further experimentation in the six-day differentiation method.

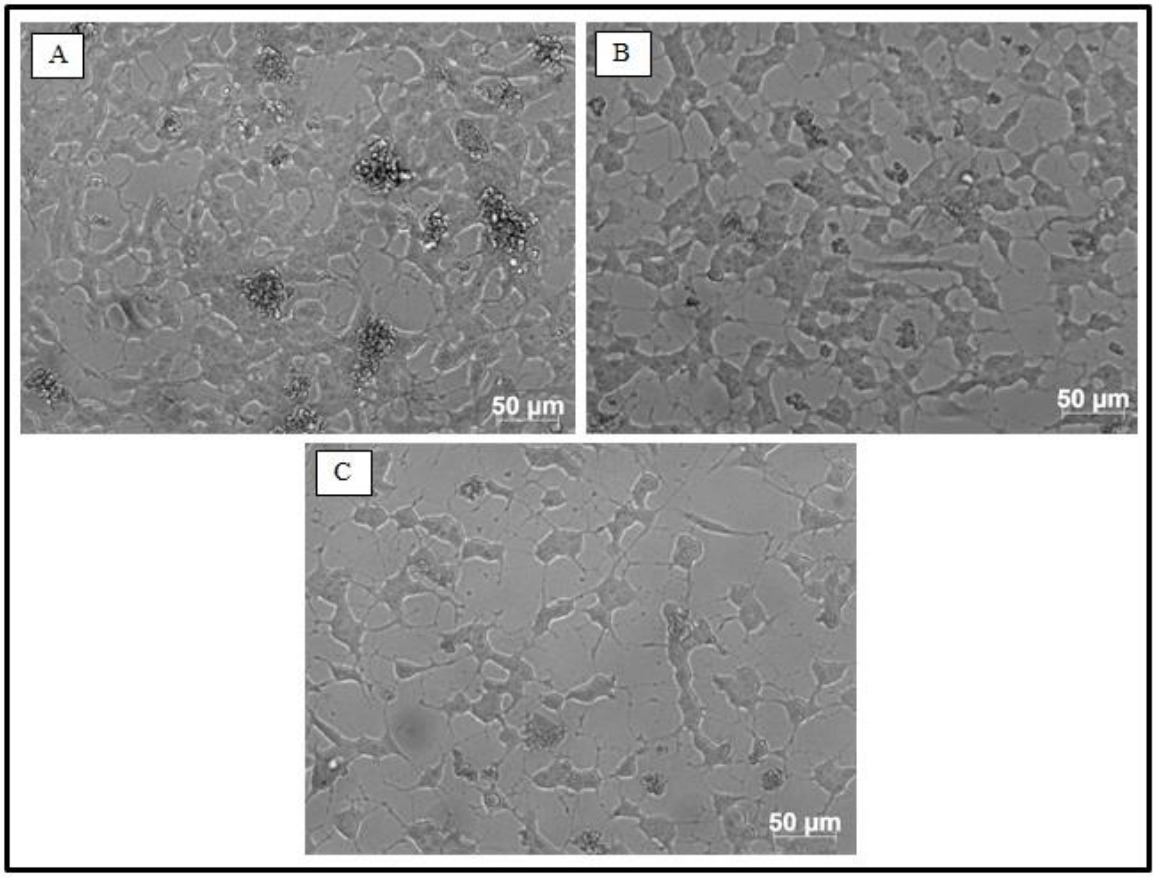

Figure 13: Photomicrographs of SH-SY5Y cells at the end of the six-day differentiation cycle. SH-SY5Y cells were seeded at a density of 85 × 10^3 cells/well (A), 80 × 10^3 cells/well (B) and 75 × 10^3 cells/well (C). [20X magnification]

3.1.1.2. Eighteen-day differentiation

To implement the eighteen-day differentiation protocol, the method by Shipley *et al.*[98] was followed with modifications to the seeding density and the frequency of cell passaging, where the cells were seeded in six-well plates at a density of 1 × 10^5 cells/well and was passaged twice (Days 7 and 10). This resulted in a low cellular density with single neurons rather than expected colonies of neurons (Figure 14A). To resolve this, the seeding density was reduced to 85 × 10^3 cells/well. Additionally, the trypsinisation step on Day 7 was omitted. This resulted in a decrease of cell death, with more time for cells to multiply before they needed to be transferred to new ECM-coated plates, and ultimately colonies of connecting neurons were produced at the end of the differentiation process (Figure 14B).

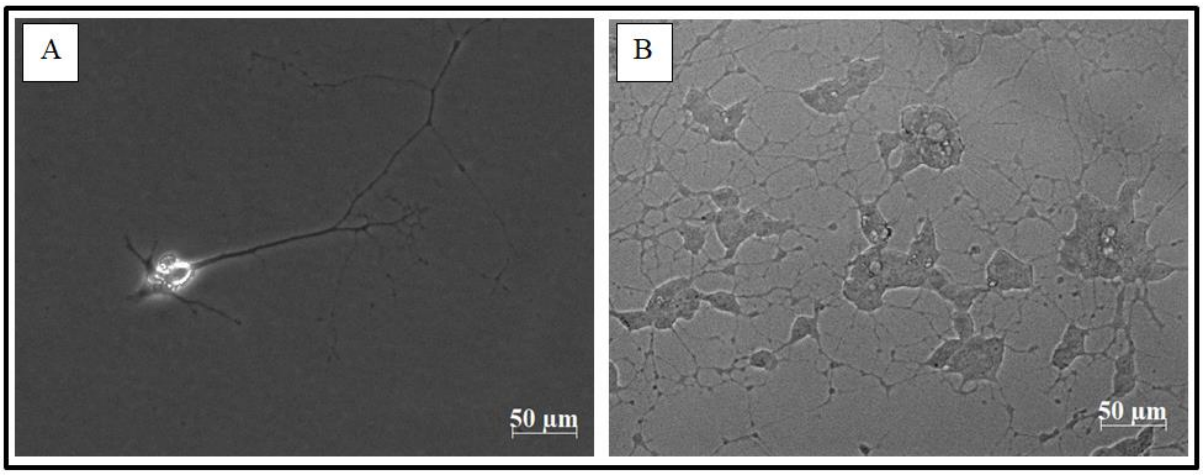

Figure 14: Photomicrographs of SH-SY5Y cells at the end of the eighteen-day differentiation cycle. SH-SY5Y cells were seeded at a density of 1×10^5 cells/well (A) and 85×10^3 cells/well (B). [20X magnification]

3.2. Cell morphology

3.2.1. Neurite outgrowth

The ultimate goal of differentiation is to ensure that SH-SY5Y cells develop as neurons, being more representative of the *in vitro* environment, than the current models where cells are not differentiated. The differentiation process was captured and compared to the published methods that were followed.

3.2.1.1. Six-day differentiation

On Day 1 cells exhibited few and short neuritic processes with a flat, retracted and neuroblast-like phenotype indicating undifferentiated cells (Figure 15A). On Day 3, longer, extended neurites were observed which was accompanied by a decrease in cellular proliferation (Figure 15B). When compared to the photomicrographs by Forster *et al.*,[105] cells were denser than those of the authors (Figure 15D, 15E). On Day 6, cells appeared more evenly distributed with a network of mature neurons indicated by the longer neuritic projections that connected to other cells (Figure 15C). The cells on the final day of differentiation corresponded to the

photomicrographs presented by Forster *et al.*[105] (Figure 15C). This, morphologically, indicated that the changes were comparable to the original method.

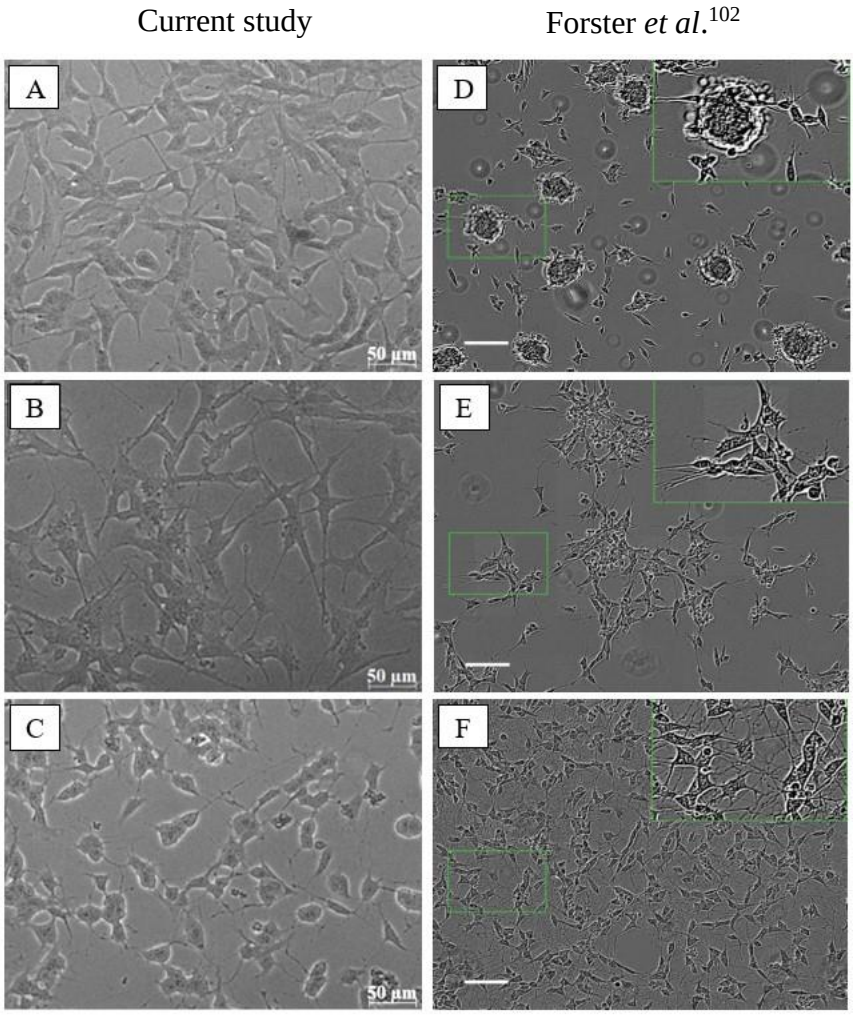

Figure 15: Photomicrographs of SHSY-5Y cells taken throughout the six-day differentiation cycle (A-C). Day 1 (A), Day 3 (B) and Day 6 (C). (Scale bar: 50 µm; 20X magnification) Differentiation micrographs by Forster *et al.*[105] (D-F). Day 1 (D), Day 3 (E) and Day 6 (F). (Scale bar: 100µM). (Reproduced with permission under Creative Commons Attribution-NonCommercial 3.0 License).

3.2.1.2. Eighteen-day differentiation

On Day 1 cells exhibited few and short neuritic processes with a flat, retracted and neuroblast-like phenotype indicating undifferentiated cells (Figure 16A). On Days 5, 7 and 10 (Figures 16B, 16C, 16D, respectively), longer, extended neurites were observed which was accompanied by a decrease in cellular proliferation. On Day 11, short and long neuritic

projections, as well as cellular clumping were observed after the cells were passaged. It was noted that cells were sparsely distributed in the wells post passaging. The ECM provides a three-dimensional platform for the cells,[127] and as a result, cells may clump as occurred on Day 18 (Figure 16F). On Day 18, the mature neuronal cultures presented with a pyramidal shaped cell body and long neuritic projections that connected to other cells (Figure 16F). In comparison to Shipley *et al*.,[98] the elimination of one trypisinisation step increased the amount of cells at the end of differentiation. The cells on the final day of differentiation corresponded to the photomicrographs presented by Shipley *et al*.[98] (Figure 16G), which morphologically indicated that the changes were comparable to the original method.

Various compounds are employed in cell differentiation assays and include RA, BDNF[98,105] and db-cAMP.[98] Retinoic acid is undoubtedly the compound that is most widely used to differentiate cells into cholinergic neurons,[128,129] and according to the published method was employed in the first phase of the six-day differentiation method and throughout the eighteen-day differentiation method. Retinoic acid activates tropomyosin kinase B (TrkB) by arresting the cell cycle, thus reducing cellular proliferation, permitting axonal outgrowth and further treatment with BDNF to produce more and longer neurites.[100] Cellular proliferation, axonal outgrowth and longer neuritic projections were observed in Figures 15C and 16F, suggestive thereof that TrkB was induced by RA. Undifferentiated cells are known to have an expeditious proliferation rate,[129] therefore, the visible reduction in cellular proliferation is indicative of cellular differentiation (Figures 15 and 16).[128] Differentiation induced by RA in the P19 cell line (mouse teratocarcinoma) produced more intricate networks of mature connecting neurons with increased neurite length than the SH-SY5Y cells.[130] Treatment with RA produced visible neurons in human NTera2 (NT2) cell line,[131] long neurites with branches and decreased cellular proliferation in both A126-1B2 cells and 123.7 cells (mutant lines of PC12)[132] as well as B35 (rat neuroblastoma) cells.[133] Human tonsil-derived mesenchymal stem cells were differentiated with RA to motor neuron-like cells and were represented by connecting neuritic projections.[134]

During differentiation the neural cells are initially treated with RA, and thereafter BDNF.[98,100,105] Cells are more receptive to BDNF treatment after induction of TrkB.[100] In the present study, as well as the studies by Forster *et al.*[105] and Shipley *et al*.,[98] treatment with BDNF initiated the formation of mature neuronal networks with longer neurites (Figures 15C, 15F, 16F, 16G). An increase in the expression of neuronal proteins was reported after treatment of BDNF.[100] However, this was not found to be the case in neural stem/progenitor cell

differentiation, as BDNF did not contribute to the differentiation of the cells but rather enhanced cell survival.[135]

During the six-day differentiation method, cells were subjected to consecutive treatment of RA for the first three days followed by BDNF for the next three days. In the eighteen-day differentiation method, cells were treated with both RA (Days 1 to end of the cycle) and BDNF (Days 11 to end of the cycle). It was reported that cells that were treated simultaneously with RA and BDNF exhibited a higher neuritic density than cells that were treated solely with RA.[100] This was evident in the eighteen-day differentiation method which resulted in a lower cell number, but longer neuritic projections, compared to the higher cell number and fewer and shorter neuritic projections of the six-day differentiation method (Figures 15C, 16F).

Another compound commonly used in differentiation is db-cAMP, which is a membrane-permeable compound.[136] This compound has been found to enhance neuronal differentiation, and has beneficial downstream effects in neurotrophin signalling such as the promotion of axonal regeneration and neurite growth.[136] Long neurites were visible after treatment with db-cAMP during differentiation with SH-SY5Y cells in this study (Figure 16F), as well as in the F-11 (immortalized dorsal-root ganglion) cell line[137] and after co-treatment with nerve growth factor in PC12 cells.[138] The differentiation of astrocytes, neuronal stem cells and mesenchymal stromal cells were amplified by db-cAMP.[139] It was reported that BDNF levels were upregulated in diabetic rats by db-cAMP, which as a result, improved cognitive function.[139] The upregulation of BDNF by db-cAMP was also found to have a neuroprotective effect.[139,140]

The reason for the addition of FBS to the cell culture media is to preserve growth of the cells.[104] Foetal bovine serum contains vitamins and growth factors that are essential for optimal cell growth.[104] The cell growth cycle has been shown to come to a halt when FBS is removed from the medium, ultimately halting proliferation.[104] However, the presence of FBS may conceal the effects of growth factors such as BDNF, making removal thereof necessary.[104] On Day 3 and Day 11 of the six- and eighteen-day differentiation methods, respectively, the cells are gradually introduced into a serum-deprived state as BDNF and db-cAMP are introduced into the media. Differentiated cells were found to exhibit longer neurites which was accompanied by a significant increase in the number of neuritic branches when grown in serum-deprived cells (Figures 15C, 16F), a finding corroborated by Thompson *et al.*[104] An increase in neurite length and a decrease in cellular proliferation was also visible in the differentiation of PC12 cells by FBS concentration reduction.[141]

Current study

Shipley *et al.*[95]

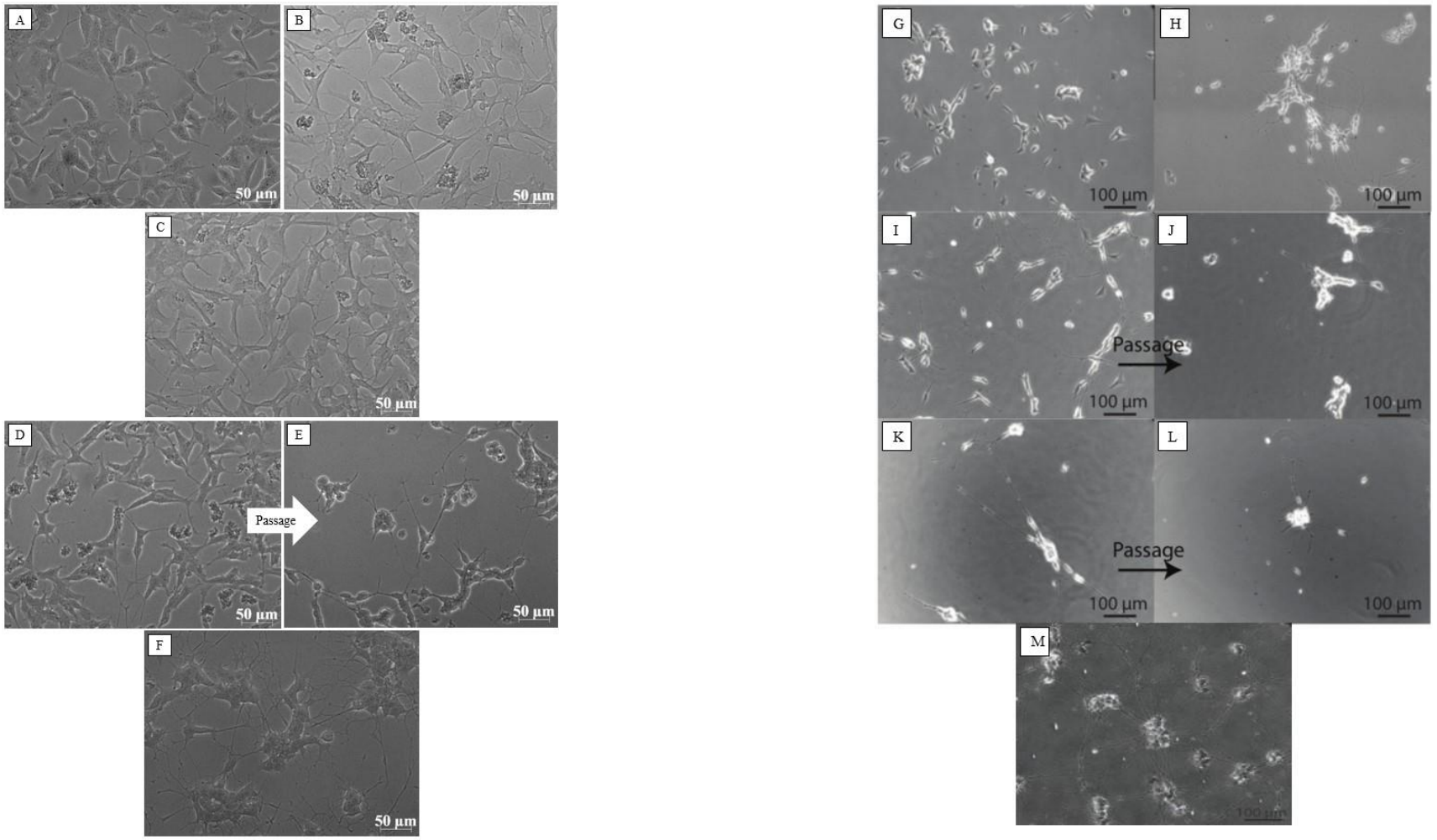

Figure 16: Photomicrographs of SH-SY5Y cells taken throughout the eighteen-day differentiation cycle (A-F). Day 1 (A), Day 5 (B), Day 7 (C), Day 10 (D), Day 11 (E), Day 18 (F). (20X magnification) Differentiation micrographs by Shipley *et al.*[98] (G-L). Day 1 (G), Day 5 (H), Day 7 (I), Day 8 (J), Day 10 (K), Day 11 (L) and Day 18 (M). (20X magnification). (Reproduced with permission from the Creative Commons Attribution License (CC BY))

3.3. Cell status

3.3.1. Cell viability

Staining with FDA/PI confirmed that the neurons were viable at the end of both differentiation methods (Figure 17) given clear conversion of FDA to fluorescein, and a lack of PI fluorescence. Additionally, cellular debris was minimal in light microscopy (as described in Section 3.2). This was corroborated by Zainullina *et al*.,[142] where the differentiated SH-SY5Y cells were viable after treatment with BDNF and reduced FBS concentration.[142] The compounds db-cAMP[139] and BDNF have been found to promote cell survival thus contributing to the viability of the differentiated cells.[142] Longer neurites, compared to the undifferentiated cells, were present in both six- (Figures 17A, 17B) and eighteen-day (Figures 17C, 17D) differentiation protocols. When compared to the photomicrographs (Figures 15C, 16F), the density of the cells was evidently higher than that of the FDA/PI composite photomicrographs (Figure 17).

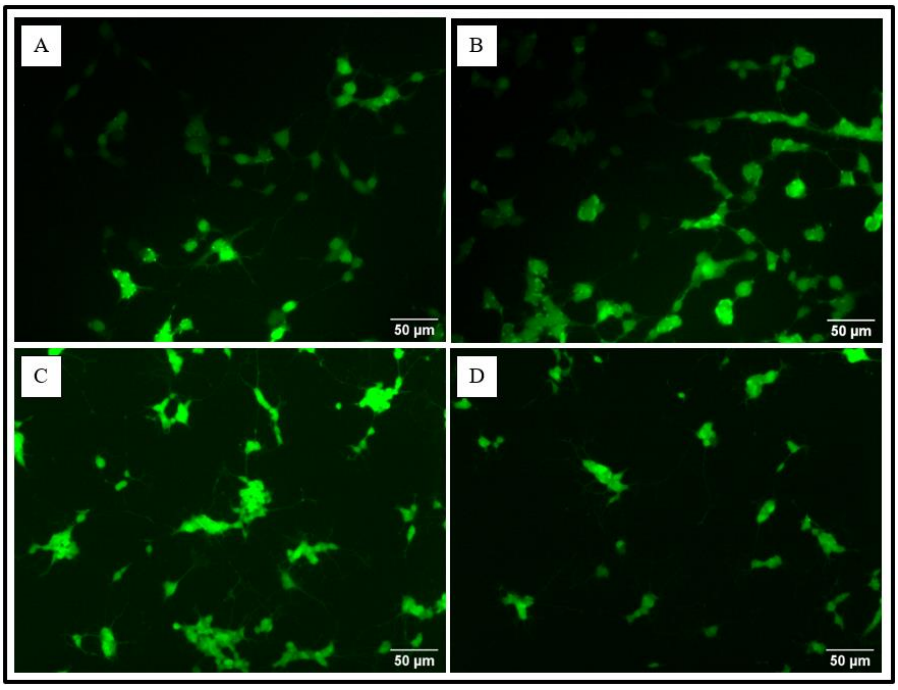

Figure 17: Composite photomicrographs of FDA/PI stained SH-SY5Y cells taken on Day 6 of the six-day differentiation cycle (A, B) and on Day 18 of the eighteen-day differentiation cycle (C, D).

3.3.2. Cell density

Cell density was assessed for undifferentiated and differentiated cells at the day at which they would be used for initiation of biological assessments. A significant ($p \leq 0.001$) increase in cellular density was observed between respective undifferentiated and differentiated cells (six-day: 3.3-fold; eighteen-day: 2-fold) (Figures 18A, 18B). The density of undifferentiated cells of the six-day differentiation method was significantly ($p \leq 0.05$) higher than the undifferentiated cells of the eighteen-day differentiation method (1.4-fold increase), which aligns to the density of cells that was initially seeded. The differentiated cells' density of the six-day differentiation method was significantly ($p \leq 0.01$) higher than the differentiated cells of the eighteen-day differentiation method with a 2.3-fold increase. The six-day differentiation method resulted in a higher percentage of cells that differentiated (Figure 18C). Despite the difference in cellular densities between the two methods, it was determined that there would still be sufficient cells at the end of the differentiation methods to continue with further testing. The differentiated cells of both differentiation methods were evidently higher than that of the cellular density of the undifferentiated cells, thus confirming that there were more cells at the end of the differentiation processes.

As previously mentioned, the cells of the six-day differentiation method were treated with RA only for the first three days of the process, which allowed the cells to continue proliferating until the end of the differentiation cycle, whereas the cells of the eighteen-day differentiation method were treated with RA throughout the differentiation cycle. The eighteen-day differentiation method consisted of a trypsinisation step which may have further decreased the cellular density. The PCNA marker, was more highly expressed in the six-day differentiation method, than in the eighteen-day differentiation method (Section 3.3.5). As a proliferation marker, PCNA, has a vital role in DNA replication, repair and cell cycle control.[143] Therefore, due to the repair and replication nature of PCNA together with RA treatment,[125] the cells of the six-day differentiation method were allowed to continue proliferating until the end of the differentiation cycle, which resulted in a higher cellular density. According to Forster *et al.*,[105] differentiated cells increase in size and complexity,[105] thereby, contributing to a larger population of fixed protein elements which are detected by the SRB assay.

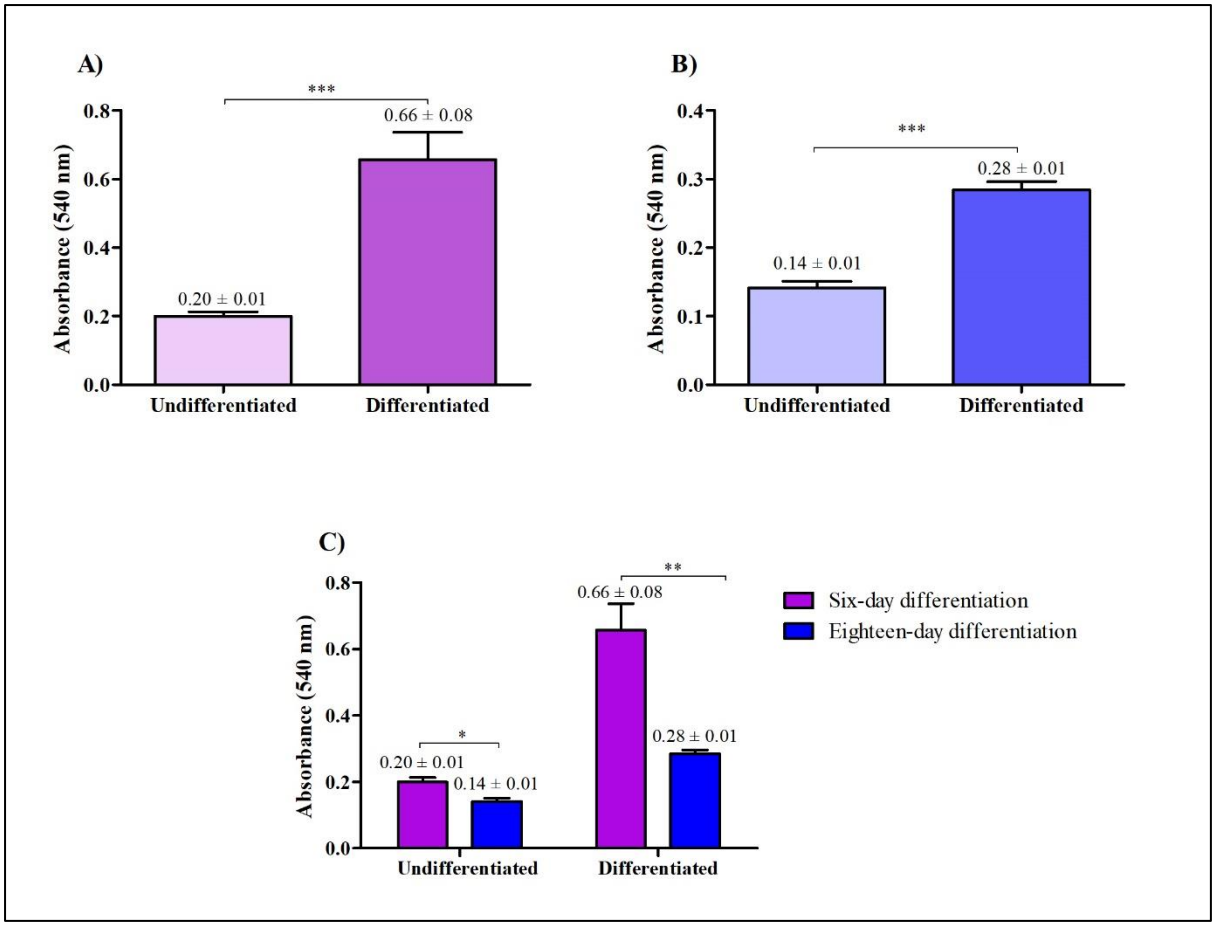

Figure 18: Cell density, expressed as the absorbance of sulforhodamine B of undifferentiated and differentiated SH-SY5Y cells at 540 nm, referenced at 630 nm. Six-day differentiation (A), eighteen-day differentiation (B), six- and eighteen-day differentiation (C). n = 3 experimental replicates. * $p \leq 0.05$, ** $p \leq 0.01$, *** $p \leq 0.001$

3.3.3. Protein content

A significant ($p \leq 0.001$) increase in protein content was observed between the undifferentiated (146.8 µg) and differentiated (303.4 µg) cell lysates of the six-day differentiation method (2.1-fold-change) (Figure 19A). Similarly, a significant ($p \leq 0.05$) increase in protein content was observed between the undifferentiated (222.9 µg) and differentiated (299.2 µg) cell lysates of the eighteen-day differentiation method (1.3-fold-change) (Figure 19B). The protein concentration of the undifferentiated cell lysates of the eighteen-day differentiation method was significantly ($p \leq 0.01$) higher than the undifferentiated cell lysates of the six-day differentiation method (1.5-fold increase) (Figure 19C). Contrary, the protein concentration of

differentiated cell lysates in the eighteen-day differentiation method did not differ significantly from that of the six-day differentiation method (Figure 19C).

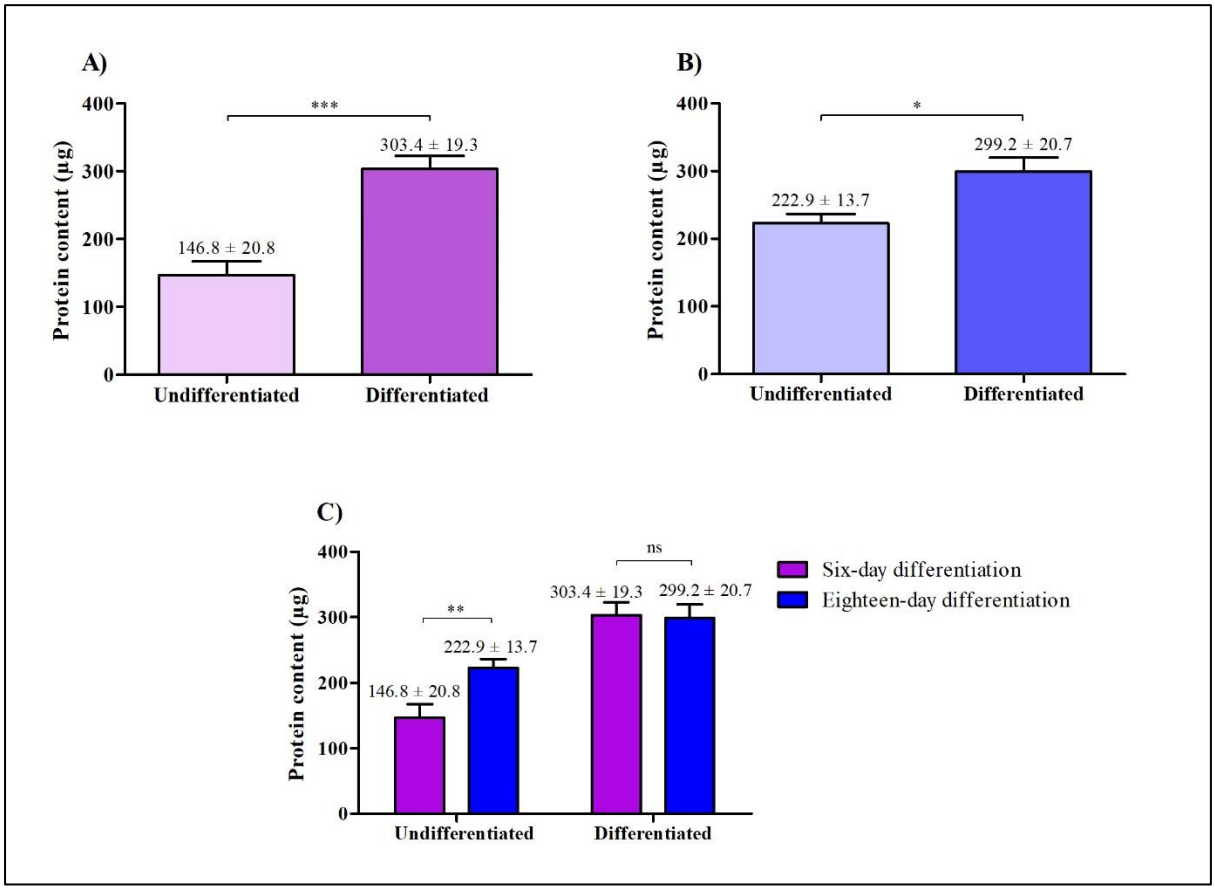

Figure 19: Protein content (µg), expressed as the protein content of undifferentiated and differentiated SH-SY5Y cells. Six-day differentiation (A), eighteen-day differentiation (B), six- and eighteen-day differentiation (C). n = 9 experimental replicates. * $p \leq 0.05$, ** $p \leq 0.01$; *** $p \leq 0.001$; not significant (ns).

A significant ($p \leq 0.001$) decrease in protein content was observed between the undifferentiated (6,431 µg) and differentiated (5,491 µg) supernatant of the six-day differentiation method (1.2-fold) (Figure 20A). A significant ($p \leq 0.001$) decrease in protein content was observed between the undifferentiated (8,715 µg) and differentiated (6,112 µg) supernatant of the eighteen-day differentiation method (1.4-fold) (Figure 20B). The protein content of the undifferentiated supernatant of the eighteen-day differentiation method was significantly ($p \leq 0.001$) higher than the undifferentiated supernatant of the six-day differentiation method (1.4-fold). The differentiated cells supernatant's protein concentration of the eighteen-day differentiation

method was significantly ($p \leq 0.01$) higher than the differentiated supernatant of the six-day differentiation method (1.1-fold). (Figure 20C).

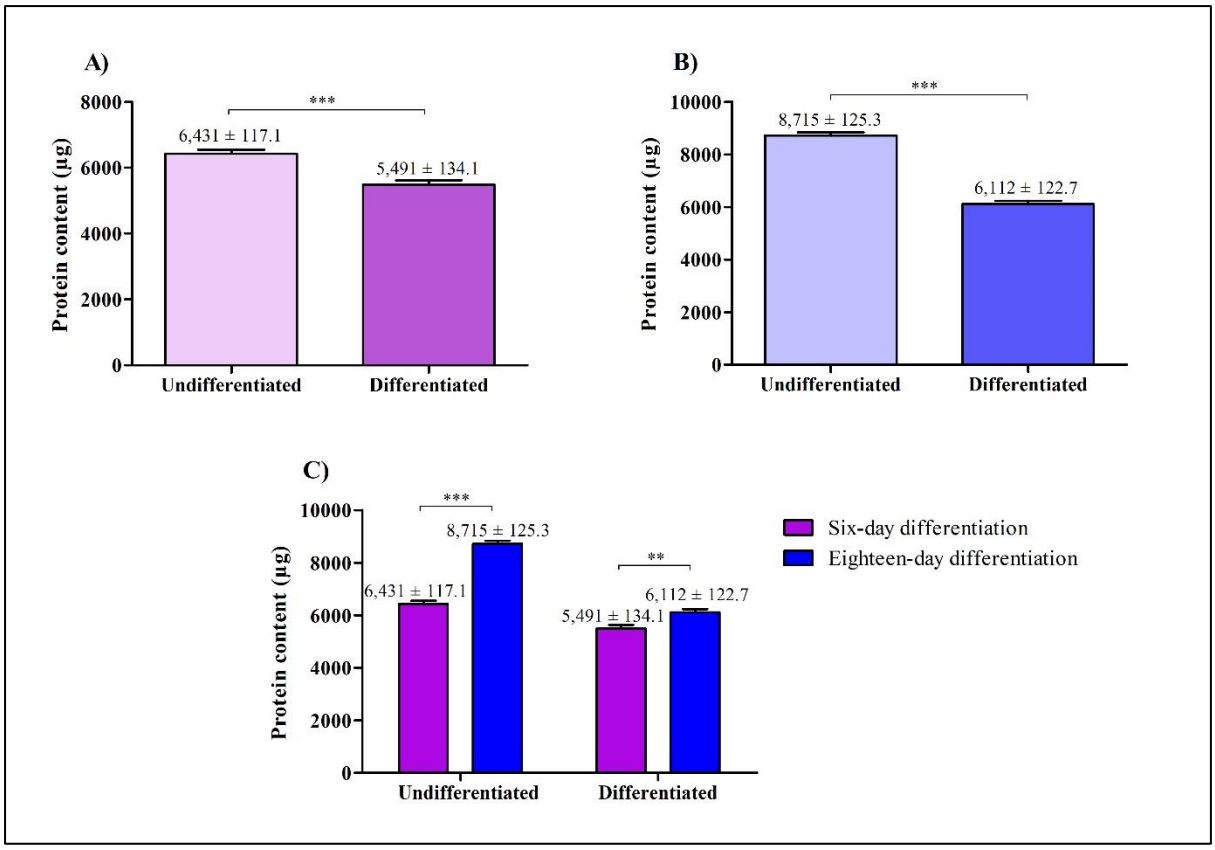

Figure 20: Protein content (µg), expressed as the protein content of undifferentiated and differentiated supernatant. Six-day differentiation (A), eighteen-day differentiation (B), six- and eighteen-day differentiation (C). n = 9 experimental replicates. ** $p \leq 0.01$; *** $p \leq 0.001$.

For the six-day differentiation method, cells were seeded in medium containing RA and reduced FBS concentration (5%), whereas in the eighteen-day differentiation method cells were seeded in standard medium. Due to the former, the protein content of the undifferentiated cell lysates and supernatant of the six-day differentiation method was lower than that of the differentiated cell lysates and supernatant of the eighteen-day differentiation method, as RA[100] and decreased FBS concentration reduces cellular proliferation.[104] The eighteen-day differentiation method also had a higher cellular seeding density which allowed a higher protein content in the undifferentiated cells. This corresponds to the cellular density of undifferentiated

cells (Figures 18A, 18C). However, the protein content of the differentiated cell lysates (Figure 19C) did not correspond with the cellular density (Section 3.3.2; Figure 18C).

3.3.4. Acetylcholine and acetylcholinesterase levels

A significant ($p \leq 0.01$) decrease in the ACh level was observed between the undifferentiated and differentiated cell lysates for both the six-day method (0.57-fold; Figure 21A) and eighteen-day method (0.64-fold; Figure 21B). There was no significant difference in the ACh level between the undifferentiated cell lysates of the six-day differentiation method and the eighteen-day differentiation method (Figure 21C). The difference between the ACh level in differentiated cell lysates of the six-day differentiation method and the eighteen-day differentiation method was not significant (Figure 21C).

A significant ($p \leq 0.01$) decrease in the ACh level was observed in the supernatant of undifferentiated and differentiated cells for the six-day method (0.6-fold; Figure 22A) and the eighteen-day method (0.65-fold; Figure 22B). The ACh level in the supernatant of the eighteen-day differentiation method was significantly ($p \leq 0.05$) higher than the six-day differentiation method (1.08-fold; Figure 22C).

The synthesis of ACh is controlled by CHaT.[36] The simultaneous treatment of RA and BDNF has been reported to increase the activity of CHaT, which would stimulate ACh synthesis.[100] Potassium chloride has also been reported to stimulate the release of ACh.[144] As potassium chloride (KCl) is included in the treatment regime of the eighteen-day differentiation method from Day 11, it would be expected that ACh levels would be higher in the cell lysates. However, this was not the case in this study as no significant increase in ACh levels was noted. Rapid ACh hydrolysis by AChE,[145] could result in the low levels of ACh detected in the differentiated cell lysates of this study. It has been reported that nicotinic ACh receptors are present in undifferentiated SH-SY5Y cells,[146] thus, it is possible that ACh is released in undifferentiated cell lysates (Figures 21A, 21B). The release of ACh in N18TG2 neuroblastoma 2/4 cloned differentiated cells as well as into the medium is reported to be enhanced by db-cAMP.[144] Furthermore, ACh was found to stimulate fiber outgrowth of the differentiated cell lysate,[144] which is observed in Figure 16F.

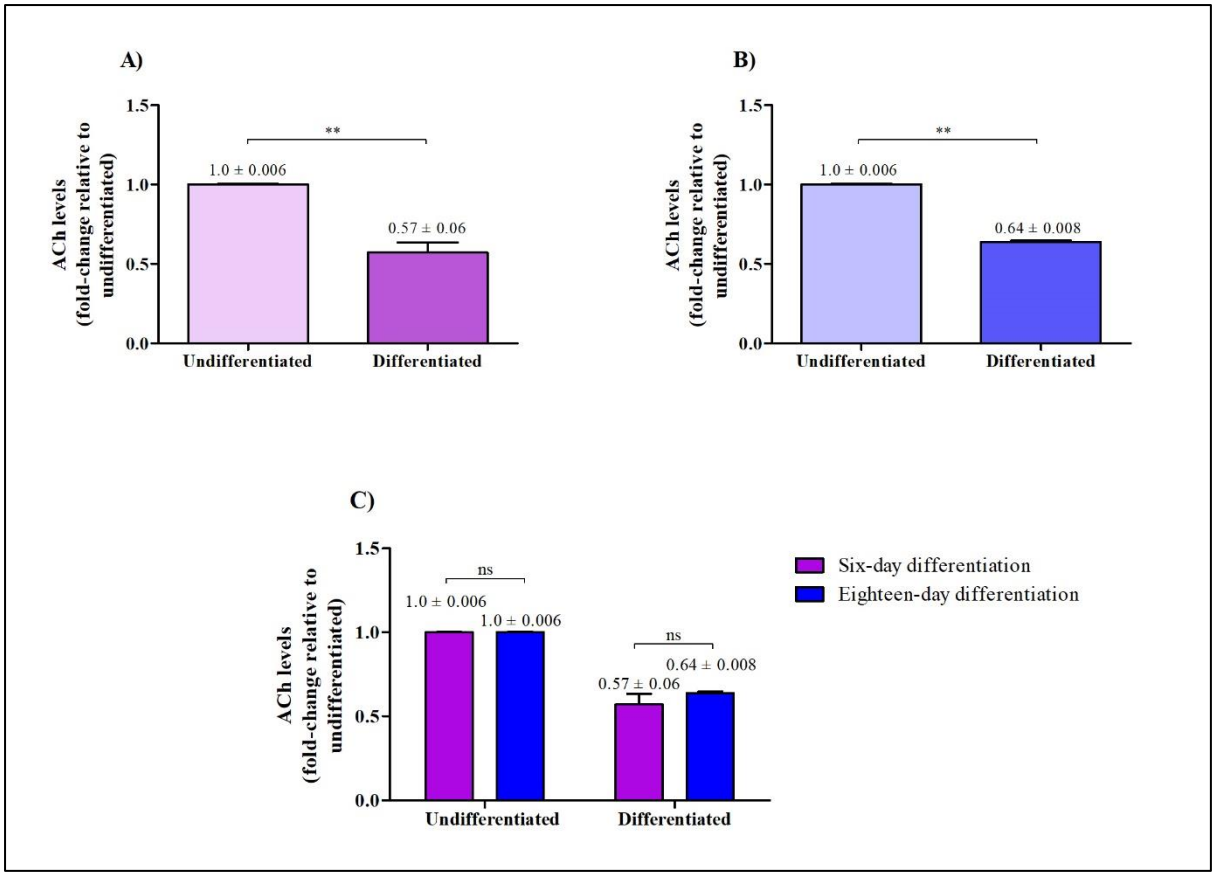

Figure 21: Acetylcholine levels in SH-SY5Y cell lysates, expressed as fold-change. Six-day differentiation (A), eighteen-day differentiation (B), six- and eighteen-day differentiation (C). n = 3 experimental replicates. ** $p \leq 0.01$; not significant (ns).

Similar to ACh levels, a significant ($p \leq 0.01$) decrease in the AChE level was observed between respective undifferentiated and differentiated cell lysates (six-day: 0.58-fold; eighteen-day: 0.51-fold) (Figure 23A, B). The difference between the AChE level in differentiated cell lysates of the six-day differentiation method and the eighteen-day differentiation method was however not significant (Figure 23C).

As for the level of AChE in the supernatant, a significant ($p \leq 0.01$) decrease in the AChE level was observed in the supernatant of the undifferentiated and differentiated cells of the six-day differentiation method (0.48-fold; Figure 24A) and the eighteen-day differentiation method (0.50-fold; Figure 24B). The difference in the level of AChE in the supernatant was not significant in the differentiated cells for either of the differentiation methods (Figure 24C).

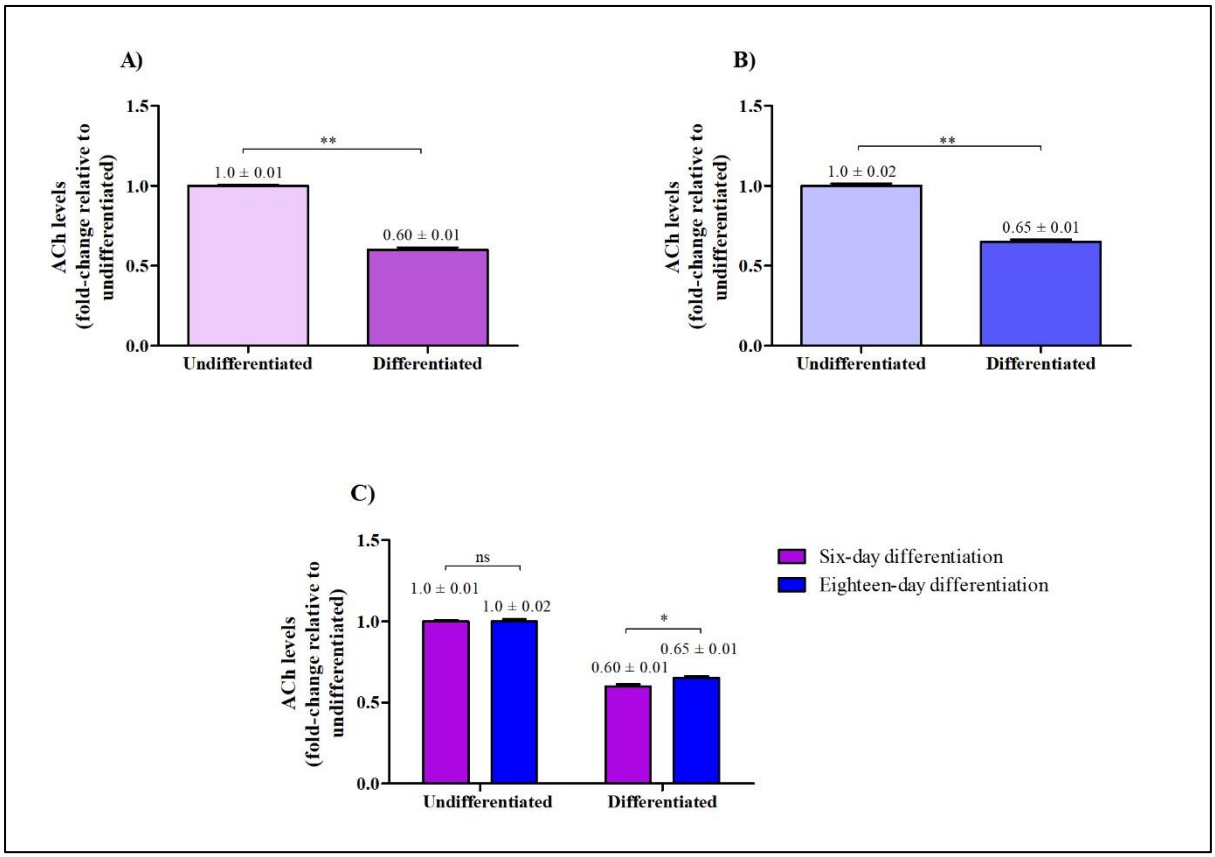

Figure 22: Acetylcholine levels in the supernatant, expressed as fold-change. Six-day differentiation (A), eighteen-day differentiation (B), six- and eighteen-day differentiation (C). n = 3 experimental replicates. * $p \leq 0.05$; ** $p \leq 0.01$; not significant (ns).

In SH-SY5Y cells, simultaneous treatment of RA and BDNF resulted in increased levels of AChE, when compared to RA-only treatment.[100] However, in the current study, AChE levels did not increase in either the differentiated cells or the supernatant as expected, even though cells were sequentially treated with RA and BDNF in the six-day differentiation method and simultaneously treated with RA and BDNF in the eighteen-day differentiation method, (Figures 23A, 23B, 24A, 24B). However, AChE was expressed in the supernatants as well as the undifferentiated cells (Figures 23A, 23B, 24A, 24B). It has been reported that AChE is isolated in neurites and is dispersed in the cytoplasm (supernatant) of SH-SY5Y cells,[147] and that undifferentiated cells also exhibited AChE level.[100] Although an increase in AChE levels was expected at the end of differentiation, this was not found as the undifferentiated cells expressed higher AChE levels. According to Thullbery *et al.*, the relationship between AChE protein expression and catalytic activity of AChE does not correspond, which may be a result

of genomic alterations due to the tumour-nature of SH-SY5Y cells,[147] thereby, AChE is present in the cells but not catalytically active. Retinoic acid has also been found to stimulate the expression of AChE in A126-1B2 (mutant line of PC12) cells.[132]

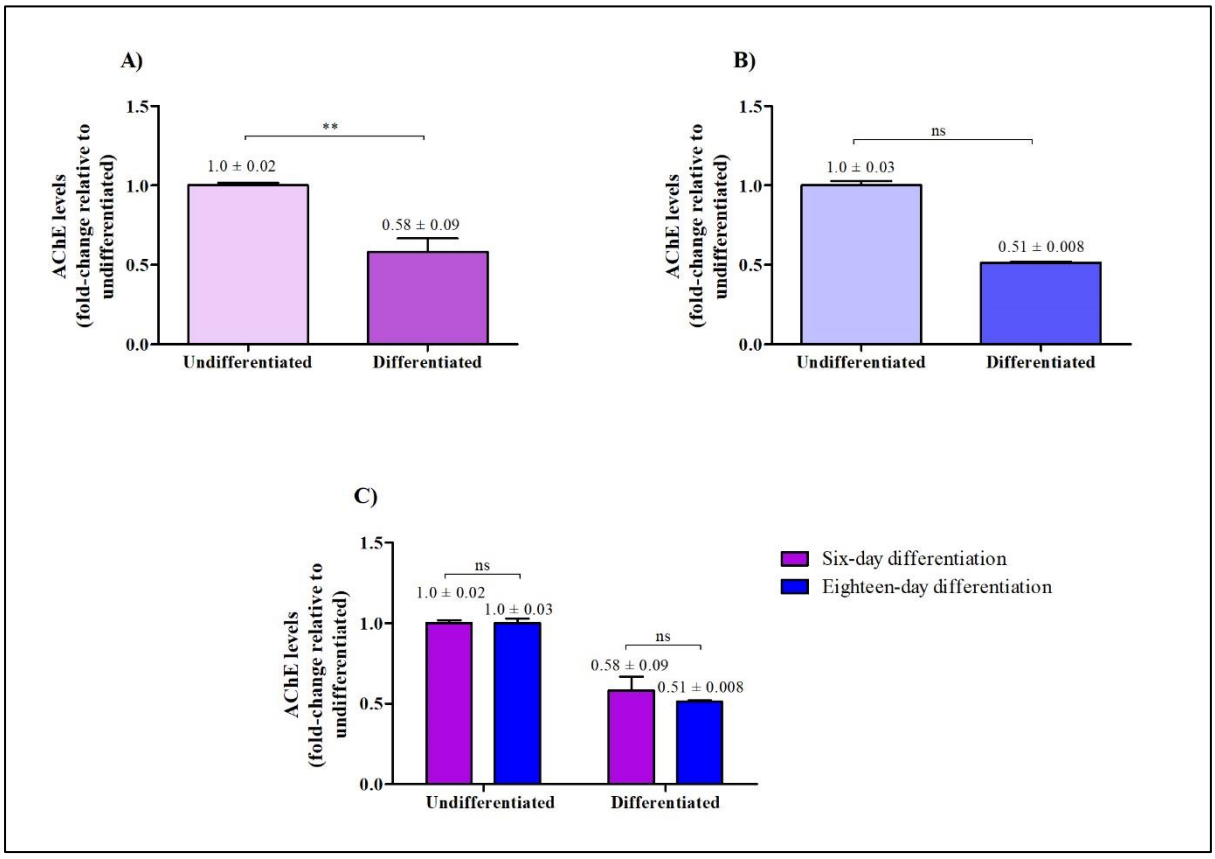

Figure 23: Acetylcholinesterase levels in SH-SY5Y cell lysates, expressed as fold-change. Six-day differentiation (A), eighteen-day differentiation (B), six- and eighteen-day differentiation (C). n = 3 experimental replicates. ** $p \leq 0.01$; not significant (ns).

It is unclear why the differentiation methods did not lead to the expected increased production of ACh and AChE. Even though differentiation of the cells took place morphologically, the differentiation processes did not appear to produce molecular outcomes that paralleled the morphological features. According to Yang *et al.*,[148] the morphology, genome and phenotype of cells *in vitro* can be altered by multiple passaging steps, thus, the reduced number of passages in the eighteen-day differentiation may have resulted in an altered phenotype and genotype.

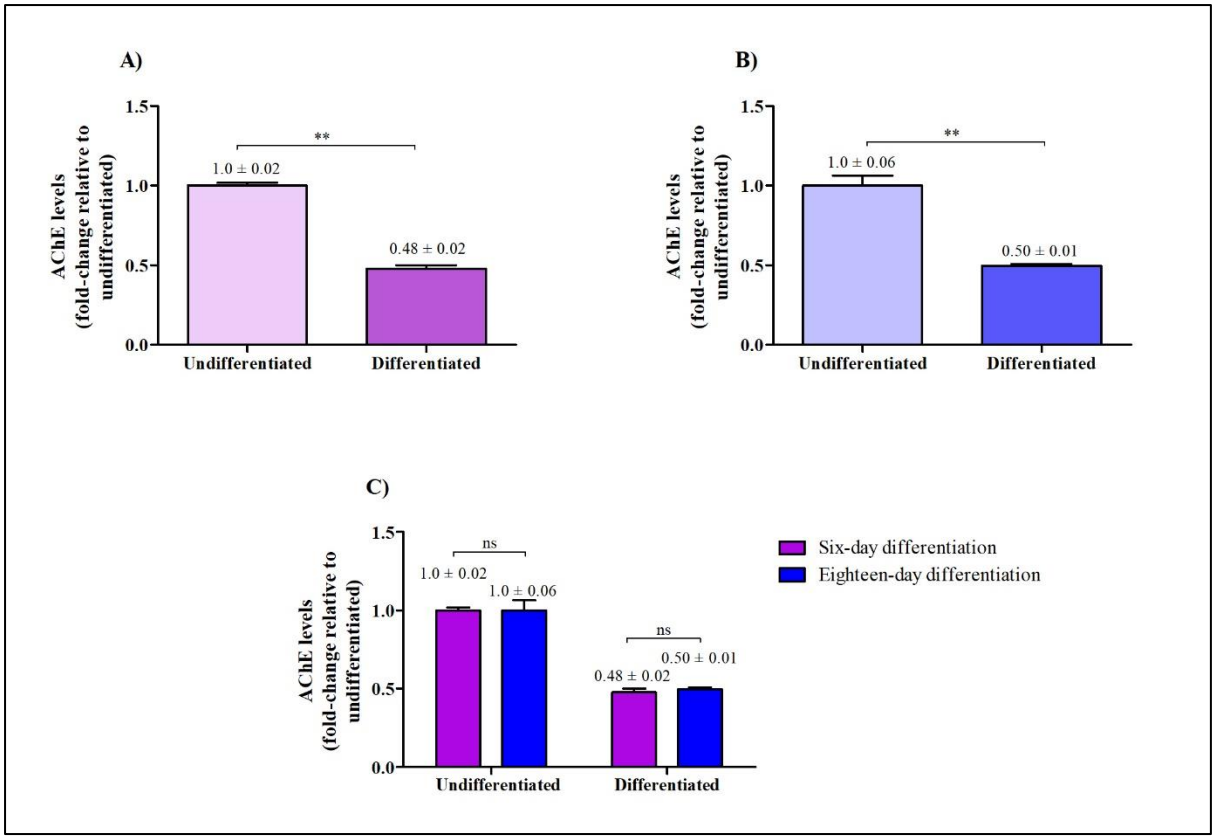

Figure 24: Acetylcholinesterase levels in the supernatant, expressed as fold-change. Six-day differentiation (A), eighteen-day differentiation (B), six- and eighteen-day differentiation (C). n = 3 experimental replicates. ** $p \leq 0.01$; not significant (ns).

3.3.5. Biomarkers

Flow cytometry was used to determine the expression of mature (APP and BACE-1) and immature (PCNA) biomarkers in differentiated and undifferentiated cells of the two differentiation methods. The presence of PCNA in the undifferentiated cells provides confirms the presence of the protein in SH-SY5Y cells. The expression of PCNA is lower in differentiated SH-SY5Y cells, thus, it is suggestive that differentiation is complete as proliferation is reduced in differentiated cells. The mature markers in differentiated cells are indicators that differentiation of the SH-SY5Y cells occurred. The SH-SY5Y cells were stained with fluorophore-conjugated antibodies.

The positive control was established by differentiating the SHSY-5Y cells for four days with RA (Section 2.3.7.1). The unstained samples of the positive control were not treated with

fluorophore-conjugated antibodies (Figure 25). The samples of the positive control were used to establish regions of expression and non-expression (Figure 26). In the positive control, only 1.36% of the cell population expressed the immature biomarker (PCNA) (Figure 26A). In contrast, the positive control expressed the mature biomarkers, APP (77.21%) and BACE-1 (59.71%) (Figures 26B, 26C).

Only 27.68% of undifferentiated cells expressed PCNA (Figure 27A), while a total of 50.98% and 97.70% of undifferentiated cells expressed APP and BACE-1, respectively (Figures 27B, 27C).

The samples of the six-day differentiated cells expressed 25.96% of the immature biomarker (Figure 28A) whereas, 74.48% and 21.71% of the six-day differentiated cells expressed APP and BACE-1, respectively (Figures 28B, 28C). The expression of PCNA and BACE-1 was lower than the expression of APP.

The samples of the eighteen-day differentiated cells expressed 4.27% of the immature biomarker (Figure 29A). The eighteen-day differentiated cells only expressed 29.33% and 22.12% of APP and BACE-1, respectively (Figures 29B, 29C).

In summary, the PCNA biomarker was slightly expressed in both undifferentiated cells and cells that were differentiated for six days (Figure 30A). The mature biomarker, APP was expressed in the undifferentiated, six- and eighteen-day differentiated cells with the six-day differentiation method having the higher expression of APP than the eighteen-day differentiation method (Figure 30B). The BACE-1 enzyme was present in the undifferentiated, six- and eighteen-day differentiated cells with the undifferentiated cells having the highest expression (97.70%) and the six-day differentiation having the lowest expression (21.71%) (Figure 30C). Overall, the undifferentiated cells expressed both the mature biomarkers (APP and BACE-1) to a higher degree than the six- and eighteen-day differentiated cells (Figure 30).

Although PCNA is expressed in both undifferentiated and differentiated SH-SH5Y cells, the level of expression is lower after the differentiation process.[149] The level of PCNA expression was substantially lower in the differentiated SH-SY5Y cells of the eighteen-day differentiation method than the undifferentiated cells and the differentiated cells of the six-day method (Figure 30). The SH-SH5Y cells are neuroblastoma cells. The PCNA biomarker is known to be overexpressed in cancer cells.[143] As mentioned earlier (Section 3.2.1.2), the removal of FBS from the medium contributes to the termination of the cell cycle.[104] The eighteen-day

differentiation method is exposed to a longer and gradual reduction of FBS concentration, whereas the FBS concentration in the six-day differentiation method was rapidly reduced over a short time. The expression of PCNA was lower in the eighteen-day differentiation method than in the six-day differentiation method, thus indicating that the longer exposure of cells to a serum-free environment reduced cellular proliferation.

The transmembrane protein, APP, is expressed in both undifferentiated and differentiated SH-SY5Y cells.[97] This was confirmed (Figure 30), however, differentiated cells of the six-day differentiation method (sequentially treated with RA and BDNF) expressed higher levels of APP than the differentiated cells of the eighteen-day method (simultaneously treated with RA and BDNF). The level of expression of APP was reported to be higher in cells that are treated with RA, when compared to undifferentiated cells or cells treated with the combination of RA and BDNF.[97] Riegerová *et al*.,[97] proposed that in fully differentiated SH-SY5Y cells, proteases quickly process APP thereby producing lower levels of the protein.[97] The latter may explain the low expression of APP in the differentiated cells of the eighteen-day method. Contrary, this has not been found to the case in differentiated human iPSCs, where the expression of APP was noted to be consistent throughout the differentiation process.[150] Furthermore, the correct balance of APP expression was found to contribute to faster axonal outgrowth rate.[151] This finding was noted in the eighteen-day differentiation method (Figures 16F, 30B). Over-expressed APP has been reported to reduce the outgrowth rate.[151] This was observed in the six-day differentiation method (Figures 15C, 30B).

In this study, undifferentiated and differentiated SH-SY5Y cells expressed BACE-1 (Figure 30), a finding supported by Riegerová *et al*.[97] The differentiated cells expressed BACE-1 to a lesser extent than the undifferentiated cells, however, according to Riegerová *et al*.,[97] undifferentiated SH-SY5Y cells express low levels of BACE-1.[97] Furthermore, it has been reported that the level of BACE-1 expression increases after RA treatment and drops after exposure to BDNF.[97] This was noted when comparing the positive control (Figure 26C) to the differentiated cells in the current study (Figures 28C, 29C). It has been proposed that non-amyloidogenic proteolytic cleavage of APP is triggered by RA and BDNF treatment, thus yielding more sAPPα.[97] The level of activity of BACE-1 in turn is hindered by the increase in sAPPα,[97] resulting in lower levels of the marker. This finding was noted in differentiated SH-SY5Y cells (Figure 30). Low levels of BACE-1 were found in the brains of adult mice and higher expression levels of the biomarker were detected in the early postnatal phase.[152] It is also reported that transgenic mice (Tg2576), lipopolysaccharide-treated mice and cultured

neurons express high levels of BACE-1, however, the anti-inflammatory properties of RA supress BACE-1 expression.[153] It was noted that amount of mature proteins being expressed after differentiation were low (Figures 30B, 30C), a finding which is corroborated by Červenka J *et al*.[154]

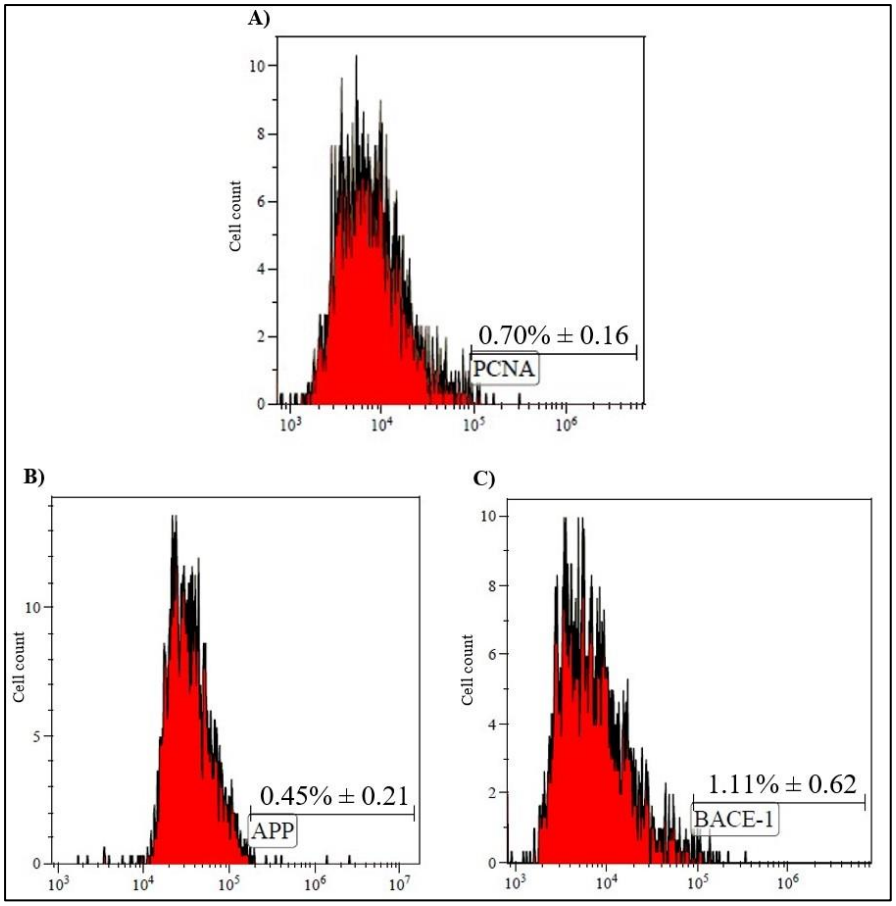

Figure 25: The expression of the biomarkers: PCNA (A), APP (B), BACE-1 (C) in unstained cells of the positive control (four-day differentiation of SHSY-5Y cells with RA). PCNA APC-A; APP PC5.5-A; BACE APC CY7 APC-A750-A. PCNA: proliferating cell nuclear antigen, APP: amyloid precursor protein, BACE-1: Beta-site APP cleaving enzyme-1.

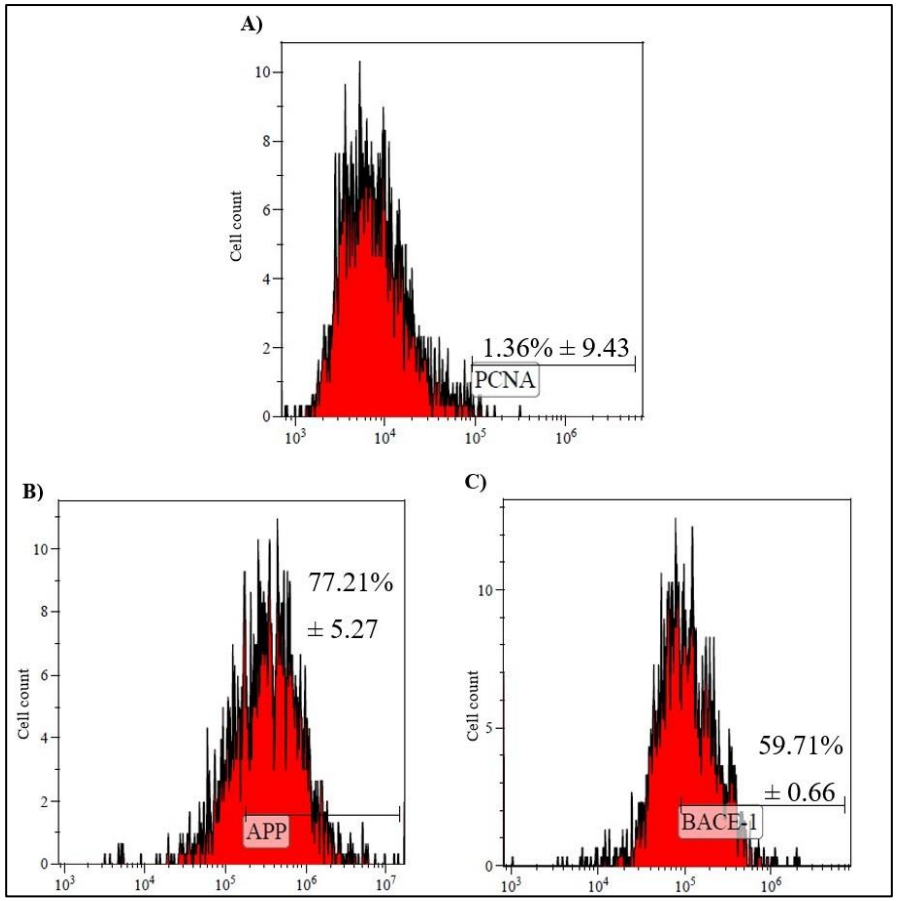

Figure 26: The expression of the biomarkers: PCNA (A), APP (B), BACE-1 (C) in SH-SY5Y cells of the positive control (four-day differentiation of SHSY-5Y cells with RA). PCNA APC-A; APP PC5.5-A; BACE APC CY7 APC-A750-A. PCNA: proliferating cell nuclear antigen, APP: amyloid precursor protein, BACE-1: Beta-site APP cleaving enzyme-1.

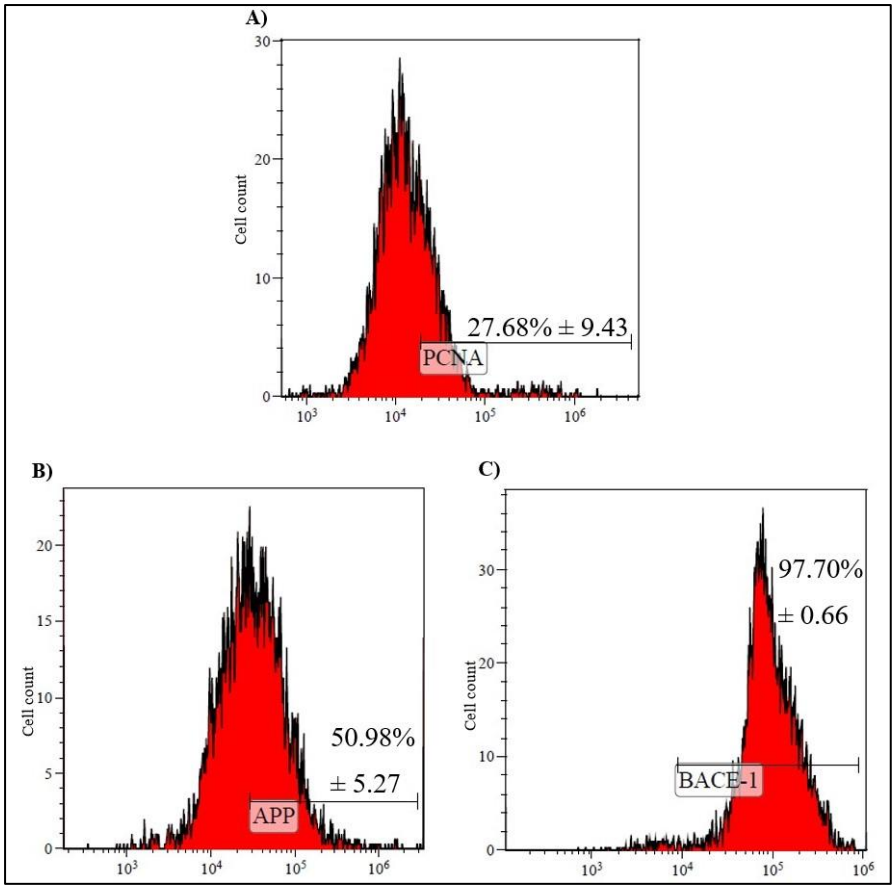

Figure 27: The expression of the biomarkers: PCNA (A), APP (B), BACE-1 (C) in undifferentiated SH-SY5Y cells. PCNA APC-A; APP PC5.5-A; BACE APC CY7 APC-A750-A. PCNA: proliferating cell nuclear antigen, APP: amyloid precursor protein, BACE-1: Beta-site APP cleaving enzyme-1.

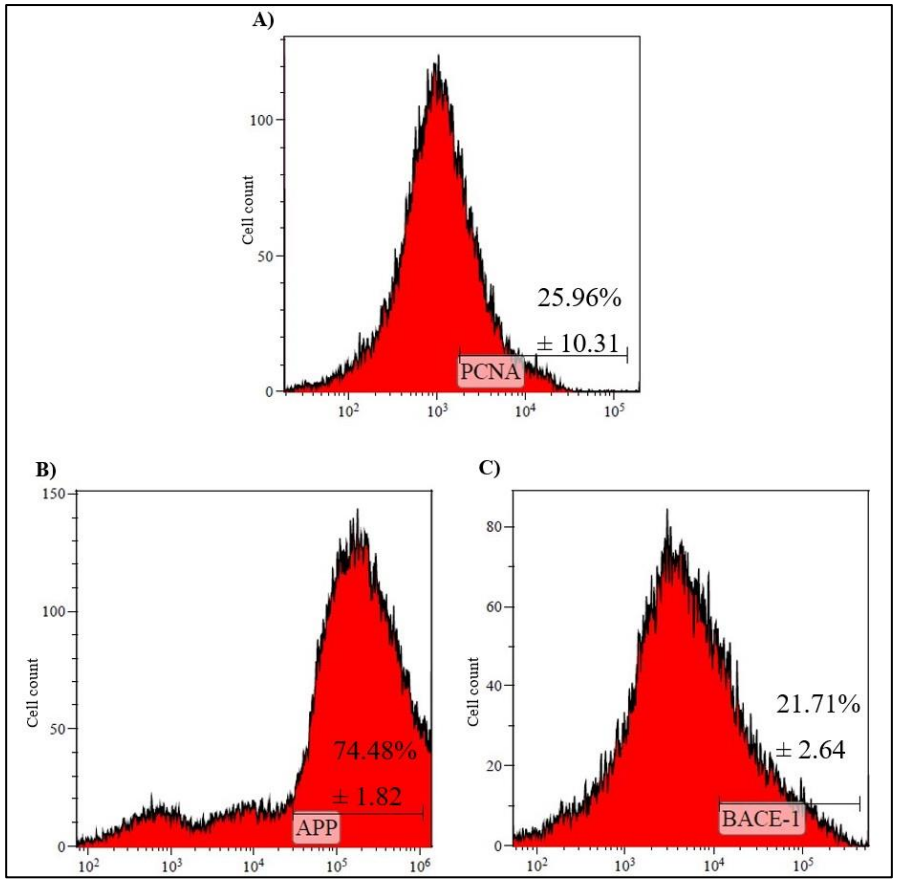

Figure 28: The expression of the biomarkers: PCNA (A), APP (B), BACE-1 (C) in SH-SY5Y cells of the six-day differentiation method. PCNA APC-A; APP PC5.5-A; BACE APC CY7 APC-A750-A. PCNA: proliferating cell nuclear antigen, APP: amyloid precursor protein, BACE-1: Beta-site APP cleaving enzyme-1.

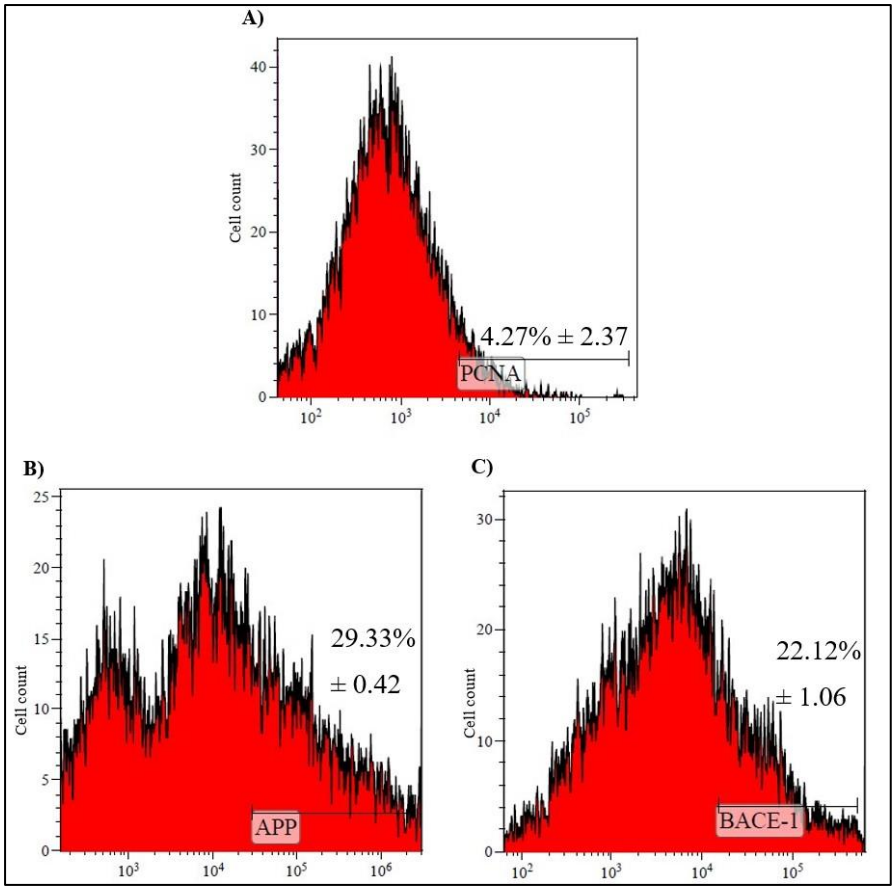

Figure 29: The expression of the biomarkers: PCNA (A), APP (B), BACE-1 (C) in SH-SY5Y cells of the eighteen-day differentiation method. PCNA APC-A; APP PC5.5-A; BACE APC CY7 APC-A750-A. PCNA: proliferating cell nuclear antigen, APP: amyloid precursor protein, BACE-1: Beta-site APP cleaving enzyme-1.

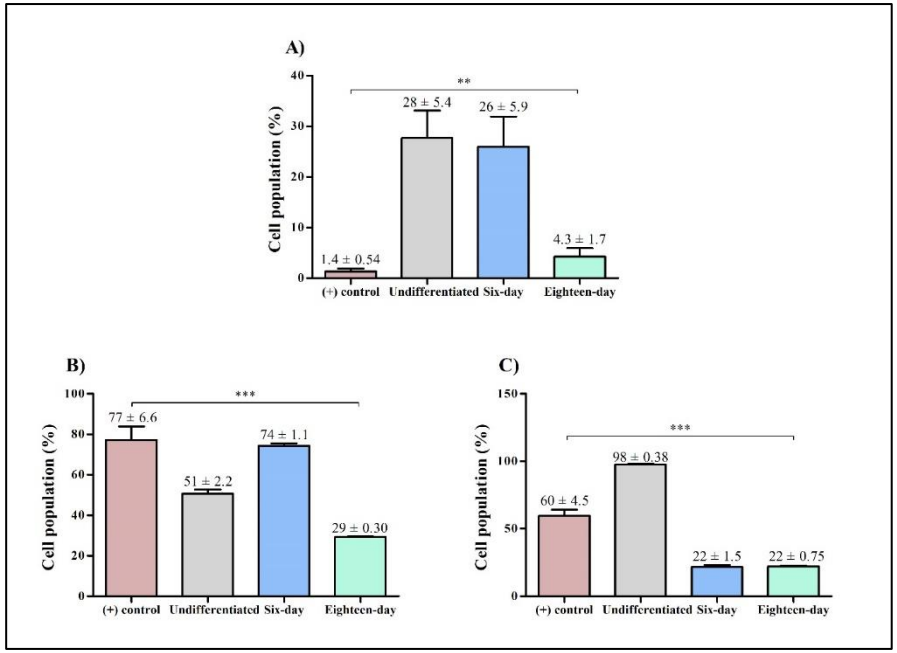

Figure 30: Average expression of the biomarkers: PCNA (A), APP (B), BACE-1 (C) of the cell population (%) in cells of the positive control, undifferentiated SH-SY5Y cells and the six- and eighteen-day differentiation methods, respectively. PCNA: proliferating cell APP: amyloid precursor protein, BACE-1: Beta-site APP cleaving enzyme-1

Chapter 4 Conclusion

Current AD treatment regimens only offer symptomatic relief as there is currently no cure. *In vitro* studies for potential models for AD drug development are more economical as they are capable of large-scale production of cell cultures, and are less labour intensive. The SH-SY5Y cell line produces phenotypically homogenous cells and is capable of expressing human-specific proteins. It is imperative to differentiate SH-SY5Y cells in order to establish a more mature neuronal phenotype as well as the expression of mature biomarkers. The aim of the study was to compare two differentiation protocols of SH-SY5Y neuroblastoma cells for the purpose of developing an *in vitro* AD drug development platform.

Two methods were compared for their ability to yield differentiated SH-SY5Y cells: a six-day and an eighteen-day differentiation procedure. The undifferentiated SH-SY5Y cells were compared to the differentiated SH-SY5Y cells in order to select the most representative model for the development of an in-house AD drug development platform.

The SRB assay confirmed that more cells were present at the end of the differentiation processes and staining with FDA/PI confirmed that the cells were viable after differentiation. The increase in cells over time without noticeable death was supported by the increase in protein concentration. However, the levels of ACh and AChE unexpectedly decreased after the differentiation process.

Undifferentiated SH-SY5Y cells possess a flat, retracted and neuroblast-like phenotype with short neuritic processes. Differentiated cells produced a high number of longer neuritic projections that connected to other cells. A reduction in cellular proliferation was observed after RA-treatment. The differentiated SH-SY5Y cells were more evenly distributed and exhibited a pyramidal shaped cell body. The eighteen-day differentiation method resulted in fewer neurons, however with longer neuritic projections, ascribed to the simultaneous exposure to RA and BDNF when compared to the six-day differentiation method where there were more neurons, but fewer neuritic projections, as cells were consecutively treated with RA and BDNF.

The PCNA biomarker was slightly expressed in SH-SY5Y cells that were differentiated for six days. The six-day differentiation method exhibited a higher expression of APP than the eighteen-day differentiation method. Low levels of the BACE-1 enzyme was expressed in the differentiatiated SH-SY5Y cells. The undifferentiated cells expressed proteins of both the immature (PCNA) and mature biomarkers (APP and BACE-1).

In conclusion, it was observed that the simulaneous treatment of RA and BDNF played an important role in cellular differentiation. The eighteen-day differentiation method involves the simultaneous treatment of RA and BDNF, whereas the six-day differentiation method includes the consecutive treatment of RA and BDNF. Morphologically, the eighteen-day differentiation method produced longer neurites with an intrinsic network of neurites connecting cells wheras the six-day differentiation method produced more neurons, but fewer neuritic projections. The eighteen-day differentiated cells exhibited the lowest PCNA (immature biomarker) expression whereas the six-day differentiation method had a higher PCNA expression than the eighteen-day differentiation method. The combination treatment of RA and BDNF (consecutive and simultaneous) resulted in low expression of BACE-1 in the differentiated cells. In fully differentiated cells, cells exhibit low APP expression, which was evident in the eighteen-day differentiation method. This implies that the six-day differentiation method did not produce fully differentiated cells since the cells exhibited high APP expressions. Therefore, the results support morphological differentiation and some molecular alterations, but it is not recommended to investigate the mature cholinergic system using the differentiated SH-SY5Y cells. Further method development is required to ascertain the correct cocktail of differentiation factors to yield a mature phenotype expressing markers relevant to AD, including APP and BACE-1, and functional neurotransmitter systems, such as ACh and AChE.

Chapter 5 Study limitations and recommendations

In this study, the morphology of the neurons such as neurite length, branching and the complexity thereof was constantly being compared by mere visual analysis. For future studies neurite outgrowth and branching analysis should be assessed using an ImageJ plugin called Neuron J or by a neurite outgrowth assay which would make analysis in more complex 3D models more reliable.

Another aspect that was commonly referred to was cellular proliferation. The reduction of cellular proliferation was one of the characteristics of differentiated cells. In addition to PCNA, the inclusion of either a proliferation marker (ki-67) or a cellular proliferation assay such as CellTrace Violet^{TM} would have been beneficial to confirm the findings.

The eighteen-day differentiation method utilised ECM, whereas the six-day differentiation method did not. The use of ECM is advantageous as it provides a scaffold for the cells thus making the cells more visually appealing when comparing the photomicrographs of the two differentiation methods. For visually comparative purposes, future studies should keep the use of ECM constant by either using ECM in both methods or omitting it completely.

The level of ACh was expected to be higher in differentiated cells, however this was not case. The inclusion of immunohistochemistry would have allowed the determination of whether the reduction of ACh and AChE levels were due to experimental artifacts.

Initially, GAPDH was used as a control throughout flow cytometry analysis. However, the antibody stock ran out and could not be included in further experimentation. Another limitation to flow cytometry was that other antibodies (anti-APP, anti-BACE-1, anti-PCNA) were also low in stock, thus only one undifferentiated sample was used to represent both six- and eighteen-day differentiation methods. The study was also limited to three biomarkers; and it is recommended that in future studies biomarkers such as nestin and MAP2 should also be assessed. The assessment of the mature biomarker, MAP2, is imperative as β-amyloids destabilise these microtubules during the progression of AD. The analysis of MAP2 via immunocytochemistry would allow for the identification of the location of tau pre- and post-differentiation, being indicative of hyperphosphorylation.

If these limitations are addressed in future studies, the assessments would be more robust. Due to the multifaceted nature of AD, other targets such as MAP2 (monitor the complete effect of the β-amyloids in the AD model) and TrkB must be taken into consideration for future work.

References

1. Sweeney P, Park H, Baumann M, Dunlop J, Frydman J, Kopito R, McCampbell A, Leblanc G, Venkateswaran A, Nurmi A, Hodgson R. Protein misfolding in neurodegenerative diseases: implications and strategies. Translational Neurodegeneration. 2017;6(6):1-13.
2. Alzheimer's Association. 2019 Alzheimer's disease facts and figures. Alzheimer's & Dementia. 2019;15(3):321-87.
3. Heffernan AL, Hare DJ. Tracing environmental exposure from neurodevelopment to neurodegeneration. Trends in Neuroscience. 2018;41(8):496-501.
4. Patterson C. World Alzheimer Report 2018. London: Alzheimer's Disease International; 2018.
5. Rahman MA, Rahman MS, Uddin MJ, Mamum-Or-Rashid ANM, Pang MG, Rhim H. Emerging risk of environmental factors: insight mechanisms of Alzheimer's diseases. Environmental Science and Pollution Research. 2020;27(36):44659-72.
6. Gołaszewska A, Bik W, Motyl T, Orzechowski A. Bridging the gap between Alzheimer's disease and Alzheimer's-like diseases in animals. International Journal of Molecular Sciences. 2019;20(7).
7. Holmes C, Amin J. Dementia. Medicine. 2020;48(11):742-5.
8. World Health Organization. Dementia. 2019. [Accessed May 2019]. Available from: https://www.who.int/en/news-room/fact-sheets/detail/dementia.
9. Prince M, Comas-Herrera A, Knapp M, Guerchet M, Karagiannidou M. World Alzheimer report 2016. Annual Report London; 2016.
10. Kumar A, Sidhu J, GoyaL A, Tsao JW. Alzheimer Disease. StatPearls. Treasure Island (FL): StatPearls Publishing; 2021.
11. Reisberg B. Clinical stages of Alzheimer's. 2017. [Accessed April 2017]. Available from: https://www.alzinfo.org/understand-alzheimers/clinical-stages-of-alzheimers/.
12. Alzheimer's Association. What is preclinical Alzheimer's disease?. Northern California and Northern Nevada: Alzheimer's Association; 2016. [Updated October 2016; Accessed June 2019]. Available from: https://www.alzheimersblog.org/2016/10/27/preclinical-alzheimers-disease/.
13. Parnetti L, Chipi E, Salvadori N, D'Andrea K, Eusebi P. Prevalence and risk of progression of preclinical Alzheimer's disease stages: a systematic review and meta-analysis. Alzheimer's Research & Therapy. 2019;11(1):7.
14. Mori T, Kikuchi T, Umeda-Kameyama Y, Wada-Isoe K, Kojima S, Kagimura T, Kudoh C, Uchikado H, Ueki A, Yamashita M, Watabe T, Nishimura C, Tsuno N, Ueda T, Akishita M, Nakamura Y. ABC dementia scale: a quick assessment tool for determining Alzheimer's disease severity. Dementia and Geriatric Cognitive Disorders Extra. 2018;8(1):85-97.
15. Yiannopoulou KG, Papageorgiou SG. Current and future treatments in Alzheimer disease: an update. Journal of Central Nervous System Disease. 2020;12:1179573520907397.
16. Frozza RL, Lourenco MV, De Felice FG. Challenges for Alzheimer's disease therapy: insights from novel mechanisms beyond memory defects. Frontiers in Neuroscience. 2018;12(37).
17. Kumar A, Tsao JW. Alzheimer disease. Treasure Island (FL): StatPearls Publishing; 2018.
18. Shen L, Xia S, Zhang H, Yao F, Liu X, Zhao Y, Ying M, Iqbal J, Liu Q. Precision medicine: role of biomarkers in early prediction and diagnosis of Alzheimer's disease. 2018. In: Molecular Medicine [Internet]. IntechOpen: IntechOpen.

19. Armstrong RA. Risk factors for Alzheimer's disease. Folia neuropathologica. 2019;57(2):87-105.
20. National Institute on Aging. What causes Alzheimer's disease? 2017. [Updated 22 May 2017; Accessed May 2019]. Available from: https://www.nia.nih.gov/health/what-causes-alzheimers-disease.
21. Watermeyer TJ, Raymont V, Ritchie K. Neuroinflammation in preclinical Alzheimer's disease: a review of current evidence. Journal of Alzheimer's Disease & Parkinsonism. 2018;8(2).
22. Li P, Marshall L, Oh G, Jakubowski J, Groot D, He Y, Wang T, Petronis A, Labrie V. Epigenetic dysregulation of enhancers in neurons is associated with Alzheimer's disease pathology and cognitive symptoms. Nature Communications. 2019;10(1):2246.
23. Boskovic Z, Meier S, Wang Y, Milne MR, Onraet T, Tedoldi A, Coulson EJ. Regulation of cholinergic basal forebrain development, connectivity, and function by neurotrophin receptors. Neuronal Signalling. 2019;3(1).
24. National Institute on Aging. What happens to the brain in Alzheimer's disease? 2017. [Updated 16 May 2017; Accessed June 2019]. Available from: https://www.nia.nih.gov/health/what-happens-brain-alzheimers-disease.
25. Koval I, Schiratti JB, Routier A, Bacci M, Colliot O, Allassonnière S, Durrleman S. Spatiotemporal propagation of the cortical atrophy: population and individual patterns. Frontiers in Neurology. 2018;9(235).
26. Johnson K, Fox N, Sperling R, Klunk W. Brain imaging in Alzheimer disease. Cold Spring Harbor Perspectives in Medicine. 2012;2(4).
27. Lieff J. Does abnormal amyloid cause Alzheimer's? 2015. [Accessed August 2017]. Available from: http://jonlieffmd.com/blog/does-abnormal-amyloid-cause-alzheimers.
28. Xu J, Patassini S, Rustogi N, Riba-Garcia I, Hale BD, Phillips AM, Waldvogel H, Haines R, Bradbury P, Stevens A, Faull RLM, Dowsey AW, Cooper GJS, Unwin RD. Regional protein expression in human Alzheimer's brain correlates with disease severity. Communications Biology. 2019;2(1):43.
29. Darusman HS, Agungpriyono DR, Kusumaputri VA, Sajuthi D, Schapiro SJ, Hau J. Granulovacuolar degeneration in brains of senile cynomolgus monkeys. Frontiers in Aging Neuroscience. 2019;11(50).
30. Didonna A, Opal P. The role of neurofilament aggregation in neurodegeneration: lessons from rare inherited neurological disorders. Molecular Neurodegeneration. 2019;14(1):19.
31. Serrano-Pozo A, Frosch M, Masliah E, Hyman B. Neuropathological alterations in Alzheimer disease. Cold Spring Harbor Perspectives in Medicine. 2011;1(1).
32. Braak H, Alafuzoff I, Arzberger T, Kretzschmar H, Tredici K. Staging of Alzheimer disease-associated neurofibrillary pathology using paraffin sections and immunocytochemistry. Acta Neuropathologica. 2006;112(4):389–404.
33. Brai E, Alina Raio N, Alberi L. Notch1 hallmarks fibrillary depositions in sporadic Alzheimer's disease. Acta Neuropathologica Communications. 2016;4(1):64.
34. Ferreira-Vieira TH, Guimaraes IM, Silva FR, Ribeiro FM. Alzheimer's disease: targeting the cholinergic system. Current Neuropharmacology. 2016;14, 101-115.
35. Trang A, Khandhar PB. Physiology, acetylcholinesterase. Treasure Island (FL): StatPearls Publishing; 2019.
36. Merck. Acetylcholine synthesis and metabolism. Germany.2019. [Accessed May 2019]. Available from: https://www.sigmaaldrich.com/technical-documents/articles/biology/rbi-handbook/non-peptide-receptors-synthesis-and-metabolism/acetylcholine-synthesis-and-metabolism.html.

37. Hernández-Zimbrón L, Gorostieta-Salas E, Díaz- Hung ML, Pérez-Garmendia R, Gevorkian G, Quiroz-Mercado H. Beta amyloid peptides: extracellular and intracellular mechanisms of clearance in Alzheimer's disease. 2016. In: Update on dementia [Internet]. IntechOpen: IntechOpen. Available from: https://www.intechopen.com/books/update-on-dementia/beta-amyloid-peptides-extracellular-and-intracellular-mechanisms-of-clearance-in-alzheimer-s-disease.
38. Hicks D, Jones AC, Pickering-Brown SM, Hooper NM. The cellular expression and proteolytic processing of the amyloid precursor protein is independent of TDP-43. Bioscience Reports. 2020;40(4).
39. Gireud M, Sirisaengtaksin N, Bean A. Molecular Mechanisms of Neurological Disease. From Molecules to Networks: An Introduction to Cellular and Molecular Neuroscience: Third Edition. 2014:639-61.
40. Zhang Y, Thompson R, Zhang H, Xu H. APP processing in Alzheimer's disease. Molecular Brain. 2011;4.
41. Alzheimer's Association. Brain tour. 2021. [Accessed September 2017]. Available from: http://www.alz.org/braintour/3_main_parts.asp.
42. Sheikh S, Safia, Haque E, Mir SS. Neurodegenerative diseases: multifactorial conformational. Journal of Neurodegenerative Diseases. 2012;2013:1-8.
43. Salahuddin P. Protein folding, misfolding, aggregation and amyloid formation: mechanisms of AB oligomer mediated toxicities. Journal of Biochemistry and Molecular Biology Research. 2015;1(2):36-45.
44. Van Eldik LJ, Carrillo MC, Cole PE, D Feuerbach, Greenberg BD, Hendrix JA, Kennedy M, Kozauer N, Margolin RA, Molinuevo JL, Mueller R, Ransohoff RM, Wilcock DM, Bain L, Bales K. The roles of inflammation and immune mechanisms in Alzheimer's disease. Alzheimer's & Dementia: Translational Research & Clinical Interventions. 2016;2:99-109.
45. Shal B, Ding W, Ali H, Kim YS, Khan S. Anti-neuroinflammatory potential of natural products in attenuation of Alzheimer's disease. Frontiers in Pharmacology. 2018;9(548):1-17.
46. Hromadkova L, Bezdekova D, Pala J, Schedin-Weiss S, Tjernberg LO, Hoschl C, Ovsepian SV. Brain-derived neurotrophic factor (BDNF) promotes molecular polarization and differentiation of immature neuroblastoma cells into definitive neurons. Biochimica et Biophysica Acta (BBA) - Molecular Cell Research. 2020;1867(9):118737.
47. Abcam. Tau in Alzheimer's disease: Abcam; 2019. [Accessed June 2019]. Available from: https://www.abcam.com/neuroscience/tau-in-alzheimers-disease.
48. Caire MJ, Varacallo M. Physiology, synapse. Treasure Island (FL): StatPearls Publishing; 2018. Available from: https://www.ncbi.nlm.nih.gov/books/NBK526047/#_NBK526047_pubdet_.
49. Lehner K, Silverman H, Addorisio M, Roy A, Al-Onaizi M, Levine Y, Olofsson P, Chavan S, Gros R, Nathanson N, Al-Abed Y, Metz C, Prado V, Prado M, Tracey K, Pavlov V. Forebrain cholinergic signaling regulates innate immune responses and inflammation. Frontiers in Immunology. 2019;10(585).
50. Cell Biolabs Inc. Acetylcholine assay kit (colorimetric). 2016. [Accessed February 2018]. Available from: https://www.cellbiolabs.com/sites/default/files/STA-603-acetylcholine-choline-assay-kit.pdf.
51. Sam C, Bordoni B. Physiology, acetylcholine. Treasure Island (FL): StatPearls Publishing; 2021.

52. Colangelo C, Shichkova P, Keller D, Markram H, Ramaswamy S. Cellular, synaptic and network effects of acetylcholine in the neocortex. Frontiers in Neural Circuits. 2019;13(24).
53. Kudlak M, Tadi P. Physiology, muscarinic receptor. Treasure Island (FL): StatPearls Publishing; 2021. Available from: https://www.ncbi.nlm.nih.gov/books/NBK555909/.
54. Wang X, Daley C, Gakhar V, Lange HS, Vardigan JD, Pearson M, Zhou X, Warren L, Miller CO, Belden M, Harvey AJ, Grishin AA, Coles CJ, O'Connor SM, Thomson F, Duffy JL, Bell IM, Uslaner JM. Pharmacological characterization of the novel and selective α7 nicotinic acetylcholine receptor-positive allosteric modulator BNC375. Journal of Pharmacology and Experimental Therapeutics. 2020;373(2):311-24.
55. Dineley KT, Pandya AA, Yakel JL. Nicotinic ACh receptors as therapeutic targets in CNS disorders. Trends in Pharmacological Sciences. 2015;36(2):96-108.
56. Hampel H, Mesulam MM, Cuello AC, Farlow MR, Giacobini E, Grossberg GT, Khachaturian AS, Vergallo A, Cavedo E, Snyder PJ, Khachaturian ZS. The cholinergic system in the pathophysiology and treatment of Alzheimer's disease. Brain. 2018;141(7):1917-33.
57. Kennedy MB. Synaptic signaling in learning and memory. Cold Spring Harbor Perspectives in Biology. 2016;8(2).
58. Miyazaki K, Lisman JE, Ross WN. Improvements in simultaneous sodium and calcium imaging. Frontiers in Cellular Neuroscience. 2019;12(514).
59. Grider MH, Glaubensklee CS. Physiology, action potential. Treasure Island (FL): StatPearls Publishing; 2019.
60. Georgia Highlands College. The nervous system: organization and tissue. 2013. [Accessed 08/09 2017/]. Available from: http://www2.highlands.edu/academics/divisions/scipe/biology/faculty/harnden/2121/notes/nervous.htm.
61. Lashley T, Schott JM, Weston P, Murray CE, Wellington H, Keshavan A, Foti SC, Foiani M, Toombs J, Rohrer JD, Heslegrave A, Zetterberg H. Molecular biomarkers of Alzheimer's disease: progress and prospects. Disease Models and Mechanisms. 2018;11(5).
62. Benfeito S, Fernandes C, Vilar S, Remião F, Uriarte E, Borges F. Exploring the multi-target performance of mitochondriotropic antioxidants against the pivotal Alzheimer's disease pathophysiological hallmarks. Molecules. 2020;25(2).
63. Liu J, Chang L, Song Y, Li H, Wu Y. The role of NMDA receptors in Alzheimer's disease. Frontiers in Neuroscience. 2019;13(43).
64. Alzheimer's Association. Medications for memory: Alzheimer's Association; 2019. [Accessed July 2019]. Available from: https://www.alz.org/alzheimers-dementia/treatments/medications-for-memory.
65. Zhang Y, Li P, Feng J, Wu M. Dysfunction of NMDA receptors in Alzheimer's disease. Journal of the Neurological Sciences. 2016;37:1039-47.
66. Sestito S, Daniele S, Pietrobono D, Citi V, Bellusci L, Chiellini G, Calderone V, Martini C, Rapposelli S. Memantine prodrug as a new agent for Alzheimer's disease. Scientific Reports. 2019;9(1):4612.
67. McShane R, Westby M, Roberts E, Minakaran N, Schneider L, Farrimond L, Maayan N, Ware J, Debarros J. Memantine for dementia. Cochrane Database of Systematic Reviews. 2019(3).
68. Cummings J, Aisen P, Lemere C, Atri A, Sabbagh M, Salloway S. Aducanumab produced a clinically meaningful benefit in association with amyloid lowering. Alzheimer's Research & Therapy. 2021;13(1):98.

69. Dunn B, Stein P, Cavazzoni P. Approval of aducanumab for Alzheimer disease—the FDA's perspective. Journal of the American Medical Association. 2021.
70. Cummings JL, Tong G, Ballard C. Treatment combinations for Alzheimer's disease: current and future pharmacotherapy options. Journal of Alzheimers Disease. 2018;67(3):779-94.
71. Alzheimer's Association. Treatment horizon Chicago: Alzheimer's Association; 2019. [Accessed July 2019]. Available from: https://www.alz.org/alzheimers-dementia/research_progress/treatment-horizon.
72. Alzforum. Posiphen: Alzforum; 2021. [Updated 30 July 2021; Accessed August 2021]. Available from: https://www.alzforum.org/therapeutics/posiphen.
73. Alzforum. Rasagiline: Alzforum; 2021. [Updated 10 May 2021; Accessed August 2021]. Available from: https://www.alzforum.org/therapeutics/rasagiline.
74. Timmers M, Streffer JR, Russu A, Tominaga Y, Shimizu H, Shiraishi A, Tatikola K, Smekens P, Börjesson-Hanson A, Andreasen N, Matias-Guiu J, Baquero M, Boada M, Tesseur I, Tritsmans L, Van Nueten L, Engelborghs S. Pharmacodynamics of atabecestat (JNJ-54861911), an oral BACE1 inhibitor in patients with early Alzheimer's disease: randomized, double-blind, placebo-controlled study. Alzheimer's Research & Therapy. 2018;10(85):1-26.
75. Huang LK, Chao SP, Hu CJ. Clinical trials of new drugs for Alzheimer disease. Journal of Biomedical Science. 2020;27(1):18.
76. Klein G, Delmar P, Voyle N, Rehal S, Hofmann C, Abi-Saab D, Andjelkovic M, Ristic S, Wang G, Bateman R, Kerchner GA, Baudler M, Fontoura P, Doody R. Gantenerumab reduces amyloid-β plaques in patients with prodromal to moderate Alzheimer's disease: a PET substudy interim analysis. Alzheimer's Research & Therapy. 2019;11(1):101.
77. Portron A, Jordan P, Draper K, Muenzer C, Dickerson D, van Iersel T, Hofmann C. A Phase I study to assess the effect of speed of injection on pain, tolerability, and pharmacokinetics after high-volume subcutaneous administration of gantenerumab in healthy volunteers. Clinical Therapeutics. 2020;42(1):108-20.e1.
78. Novak P, Kovacech B, Katina S, Schmidt R, Scheltens P, Kontsekova E, Ropele S, Fialova L, Kramberger M, Paulenka-Ivanovova N, Smisek M, Hanes J, Stevens E, Kovac A, Sutovsky S, Parrak V, Koson P, Prcina M, Galba J, Cente M, Hromadka T, Filipcik P, Piestansky J, Samcova M, Prenn-Gologranc C, Sivak R, Froelich L, Fresser M, Rakusa M, Harrison J, Hort J, Otto M, Tosun D, Ondrus M, Winblad B, Novak M, Zilka N. ADAMANT: a placebo-controlled randomized phase 2 study of AADvac1, an active immunotherapy against pathological tau in Alzheimer's disease. Nature Aging. 2021;1(6):521-34.
79. Cummings J, Lee G, Zhong K, Fonseca J, Taghva K. Alzheimer's disease drug development pipeline: 2021. Alzheimer's & Dementia. 2021;7(1):e12179-e.
80. Alzforum. Sargramostim: Alzforum; 2021. [Updated 22 July 2021; Accessed August 2021]. Available from: https://www.alzforum.org/therapeutics/sargramostim.
81. Jansen CU, Qvortrup KM. Small molecule drugs for treatment of Alzheimer's diseases developed on the basis of mechanistic understanding of the serotonin receptors 4 and 6. IntechOpen Book Series: IntechOpen; 2021.
82. Alzforum. Pimavanserin: Alzforum; 2021. [Updated 22 July 2021; Accessed August 2021]. Available from: https://www.alzforum.org/therapeutics/pimavanserin.
83. Martins M, Silva R, Pinto MMM, Sousa E. Marine natural products, multitarget therapy and repurposed agents in Alzheimer's disease. Pharmaceuticals (Basel, Switzerland). 2020;13(9).

84. Gray NE, Zweig JA, Caruso M, Zhu JY, Wright KM, Quinn JF, Soumyanath A. Centella asiatica attenuates hippocampal mitochondrial dysfunction and improves memory and executive function in β-amyloid overexpressing mice. Molecular and Cellular Neuroscience. 2018;93(2018):1-9.
85. Salinaro AT, Pennisi M, Paola RD, Scuto M, Crupi R, Cambria MT, Ontario ML, Tomasello M, Uva M, Maiolino L, Calabrese EJ, Cuzzocrea S, Calabrese V. Neuroinflammation and neurohormesis in the pathogenesis of Alzheimer's disease and Alzheimer-linked pathologies: modulation by nutritional mushrooms. Immunity & Ageing. 2018;15(8):17.
86. Chin-Chan M, Navarro-Yepes J, Quintanilla-Vega B. Environmental pollutants as risk factors for neurodegenerative disorders: Alzheimer and Parkinson diseases. Frontiers in Cellular Neuroscience. 2015;9:124.
87. Vitek MP, Araujo JA, Fossel M, Greenberg BD, Howell GR, Rizzo SJS, Seyfried NT, Tenner AJ, Territo PR, Windisch M, Bain LJ, Ross A, Carrillo MC, Lamb BT, Edelmayer RM. Translational animal models for Alzheimer's disease: an Alzheimer's association business consortium think tank. Alzheimer's & Dementia: Translational Research & Clinical Interventions. 2020;6(1):e12114.
88. LaFerla F, Green K. Animal models of Alzheimer disease. Cold Spring Harb Perspect Med. 2012;2(11).
89. Paldino E, Balducci C, La Vitola P, Artioli L, D'Angelo V, Giampà C, Artuso V, Forloni G, Fusco FR. Neuroprotective effects of doxycycline in the R6/2 mouse model of Huntington's disease. Molecular Neurobiology. 2020;57(4):1889-903.
90. Heneka MT, Carson MJ, El Khoury J, Landreth GE, Brosseron F, Feinstein DL, Jacobs AH, Wyss-Coray T, Vitorica J, Ransohoff RM, Herrup K, Frautschy SA, Finsen B, Brown GC, Verkhratsky A, Yamanaka K, Koistinaho J, Latz E, Halle A, Petzold GC, Town T, Morgan D, Shinohara ML, Perry VH, Holmes C, Bazan NG, Brooks DJ, Hunot S, Joseph B, Deigendesch N, Garaschuk O, Boddeke E, Dinarello CA, Breitner JC, Cole GM, Golenbock DT, MP. K. Neuroinflammation in Alzheimer's disease. The Lancet Neurology. 2015;14(4):388-405.
91. Heneka MT, Sastre M, Dumitrescu-Ozimek L, Dewachter I, Walter J, T. K, F. VL. Focal glial activation coincides with increased BACE1 activation and precedes amyloid plaque deposition in APP[V717I] transgenic mice. Journal of Neuroinflammation. 2005;2:22.
92. Janelsins MC, Mastrangelo MA, Oddo S, LaFerla FM, Federoff H, J. BW. Early correlation of microglial activation with enhanced tumor necrosis factor-alpha and monocyte chemoattractant protein-1 expression specifically within the entorhinal cortex of triple transgenic Alzheimer's disease mice. Journal of Neuroinflammation. 2005;2(1):23.
93. Dubey SK, Ram MS, Krishna KV, Saha RN, Singhvi G, Agrawal M, Ajazuddin, Saraf S, Saraf S, Alexander A. Recent expansions on cellular models to uncover the scientific barriers towards drug development for Alzheimer's disease. Cellular and Molecular Neurobiology. 2019;39(2):181-209.
94. Doke SK, Dhawale SC. Alternatives to animal testing: a review. Saudi Pharmaceutical Journal. 2015;23(3):223-9.
95. Sittampalam GS, Coussens NP, Brimacombe K, Grossman A, Arkin M, Auld D, Austin C, Baell J, Bejcek B, Chung TDY, Dahlin JL, Devanaryan V, Foley TL, Glicksman M, Hall MD, Hass JV, Inglese J, Iversen PW, Kahl SD, Kales SC, Lal-Nag M, Li Z, McGee J, McManus O, Riss T, Trask OJ, Weidner JR, Xia M, Xu X. Assay guidance manual. Bethesda, MD: Eli Lilly & Company and the National Center for Advancing Translational Sciences; 2017.

96. National Research Council (US) Committee on Methods of Producing Monoclonal Antibodies. Monoclonal antibody production. Washington (DC): National Academies Press (US); 1999.
97. Riegerová P, Brejcha J, Bezděková D, Chum T, Mašínová E, Čermáková N, Ovsepian SV, Cebecauer M, Štefl M. Expression and localization of AβPP in SH-SY5Y cells depends on differentiation state. Journal of Alzheimer's Disease. 2021;82:485-91.
98. Shipley M, Mangold C, Szpara ML. Differentiation of the SH-SY5Y human neuroblastoma cell line. Journal of Visualized Experiments. 2017;108.
99. Carolindah MN, Rosli R, Adam A, Nordin N. An *in vitro* research models for Alzheimer's disease (AD). Regenerative Research. 2013;2(2):8-13.
100. de Medeiros LM, De Bastiani MA, Rico EP, Schonhofen P, Pfaffenseller B, Wollenhaupt-Aguiar B, Grun L, Barbé-Tuana F, Zimmer ER, Castro MAA, Parsons RB, Klamt F. Cholinergic differentiation of human neuroblastoma SH-SY5Y cell line and its potential use as an *in vitro* model for Alzheimer's disease studies. Molecular Neurobiology. 2019;56(11):7355-67.
101. Arber C, Lovejoy C, Wray S. Stem cell models of Alzheimer's disease: progress and challenges. Alzheimer's Research & Therapy. 2017;9(42):1-17.
102. Duncan T, Valenzuela M. Alzheimer's disease, dementia, and stem cell therapy. Stem Cell Research & Therapy. 2017;8(111):1-9.
103. Şahin M, Öncü G, Yılmaz MA, Özkan D, Saybaşılı H. Transformation of SH-SY5Y cell line into neuron-like cells: investigation of electrophysiological and biomechanical changes. Neuroscience Letters. 2021;745:135628.
104. Thomson AC, Schuhmann T, de Graaf TA, Sack AT, Rutten BPF, Kenis G. The effects of serum removal on gene expression and morphological plasticity markers in differentiated SH-SY5Y cells. Cell Molecular Neurobiology. 2021.
105. Forster JI, Köglsberger S, Trefois C, Boyd O, Baumuratov AS, Buck L, Balling R, Antony PMA. Characterization of differentiated SH-SY5Y as neuronal screening model reveals increased oxidative vulnerability. Journal of Biomolecular Screening. 2016; 21(5):496 –509
106. Teppola H, Sarkanen J, Jalonen T, Linne M. Morphological differentiation towards neuronal phenotype of SH-SY5Y neuroblastoma cells by estradiol, retinoic acid and cholesterol. Neurochemical Research. 2016;41:731-47.
107. Kim AC, Lim S, Kim YK. Metal ion effects on Aβ and tau aggregation. International Journal of Molecular Sciences. 2018;19(1).
108. Li Y, Jiao Q, Xu H, Du X, Shi L, Jia F, Jiang H. Biometal dyshomeostasis and toxic metal accumulations in the development of Alzheimer's disease. Frontiers in Molecular Neuroscience. 2017;10(339).
109. Chung H, Lee J, Kim J, Roh E, Lee Y, Hong S, Kim N, Yoo H, Seo J, Kim S, Kim N, Baik S, Choi K. Variability in total cholesterol concentration is associated with the risk of dementia: a nationwide population-based cohort study. Frontiers in Neurology. 2019;10(441).
110. Beel A, Sakakura M, Barrett P, Sanders C. Direct binding of cholesterol to the amyloid precursor protein: an important interaction in lipid-Alzheimer's disease relationships. Biochimica et Biophysica Acta. 2010;1801(8):975–82.
111. Dias IHK, Mistry J, Fell S, Reis A, Spickett C, Polidori M, Lip GY, Griffithsa HR. Oxidized LDL lipids increase β-amyloid production by SH-SY5Y cells through glutathione depletion and lipid raft formation. Free Radical Biology and Medicine. 2014;75:48-59.

112. Hui L, Soliman ML, Geiger NH, Miller NM, Afghah Z, Lakpa KL, Chen X, Geiger JD. Acidifying endolysosomes prevented LDL-induced amyloidogenesis. Journal of Alzheimer's Disease. 2019;67(1):393-410.
113. Molecular Probes Inc. Amplex® red acetylcholine/acetylcholinesterase assay kit (A12217). 2004. [Accessed July 2017]. Available from: https://assets.thermofisher.com/TFS-Assets/LSG/manuals/mp12217.pdf.
114. Vichai V, Kirtikara K. Sulforhodamine B colorimetric assay for cytotoxicity screening. Nature Protocols. 2006;1(3):1112-6.
115. Orellana EA, Kasinski AL. Sulforhodamine B (SRB) Assay in Cell Culture to Investigate Cell Proliferation. Bio-protocol. 2016;6(21):e1984.
116. Boyd V, Cholewa OM, Papas KK. Limitations in the use of fluorescein diacetate/propidium iodide (FDA/PI) and cell permeable nucleic acid stains for viability measurements of isolated islets of langerhans. Current Trends in Biotechnology and Pharmacy. 2008 2(2):66-84.
117. Jones K, Kim DW, Park JS, Khang CH. Live-cell fluorescence imaging to investigate the dynamics of plant cell death during infection by the rice blast fungus *Magnaporthe oryzae*. BMC Plant Biology. 2016;16(1):69.
118. Rosenberg M, Azevedo NF, Ivask A. Propidium iodide staining underestimates viability of adherent bacterial cells. Scientific Reports. 2019;9(1):6483.
119. Fan G, Liu D, Lin Q. Fluorescein diacetate and propidium iodide FDA-PI double staining detect the viability of *Microcystis sp.* after ultrasonic irradiation. Journal of Food, Agriculture & Environment. 2013;11:2419-21.
120. Ibidi. Live/dead staining with FDA and PI. Application Note 332015.
121. Sigma-Aldrich. Bicinchoninic acid kit. 2018. [Accessed February 2018]. Available from: https://www.sigmaaldrich.com/life-science/proteomics/protein-quantitation/bicinchoninic-acid.html.
122. Brady PN, Macnaughtan MA. Evaluation of colorimetric assays for analyzing reductively methylated proteins: biases and mechanistic insights. Analytical Biochemistry. 2015;491:43-51.
123. ThermoFisher Scientific. BCA Assay and Lowry Assays. 2021. [Accessed May 2021].
124. Abcam. Introduction to flow cytometry: Abcam; 2019. [Accessed June 2019]. Available from: https://www.abcam.com/protocols/introduction-to-flow-cytometry.
125. McKinnon KM. Flow cytometry: an overview. Current Protocols in Immunology. 2018;120(1):5.1.-5.1.11.
126. Lv M, Zhang Y, Liang L, Wei M, Hu W, Li X, Huang Q. Effect of graphene oxide on undifferentiated and retinoic acid-differentiated SH-SY5Y cells line. Nanoscale. 2012;4:3861-86.
127. Sigma-Aldrich. MaxGel ECM. Sigma-Aldrich; 2017. p. 1.
128. Kovalevich J, Langford D. Considerations for the use of SH-SY5Y neuroblastoma cells in neurobiology. Methods in Molecular Biology. 2013;2013(1078):9-21.
129. Serdar BS, Erkmen T, Ergür BU, Akan P, Koçtürk S. Which medium and ingredients provide better morphological differentiation of SH-SY5Y cells? Proceedings of the National Academy of Sciences of the United States of America. 2018;2(1557).
130. Popova D, Karlsson J, Jacobsson SOP. Comparison of neurons derived from mouse P19, rat PC12 and human SH-SY5Y cells in the assessment of chemical- and toxin-induced neurotoxicity. BMC Pharmacology and Toxicology. 2017;18(1):42.
131. Taylor MA, Kan HL, Gollapudi BB, Marty MS. An *in vitro* developmental neurotoxicity screening assay for retinoic acid-induced neuronal differentiation using the human NT2/D1 cell line. NeuroToxicology. 2019;73:258-64.

132. Scheibe RJ, Ginty DD, Wagner JA. Retinoic acid stimulates the differentiation of PC12 cells that are deficient in cAMP-dependent protein kinase. Journal of Cell Biology. 1991;113(5):1173-82.
133. López-García I, Gerő D, Szczesny B, Szoleczky P, Olah G, Módis K, Zhang K, Gao J, Wu P, Sowers LC, DeWitt D, Prough DS, Szabo C. Development of a stretch-induced neurotrauma model for medium-throughput screening *in vitro*: identification of rifampicin as a neuroprotectant. British Journal of Pharmacology. 2018;175(2):284-300.
134. Park S, Kim JY, Myung S, Jung N, Choi Y, Jung SC. Differentiation of motor neuron-like cells from tonsil-derived mesenchymal stem cells and their possible application to neuromuscular junction formation. International Journal of Molecular Sciences. 2019;20(11).
135. Hachem LD, Mothe AJ, Tator CH. Effect of BDNF and other potential survival factors in models of *in vitro* oxidative stress on adult spinal cord–derived neural stem/progenitor cells. BioResearch Open Access. 2015;4(1):146-59.
136. Kim H, Zahir T, Tator CH, Shoichet MS. Effects of dibutyryl cyclic-AMP on survival and neuronal differentiation of neural stem/progenitor cells transplanted into spinal cord injured rats. The Public Library of Science ONE. 2011;6(6):12.
137. Haberberger RV, Barry C, Matusica D. Immortalized Dorsal Root Ganglion Neuron Cell Lines. Frontiers in Cellular Neuroscience. 2020;14(184).
138. Ng YP, Wu Z, Wise H, Tsim KWK, Wong YH, Ip NY. Differential and synergistic effect of nerve growth factor and cAMP on the regulation of early response genes during neuronal differentiation. Neurosignals. 2009;17(2):111-20.
139. Al-Farhan NW, Rao M. Dibutyryl cAMP enhances cognitive functions in diabetic rats by increasing the hippocampal neurogenesis. The Federation of American Societies for Experimental Biology Journal. 2019;33(S1):lb157-lb.
140. Abd-El-Basset EM, Rao MS. Dibutyryl cyclic adenosine monophosphate rescues the neurons from degeneration in stab wound and excitotoxic injury models. Frontiers in Neuroscience. 2018;12(546).
141. Hu R, Cao Q, Sun Z, Chen J, Zheng Q, Xiao F. A novel method of neural differentiation of PC12 cells by using opti-MEM as a basic induction medium. International Journal of Molecular Medicine. 2018;41(1):195-201.
142. Zainullina LF, Vakhitova YV, Lusta AY, Gudasheva TA, Seredenin SB. Dimeric mimetic of BDNF loop 4 promotes survival of serum-deprived cell through TrkB-dependent apoptosis suppression. Scientific Reports. 2021;11(1):7781.
143. Shemesh A, Kundu K, Peleg R, Yossef R, Kaplanov I, Ghosh S, Khrapunsky Y, Gershoni-Yahalom O, Rabinski T, Cerwenka A, Atlas R, Porgador A. NKp44-derived peptide binds proliferating cell nuclear antigen and mediates tumor cell death. Frontiers in Immunology. 2018;9(1114).
144. Salani M, Anelli T, Tocco GA, Lucarini E, Mozzetta C, Poiana G, Tata AM, Biagioni S. Acetylcholine-induced neuronal differentiation: muscarinic receptor activation regulates EGR-1 and REST expression in neuroblastoma cells. Journal of Neurochemistry. 2009;108(3):821-34.
145. Nirogi R, Mudigonda K, Kandikere V, Ponnamaneni R. Quantification of acetylcholine, an essential neurotransmitter, in brain microdialysis samples by liquid chromatography mass spectrometry. Biomedical Chromatography. 2010;24(1):39-48.
146. Yang JL, Lin YT, Chen WY, Yang YR, Sun SF, Chen SD. The neurotrophic function of glucagon-like peptide-1 promotes human neuroblastoma differentiation via the PI3K-AKT axis. Biology. 2020;9(11).

147. Thullbery MD, Cox HD, Schule T, Thompson CM, George KM. Differential localization of acetylcholinesterase in neuronal and non-neuronal cells. Journal of Cellular Biochemistry. 2005;96(3):599-610.
148. Yang YHK, Ogando CR, Wang See. C, Chang TY, Barabino GA. Changes in phenotype and differentiation potential of human mesenchymal stem cells aging *in vitro*. Stem Cell Research & Therapy. 2018;9(1):131.
149. Cockova Z, Ujcikova H, Telensky P, Novotny J. Protein profiling of SH-SY5Y neuroblastoma cells: the effect of rhein. Journal of Biosciences. 2019;44(4).
150. Bergström P, Agholme L, Nazir FH, Satir TM, Toombs J, Wellington H, Strandberg J, Bontell TO, Kvartsberg H, Holmström M, Boreström C, Simonsson S, Kunath T, Lindahl A, Blennow K, Hanse E, Portelius E, Wray S, Zetterberg H. Amyloid precursor protein expression and processing are differentially regulated during cortical neuron differentiation. Scientific Reports. 2016;6:29200.
151. Sosa LJ, Cáceres A, Dupraz S, Oksdath M, Quiroga S, Lorenzo A. The physiological role of the amyloid precursor protein as an adhesion molecule in the developing nervous system. Journal of Neurochemistry. 2017;143(1):11-29.
152. Kim WH, Watanabe H, Lomoio S, Tesco G. Spatiotemporal processing of neural cell adhesion molecules 1 and 2 by BACE1 *in vivo*. Journal of Biological Chemistry. 2021;296:100372.
153. Wang R, Chen S, Liu Y, Diao S, Xue Y, You X, Park EA, FF. L. All-trans-retinoic acid reduces BACE1 expression under inflammatory conditions via modulation of nuclear factor κB (NFκB) signaling. The Journal of Biological Chemistry. 2015;290(37):22532-42.
154. Červenka J, Tylečková J, Kupcová Skalníková H, Vodičková Kepková K, Poliakh I, Valeková I, Pfeiferová L, Kolář M, Vaškovičová M, Pánková T, Vodička P. Proteomic characterization of human neural stem cells and their secretome during *in vitro* differentiation. Frontiers in Cellular Neuroscience. 2021;14(465).

Appendix I: Ethical approval

UNIVERSITEIT VAN PRETORIA
UNIVERSITY OF PRETORIA
YUNIBESITHI YA PRETORIA

Faculty of Health Sciences

Institution: The Research Ethics Committee, Faculty Health Sciences, University of Pretoria complies with ICH-GCP guidelines and has US Federal wide Assurance.
- FWA 00002567, Approved dd 22 May 2002 and Expires 03/20/2022.
- IORG #: IORG0001762 OMB No. 0990-0279 Approved for use through February 28, 2022 and Expires: 03/04/2023.

15 April 2021

Approval Certificate
Annual Renewal

Ethics Reference No.: 212/2018
Title: Comparison of differentiation protocols of SH-SY5Y cells for use as an in vitro model of Alzheimer's disease.

Dear Miss N Mullah

The **Annual Renewal** as supported by documents received between 2021-03-17 and 2021-04-14 for your research, was approved by the Faculty of Health Sciences Research Ethics Committee on 2021-04-14 as resolved by its quorate meeting.

Please note the following about your ethics approval:
- Renewal of ethics approval is valid for 1 year, subsequent annual renewal will become due on 2022-04-15.
- Please remember to use your protocol number (212/2018) on any documents or correspondence with the Research Ethics Committee regarding your research.
- Please note that the Research Ethics Committee may ask further questions, seek additional information, require further modification, monitor the conduct of your research, or suspend or withdraw ethics approval.

Ethics approval is subject to the following:
- The ethics approval is conditional on the research being conducted as stipulated by the details of all documents submitted to the Committee. In the event that a further need arises to change who the investigators are, the methods or any other aspect, such changes must be submitted as an Amendment for approval by the Committee.

We wish you the best with your research.

Yours sincerely

Professor Werdie (CW) Van Staden
MBChB MMed(Psych) MD FCPsych(SA) FTCL UPLM
***Chairperson**: Faculty of Health Sciences Research Ethics Committee*

The Faculty of Health Sciences Research Ethics Committee complies with the SA National Act 61 of 2003 as it pertains to health research and the United States Code of Federal Regulations Title 45 and 46. This committee abides by the ethical norms and principles for research, established by the Declaration of Helsinki, the South African Medical Research Council Guidelines as well as the Guidelines for Ethical Research: Principles Structures and Processes, Second Edition 2015 (Department of Health)

Research Ethics Committee
Room 4-60, Level 4, Tswelopele Building
University of Pretoria, Private Bag x323
Gezina 0031, South Africa
Tel +27 (0)12 356 3084
Email: deepika.behari@up.ac.za

Fakulteit Gesondheidswetenskappe
Lefapha la Disaense tša Maphelo

Appendix II: Reagents and chemicals

Acetic acid (1%)

Acetic acid was purchased from Merck Chemicals (South Africa) and stored at room temperature. Acetic acid (%) was prepared by diluting 1 mL acetic acid up to 100 mL distilled water. Acetic acid (1%) was stored at room temperature.

Amplex® Acetylcholine/Acetylcholinesterase activity assay kit

The Amplex® Acetylcholine/Acetylcholinesterase Assay kit was purchased from Thermo Fisher (Massachusetts, USA) and stored at -20°C. The reagents were prepared according to the manufacturer's instructions as described below:

Acetylcholine stock solution (100 mM)

Acetylcholine chloride was provided in the Amplex® Acetylcholine/Acetylcholinesterase Assay kit as a powder. A stock solution (100 mM) was prepared by dissolving acetylcholine chloride (5 mg) in distilled water (275 µL). The stock solution was made fresh before experiments.

Acetylcholinesterase stock solution (100 U/mL)

Acetylcholinesterase from electrical eel was provided in the Amplex® Acetylcholine/ Acetylcholinesterase Assay kit. A stock solution (100 U/mL) was prepared by dissolving the contents of the provided vial (60 U) with 600 µL reaction buffer (1X). The stock solution was stored -20°C in aliquots (100 µL).

Reaction buffer (1X)

The reaction buffer (1X) was prepared by diluting 5 mL Tris-HCl (5X) in 20 mL distilled water. The reaction buffer (1X) was stored at 4°C.

Acetylcholine positive control

The positive control (50 µM ACh) was prepared by diluting 5 µL ACh stock solution (100 mM) in 9.995 mL distilled water. The stock solution was used immediately.

Hydrogen peroxide positive control

The positive control (10 µM H_2O_2) was prepared by diluting H_2O_2 working solution (20 mM) in reaction buffer (1X). The solution was used immediately.

Acetylcholinesterase positive control

The positive control (AChE; 0.2 U/mL) was prepared by diluting 50 µL AChE stock solution (100 U/mL) in 50 µL reaction buffer (1X) and stored at -20°C.

Anti-APP antibody

The rabbit anti-APP antibody was purchased from Sigma-Aldrich (St. Louis, USA) and stored at -20°C. The antibody was diluted in PBS (1:500-1:1000, v/v). Anti-APP antibody was conjugated with the PE/Cy5.5® conjugation kit (ab102899) which was purchased from Abcam (Cambridge, UK) and stored at -20°C

Anti-BACE-1 antibody

The rabbit anti-BACE-1 antibody was purchased from Sigma-Aldrich (St. Louis, USA) and stored at -20°C. The antibody was diluted in PBS (1:100, v/v). Anti-BACE-1 antibody was conjugated with the APC/Cy7® conjugation kit (ab102859) which was purchased from Abcam (Cambridge, UK) and stored at -20°C.

Anti-PCNA-APC antibody

The rabbit anti-PCNA-APC antibody was already conjugated and was purchased from Miltenyi Biotec (Bergisch Gladbach, Germany) and stored at 4°C. The antibody was diluted in PBS (1:500-1:1,000, v/v).

Bicinchoninic acid

The BCA reagent consisted of reagent A and reagent B in a 50:1 ratio. The solution was discarded after use.

Reagent A was prepared by dissolving 1 g sodium bicinchoninate (0.1%), 2 g sodium carbonate decahydrate (2%), 0.16 g sodium tartrate dihydrate (0.16%), 0.4 g sodium hydroxide (4%) and 0.95 g sodium hydrogen carbonate (0.95%, pH=11.25) in 100 mL distilled water. The solution was stored at 4°C.

Reagent B contained 0.4 g copper (II) sulfate pentahydrate (4%) which was dissolved in 10 mL distilled water. The solution was covered with foil and stored at 4°C.

Brain-derived neurotrophic factor

Brain-derived neurotrophic factor was purchased from Sigma-Aldrich (St. Louis, USA) and stored at -20°C. The BDNF (10 µg/mL) was prepared in neurobasal medium and B27 supplement (1X) by dissolving 10 µg BDNF in 980 µL neurobasal medium and 20 µL B27 supplement (50X).

B27 supplement

B27 supplement (50X) was purchased from Thermo Fisher (Massachusetts, USA). B27 supplement (50X) stored at -20°C in ready to use aliquots (1 mL).

Copper (II) sulfate pentahydrate

Copper (II) sulfate pentahydrate was purchased from Sigma-Aldrich (St. Louis, USA) and stored at room temperature. Copper (II) sulfate pentahydrate (0.4 g) was dissolved in distilled water (10 mL) and stored at 4°C.

Dibutyryl cyclic adenosine monophosphate

Dibutyryl cyclic AMP was purchased from Sigma-Aldrich (St. Louis, USA) and was stored at -20°C. Dibutyryl cyclic AMP (1 M) was prepared by dissolving 1 g in distilled water (2.04 mL) and stored at 4°C.

Differentiation media I

Differentiation media I (50 mL) consisted of DMEM/Ham's F12 medium (1:1) supplemented with 2.5% FBS, 1% penicillin/streptomycin and 10 µM RA (added immediately before use). This was achieved by mixing 1.25 mL FBS (100%), 500 µL penicillin/streptomycin (100X), 100 µL RA (5 mM) and 48.15 mL DMEM/Ham's F12 medium (1:1). Unused media supplemented with RA was disposed of.

Differentiation media II

Differentiation media II (40 mL) consisted of DMEM/Ham's F12 medium (1:1) supplemented with 1% FBS, 1% penicillin/streptomycin and 10 µM RA (added immediately before use). This was achieved by mixing 400 µL FBS (100%), 400 µL penicillin/streptomycin (100X), 100 µL

RA (5 mM) and 39.10 mL DMEM/Ham's F12 medium (1:1). Unused media supplemented with RA was disposed of.

Differentiation media III

Differentiation media III (100 mL) consisted of neurobasal medium supplemented with 1% penicillin/streptomycin, B27 supplement (1X), 20 mM KCl, 2 mM GlutaMAX and 2 mM db-cAMP, 50 ng/mL BDNF (added immediately before use) and 10 µM RA (added immediately before use). This was achieved by mixing 1 mL penicillin/streptomycin (100X), 1.96 mL B27 supplement (50X), 1.96 mL KCl (1 M), 990 µL GlutaMAX (100X), 200 µL db-cAMP (1 M), 498 µL BDNF (10 ng/mL), 200 µL RA (5 mM) and 93.19 mL neurobasal medium. Unused media supplemented with RA was disposed of.

DMEM/Ham's F12

Dulbecco's Modified Eagle's Medium and Ham's F12 medium was purchased from Sigma-Aldrich (St. Louis, USA) and stored at 4°C. A dual-medium was prepared by mixing equal parts of DMEM and Ham's F12.

Edetic acid

Edetic acid (EDTA) was purchased from Sigma-Aldrich (St. Louis, USA) and stored at room temperature. Edetic acid was used undissolved.

Fluorescein diacetate

Fluorescein diacetate was purchased from Sigma-Aldrich (St. Louis, USA). The FDA stock solution was prepared by dissolving 5 mg of FDA in 1 mL of acetone (stored at -20°C).

Fluorescein diacetaten/propidium iodide staining solution

The FDA/PI staining solution was prepared by adding 8 µL of FDA stock solution and 50 µL of PI stock solution in 5 mL of PBS and used immediately.

MaxGel™ extracellular matrix

MaxGel™ ECM was purchased from Sigma-Aldrich (St. Louis, USA) and stored at -80°C. The extracellular matrix was prepared by diluting the solution with DMEM/Ham's F12 at a ratio of 1:100 (v/v).

Foetal bovine serum

Foetal bovine serum was purchased from Thermo Fisher (Massachusetts, USA), heat-inactivated and stored at -20°C. Foetal bovine serum was used undiluted.

GlutaMAX

GlutaMAX (100X) was purchased from Thermo Fisher (Massachusetts, USA) and stored at room temperature. GlutaMAX was used undiluted.

Neurobasal medium

Neurobasal medium was purchased from Thermo Fisher (Massachusetts, USA) and stored at 4°C. Neurobasal medium was used undiluted.

N-2 supplement

The N-2 supplement (100X) was purchased from Thermo Fisher (Massachusetts, USA) and stored at -20°C. The N-2 supplement was used undiluted.

Penicillin/streptomycin

Penicillin/streptomycin (100X) was purchased from Sigma-Aldrich (St. Louis, USA) and stored at -20°C. Penicillin/streptomycin was used undiluted.

Phase I medium

Phase I medium (20 mL) consisted of DMEM/Ham's F12 (1:1) supplemented with 5% FBS, 1% penicillin/streptomycin, 10 µM RA (added immediately before use). This was achieved by mixing 1 mL FBS (100%), 200 µL penicillin/streptomycin (100X), 40 µL RA (5 mM) and 18.76 mL DMEM/Ham's F12 (1:1). Unused media after the addition of RA was disposed of.

Phase II medium

Phase II medium (40 mL) consisted of neurobasal medium supplemented with 1% penicillin/streptomycin, 1X GlutaMAX, 1X N-2 supplement (added immediately before use) and 50 ng/mL BDNF (added immediately before use). This was achieved by mixing 400 µL penicillin/streptomycin (100X), 400 µL GlutaMAX (100X), 400 µL N-2 supplement (100X), 400 µL BDNF (10 µg/mL) and 38.40 mL neurobasal medium.

Phosphate-buffered saline

Phosphate-buffered saline was purchased from Sigma-Aldrich (St. Louis, USA) and stored at room temperature. Phosphate-buffered saline was prepared by dissolving 1.015 g PBS in 110 mL distilled water. Phosphate-buffered saline was stored 4°C.

Potassium chloride

Potassium chloride was purchased from Sigma-Aldrich (St. Louis, USA). Potassium chloride (1 M was prepared by dissolving 18.6 g) was dissolved in distilled water (250 mL) and stored at room temperature.

Propidium iodide

Propidium iodide was purchased from Sigma Aldrich (St Louis, USA). The PI stock solution was prepared by dissolving 2 mg of PI in 1 mL PBS (stored at 4°C).

Retinoic acid

Retinoic acid was purchased from Sigma-Aldrich (St. Louis, USA) and stored at -20°C. Retinoic acid (50 mg) was dissolved in 95% EtOH (33.3 mL) and stored in a dark bottle at 4°C after preparation. The mixture was not kept for longer than six weeks.

Radioimmunoprecipitation assay buffer

Radioimmunoprecipitation assay buffer consisted of 50 mM Tris-hydrochloride [pH 7.4], 150 mM sodium chloride (NaCl), 1% Triton X-100, 1% sodium deoxycholate, 0.1% sodium dodecyl sulfate (SDS; w/v), 1 mM EDTA. This was accomplished by mixing 2.5 mL Tris-HCl (1 M), 438.30 mg NaCl, 500 µL Triton X-100, 5 mL sodium deoxycholate (10%), 500 µL SDS stock solution (10%). Radioimmunoprecipitation assay buffer was stored at 4°C.

Sodium bicinchoninate

Sodium bicinchoninate was purchased from Sigma-Aldrich (St. Louis, USA) and stored at room temperature. Sodium bicinchoninate was used undissolved.

Sodium carbonate decahydrate

Sodium carbonate decahydrate was purchased from Sigma-Aldrich (St. Louis, USA) and stored at room temperature. Sodium carbonate decahydrate was used undissolved.

Sodium chloride

Sodium chloride was purchased from Sigma-Aldrich (St. Louis, USA) and stored at room temperature. Sodium chloride was used undissolved.

Sodium dodecyl sulfate

Sodium dodecyl sulfate was purchased from Sigma-Aldrich (St. Louis, USA) and stored at room temperature. Sodium dodecyl sulfate stock solution (10%) was prepared by dissolving 10 g of SDS in 100 mL distilled water and stored at room temperature.

Sodium deoxycholate

Sodium deoxycholate was purchased from Sigma-Aldrich (St. Louis, USA) and stored at room temperature. Sodium deoxycholate was prepared by dissolving 10 g of Sodium deoxycholate in 100 mL distilled water and stored at room temperature.

Sodium hydrogen carbonate

Sodium hydrogen carbonate was purchased from Sigma-Aldrich (St. Louis, USA) and stored at room temperature. Sodium hydrogen carbonate was used undissolved.

Sodium hydroxide

Sodium hydroxide was purchased from Sigma-Aldrich (St. Louis, USA) and stored at room temperature. Sodium hydroxide was used undissolved.

Sodium tartrate dihydrate

Sodium tartrate dihydrate was purchased from Sigma-Aldrich (St. Louis, USA) and stored at room temperature. Sodium tartrate dihydrate was used undissolved.

Sulforhodamine B

Sulforhodamine B stain was purchased from Sigma Aldrich (St Louis, USA) and was stored at room temperature. The SRB stain solution (0.057%) was prepared by dissolving 57 mg SRB stain in 100 mL distilled water. The solution was stored at 4°C in the dark.

Trichloroacetic acid (50%)

Trichloroacetic acid powder was purchased from Sigma Aldrich (St Louis, USA) and was stored at room temperature. The TCA solution (50%) was prepared by dissolving 50 g TCA powder in 100 mL distilled water. The solution was stored at 4°C.

TRIS buffer

TRIS powder was purchased from Sigma Aldrich (St Louis, USA) and stored at room temperature. The TRIS buffer was prepared by dissolving 120 mg TRIS powder in 100 mL distilled water. The buffer was adjusted to pH 10.5 and was stored at room temperature.

Triton X-100

Triton X-100 was purchased from Sigma-Aldrich (St. Louis, USA) and stored at room temperature. Triton X-100 was used undiluted.